

RADIO ASTRONOMY

Journal of the Society of Amateur Radio Astronomers
March - April 2024



SARA 2024 Western Conference – Dallas, Texas



Dr. Richard A. Russel
SARA President and Editor

Bogdan Vacaliuc
Contributing Editor

Radio Astronomy is published bimonthly as the official journal of the Society of Amateur Radio Astronomers. Duplication of uncopyrighted material for educational purposes is permitted but credit shall be given to SARA and to the specific author. Copyrighted materials may not be copied without written permission from the copyright owner.

Radio Astronomy is available for download only by SARA members from the SARA web site and may not be posted anywhere else.

It is the mission of the Society of Amateur Radio Astronomers (SARA) to: Facilitate the flow of information pertinent to the field of Radio Astronomy among our members; Promote members to mentor newcomers to our hobby and share the excitement of radio astronomy with other interested persons and organizations; Promote individual and multi station observing programs; Encourage programs that enhance the technical abilities of our members to monitor cosmic radio signals, as well as to share and analyze such signals; Encourage educational programs within SARA and educational outreach initiatives. Founded in 1981, the Society of Amateur Radio Astronomers, Inc. is a membership supported, non-profit [501(c) (3)], educational and scientific corporation.

Copyright © 2024 by the Society of Amateur Radio Astronomers, Inc. All rights reserved.

Cover Photo:
SARA

Contents

President's Page	2
Editor's Notes	3
SARA 2024 Eastern Conference	4
SARA NOTES	8
News: (March - April 2024)	10
Technical Knowledge and Education: (March-April 2024)	20
SuperSID	22
Announcing Radio JOVE 2.0	25
John Cook's VLF Report	31
BAA RA Section programme 2024.....	51
Featured Articles	52
Run GNU Radio on a Windows 11 PC with Windows Subsystem for Linux, ver. 2 (WSL 2) – Tom Hagen	52
Some Folding Algorithm Variants for Optimizing Pulsar SNR for Small Apertures - Peter W East.....	63
Notes on building a maser receiver – Dimitry Fedorov	71
Solar & Geomagnetic Storms 23-24 March 2024 - Whitham D. Reeve	83
Hydrogen Line Drift Scan Detection of M31 and M33 with a Portable 2.64 Meter Dish – Jason Burnfield	88
Observation Reports	97
Small Aperture Antenna Drive with 3D Printed Components – Nathaniel Butts.....	97
Observation report: OH masers observed with the Dwingeloo telescope – Eduard Mol, et al.....	100
Journal Archives and Other Promotions	108
What is Radio Astronomy?.....	109
Administrative	110
Officers, directors, and additional SARA contacts	110
Resources	111
Great Projects to Get Started in Radio Astronomy	111
Radio Astronomy Online Resources.....	113
SARA Brochure	116

President's Page



I want to congratulate David Westman, Bob Stricklin, Nathan Butts and Tom Jacobs for the VERY successful Western Conference!

The videos of the presentations are on the SARA You Tube channel under the 2024 Western Conference Playlist. [Keynote: Dr Linsay King - Gravitational Lensing \(youtube.com\)](#)

Officer nominations will be coming out next month. Volunteer for a board or officer position and learn how to manage an International 501(c)(3).

Rich

SARA President

Editor's Notes

We are always looking for basic radio astronomy articles, radio astronomy tutorials, theoretical articles, application and construction articles, news pertinent to radio astronomy, profiles and interviews with amateur and professional radio astronomers, book reviews, puzzles (including word challenges, riddles, and crossword puzzles), anecdotes, expository on "bad astronomy," articles on radio astronomy observations, suggestions for reprint of articles from past journals, book reviews and other publications, and announcements of radio astronomy star parties, meetings, and outreach activities.

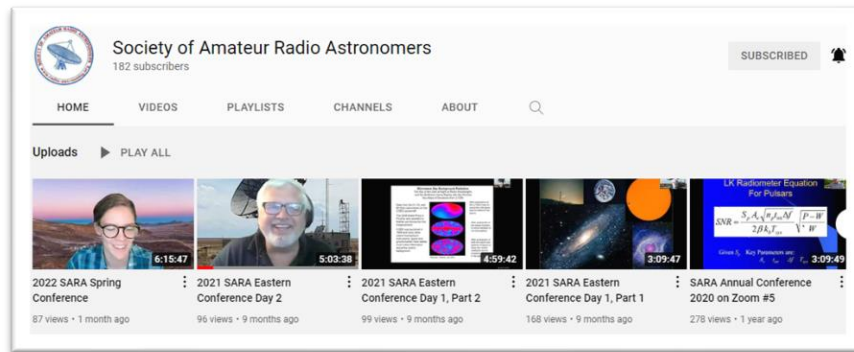
Subscribe to the SARA YouTube Channel

SARA has a YouTube channel at: <https://www.youtube.com/@radio-astronomy>



Don't forget to LIKE the videos! It helps with the YouTube distribution algorithm.

We are also looking to add content to the site. Anyone who wants to help produce a series of 5 - minute videos relating to radio astronomy technology or observations please contact me. (drrichrussel@netscape.net)



Observation Reports

We are now accepting 1-2 page observation reports. These reports should include the astronomical object's RA/DEC plus UTC of the observation. Also include the telescope configuration, process used to observe the object and results. Picture of the setup and plots of the observation are a plus to the report.

If you would like to write an article for Radio Astronomy, please follow **the newly updated Author's Guide** on the SARA web site:

http://www.radio-astronomy.org/publicat/RA-JSARA_Author's_Guide.pdf.

Let us know if you have questions; we are glad to assist authors with their articles and papers and will not hesitate to work with you. You may contact your editors any time via email here: edit@radio-astronomy.org.

The editor(s) will acknowledge that they have received your submission within two days. If they do not reply, assume they did not receive it and please try again.

Please consider submitting your radio astronomy observations for publication: any object, any wavelength. Strip charts, spectrograms, magnetograms, meteor scatter records, space radar records, photographs; examples of radio frequency interference (RFI) are also welcome.

Guidelines for submitting observations may be found here: http://www.radio-astronomy.org/publicat/RA-JSARA_Observation_Submission_Guide.pdf

**2024 SARA Eastern Conference
and
Global Radio Astronomy Symposium
Green Bank Observatory
Green Bank, West Virginia, 2024
4-7 August 2024**

The 2024 SARA Eastern Conference and Global Radio Astronomy Symposium will be held at the Green Bank Observatory, West Virginia, Sunday through Wednesday, 4-7 August 2024. The conference will also be available as a fully interactive online event.

With radio astronomy as its foundation, the Green Bank Observatory (GBO) is a world leader in advancing research, innovation, and education.

The first trailblazers of American radio astronomy called Green Bank Observatory home over 60 years ago. Today, their legacy is alive and well. Nestled in the mountain ranges and farmland of West Virginia, within the National Quiet Zone, radio astronomers are listening to the remote whispers of the universe, in order to discover answers to our most astounding astronomical questions.



Schedule: Conference meetings will be held in the main auditorium of the Jansky Laboratory at Green Bank Observatory with presentations by SARA members, GBO staff and distinguished speakers. Security and health restrictions permitting, tours of the facility, radio telescopes and laboratories will be conducted. Certain locations are open only to U.S. citizens who submit for a security review two weeks prior; however, most areas will be open to all attendees. ***Fully interactive online participation will be available for those who cannot attend in person.***

Key advantages of in-person attendance are training and hands-on use of the historical 40-foot radio telescope as well as user tutorial and supervised control of the 20 Meter radio telescope.

Sunday through Tuesday evenings, round table discussions and refreshments are scheduled in the Drake's Lounge, and there will be space outside for attendees to set up and display their own portable radio astronomy systems and optical telescopes.

Meals in the GBO cafeteria are included in the registration fee for in-person attendees.

Virtual online sessions are available for those who cannot attend in person.

Lodging is not included in the conference registration fee.

A small number of on-site dormitory rooms may become available for conference speakers, support staff and SARA officers. Other conference attendees may request rooms on a standby basis, but it is highly recommended that attendees arrange off-site accommodations.

RV/camping sites and a cabin are available at the nearby Boyer Station Campground. Call 1.304.456.4667 to inquire. The Elk Springs Resort is about 12 miles away. The Snowshoe Mountain area has several lodging facilities.

For other accommodations, please go to <https://www.snowshoemtn.com/plan-your-trip/lodging>. Numerous VRBO / Airbnb properties and private rentals are near GBO.

A list of many properties is at <https://pocahontascountywv.com/lodging/>. Many chain accommodations are located about 30 miles away in Elkins, but that drive takes at least an hour due to mountainous roads.

Registration: Registration for in-person attendance by SARA members at the Conference is \$250.00 (USD) if received by July 5, 2024, which includes meals but not lodging. The fee for family members or other guests who do not participate in conference sessions is \$75.00, which includes meals and evening activities. Registration by July 5th for non-members is \$270.00, which includes a year's membership in SARA. SARA members wishing to renew their membership at the same time as they register may also pay \$270 and should include a renewal comment with their payment.

Late registration after July 5, 2024, is \$300.00. Walk-in registration at the conference is \$350.00.

Payment can be made through PayPal, www.paypal.com by sending payment to treasurer@radio-astronomy.org Please include in comments that the payment is for the **2024 Eastern Conference**.

Online registration will be available at the SARA Store in January 2024:

[On-Site Participation](#) or [Online Participation](#)

Proposals for papers, presentations, poster displays and working exhibits are welcome. Initial proposals for papers and presentations should be submitted by May 15, 2024. Abstracts of papers presentation outlines and display details must be submitted by June 1, 2024, with all final materials due on July 5, 2024 to meet publication deadlines. All proposals are subject to peer review and approval.

Presenters who cannot attend in person may be selected for remote video conference presentation. Submit abstracts and proposals to: jwilson@radio-astronomy.org by May 15, 2024.

What Green Bank Observatory Visitors Need to Know

COVID Restrictions. GBO reserves the right to impose requirements for vaccinations and masks. SARA will notify all registrants should GBO issue a policy statement. Should GBO policies adversely impact a conference registrant, they may change their registration from in-person to virtual / online and receive a refund for the difference. Should GBO close the campus for any reason, all registrations will be changed to virtual / online.

No Cellular Phone Service. GBO is in the National Radio Quiet Zone and there is no wireless phone service in the area. Use of wi-fi devices and satellite phones such as Iridium or Globalstar near the facility is not allowed, and severe restrictions are placed on digital cameras, although film cameras without electronic flash are allowed. There is a computer lab available during the day.

Pre-Conference Activities. Suggested pre-conference activities include free self-guided tours of the Green Bank Observatory Science Center and reasonably priced guided tours of the radio telescope area. Full details with a link for ticket purchase: <https://greenbankobservatory.org/visit/>
An overall guide to other activities and attractions in the area: <https://pocahontascountywv.com/things-to-do/>

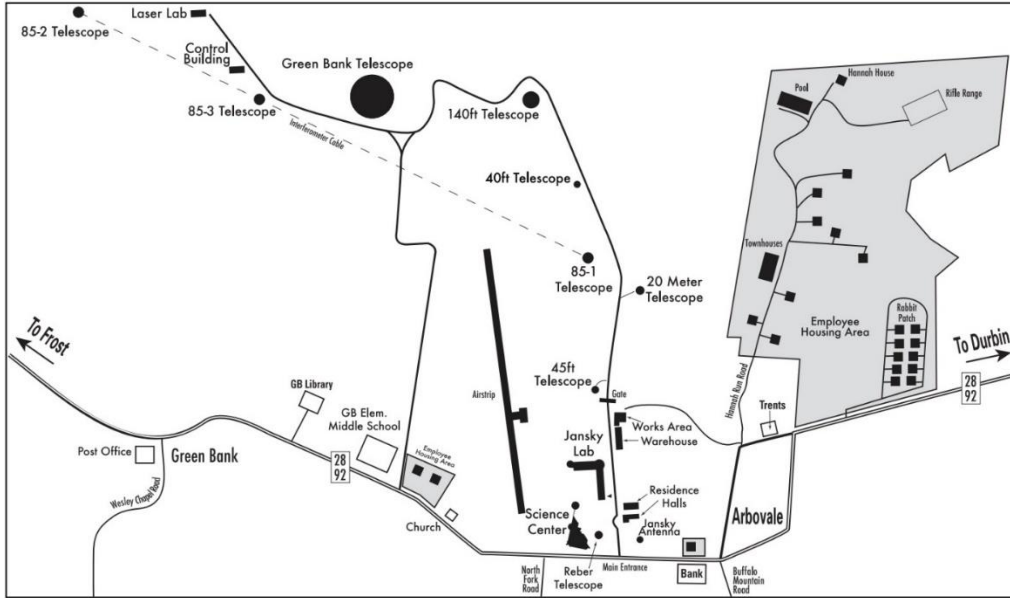
Contact: Please contact the conference coordinator, B.J. Wilson, if you have any questions or if you would like to help with the conference: vicepresident@radio-astronomy.org

Additional Information: Additional details and updates will be published online at www.radio-astronomy.org and in the SARA journal, *Radio Astronomy*, as we get closer to the conference date.

National Radio Quiet Zone and Major Roads to Green Bank



Green Bank Observatory Site Map



SARA NOTES

SARA Student & Teacher Grant Program

All, SARA has a grant program that is, sad to say, very underutilized. We will provide kits or money to students and teachers including college students to help them with a radio telescope project. SARA can supply any of the following kits:

- [1] SuperSID
- [2] Scope in a Box
- [3] IBT (Itty Bitty Telescope)
- [4] Radio Jove kit
- [5] Inspire
- [6] Sky Scan

We can also provide up to five hundred dollars (\$500.00 USD) for an approved radio telescope project.

We have on occasion provided more money based on the merits of the project and the SARA Grant Committee approval.

More information on the grant program can be found at the URL below.

[SARA Student and Teacher Project Grants | Society of Amateur Radio Astronomers \(radio-astronomy.org\)](https://www.radio-astronomy.org/SARA-Student-and-Teacher-Project-Grants)

All that is required is the SARA grant request form be filled out and sent in. If it needs more work for approval, we will work with the students to help ensure their success.

Please pass the word that SARA will fund any legitimate radio telescope project anywhere in the world.

If you have a question, contact me at crowleytj@hotmail.com.

Tom Crowley - SARA Grant Program Administrator

Drake's Lounge Australia

This new zoom forum is geared to the Melbourne, Australia time zone (UTC+10) in order to improve coordination with our Australia, New Zealand, and Japanese members. The meetings are scheduled for the 4th Friday of every month, 9 AM Melbourne time (2000 UTC December 23). A zoom announcement will be sent out to all SARA members before the meeting.

Radio Telescope Observation Party (RTOP)

RTOP is designed to demonstrate how to take observations using various radio telescopes. It will also cover how to record and analyze data.

RTOP is every month on the 1st Sunday at 2 pm Eastern time (1800 UTC). ZOOM email notifications will be sent to all members.

Drake's Lounge

Join the SARA community as we discuss the latest astronomy and radio astronomy news. The lounge also provides a forum to share and get advice on your radio astronomy projects from very experienced amateur radio astronomers.

Drake's Lounge is every month on the 3rd Sunday at 2 pm Eastern time (1800 UTC). ZOOM email notifications will be sent to all members.

News: (March - April 2024)

Large plasma plumes seen around the sun during totality were not caused by solar flares, experts say. Credit:



Petr Horálek, Josef Kujal, Milan Hlaváč

Harry Baker ~ No, you didn't see a solar flare during the total eclipse — but you may have seen something just as special

<https://www.livescience.com/space/the-sun/no-you-didnt-see-a-solar-flare-during-the-total-eclipse-but-you-may-have-seen-something-just-as-special>

Kelly Kizer Whitt ~ Total solar eclipse pics and video from the EarthSky community



<https://earthsky.org/todays-image/total-solar-eclipse-pics-april-8-2024/>

Credit: Raul Cortes

Mark Garcia ~ Station Orbits into Eclipse, Crew Works Research and Spacesuits

<https://blogs.nasa.gov/spacestation/2024/04/08/station-orbits-into-eclipse-crew-works-research-and-spacesuits/>

Credit: NASA



The Eclipse Co. ~ 2024 Total Eclipse (Interactive Map)



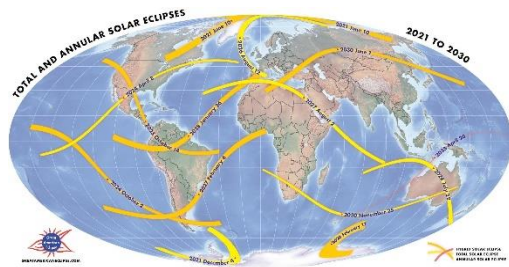
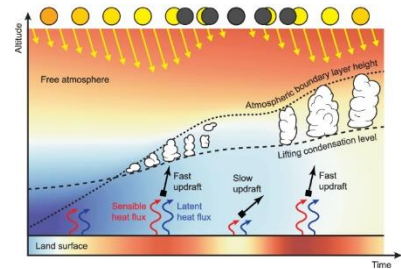
<https://theeclipsecompany/map/2024-total-eclipse>

Victor Trees ~ Clouds disappear quickly during solar eclipse

<https://www.tudelft.nl/en/2024/citg/clouds-disappear-quickly-during-solar-eclipse>

<https://www.nature.com/articles/s43247-024-01213-0>

Credit: Trees V.J.H, et al Communications on Earth Environ 5, 71 (2024)



John Uri ~ Eclipses Near and Far

<https://www.nasa.gov/history/eclipses-near-and-far/>

Credit: Great American Eclipse

Samantha Mathewson ~ Very Large Telescope snaps gorgeous shot of Milky Way's star-studded core

<https://www.space.com/eso-vlt-starry-landscape-milky-way-core>

<https://www.eso.org/public/images/potw2407a/>

<https://doi.org/10.1051/0004-6361/202348712>

Credit: ESO/F. Nogueras-Lara, et al.



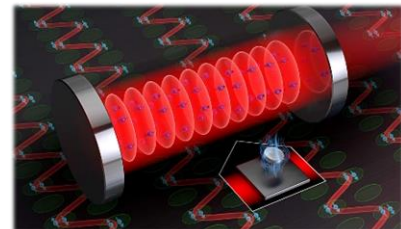
Rebecca Jacobson ~ Scientists Observe Long-Predicted Superconductor Property Using a Quantum Simulator

<https://www.nist.gov/news-events/news/2024/02/scientists-observe-long-predicted-superconductor-property-using-quantum>

<https://www.nist.gov/news-events/news/2024/02/scientists-observe-long-predicted-superconductor-property-using-quantum>

<https://doi.org/10.1038/s41586-023-06911-x>

Credit: JILA/Steven Burrows





Caitlin O'Kane ~ NASA looking for 4 volunteers to spend a year living and working inside a Mars simulator

<https://www.cbsnews.com/news/nasa-mars-simulator-4-volunteers-to-spend-a-year-living-and-working-inside-3d-printed-dune-alpha/>

<https://www.nasa.gov/humans-in-space/chapea/>

Sharon Goldman ~ With Sora, OpenAI highlights the mystery and clarity of its mission

<https://venturebeat.com/ai/with-sora-openai-highlights-the-mystery-and-clarity-of-its-mission-the-ai-beat/>

Credit: Sharon Goldman/VentureBeat

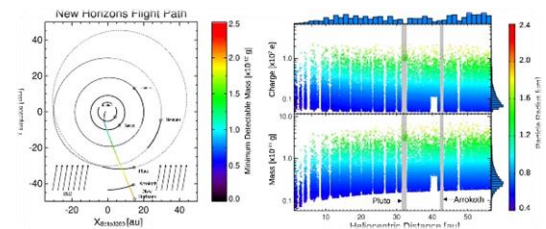


Michelle Starr ~ NASA's New Horizons Discovered a Large Surprise in The Kuiper Belt

<https://www.sciencealert.com/nasas-new-horizons-discovered-a-large-surprise-in-the-kuiper-belt>

<https://dx.doi.org/10.3847/2041-8213/ad18b0>

Credit: Alex Doner et al 2024 ApJL 961 L38



Noa Leach ~ Major quantum gravity breakthrough could spark new 'theory of everything'

<https://www.sciencefocus.com/news/breakthrough-quantum-gravity>

<https://doi.org/10.1126/sciadv.adk2949>

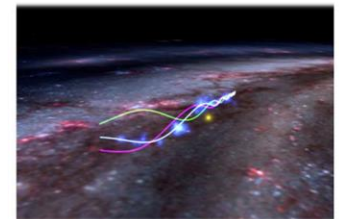
Credit: University of Southampton

Harvard University ~ Astronomers observe the Radcliffe Wave oscillating

<https://phys.org/news/2024-02-astronomers-radcliffe-oscillating.html>

<https://dx.doi.org/10.1038/s41586-024-07127-3>

Credit: Ralf Konietzka, Alyssa Goodman, and WorldWide Telescope



Michelle Starr ~ We Finally Know What Turned the Lights on at The Dawn of Time



<https://www.sciencealert.com/we-finally-know-what-turned-the-lights-on-at-the-dawn-of-time>

<https://esaweb.org/news/weic2405/?lang>

<https://www.nature.com/articles/s41586-024-07043-6>

Credit: NASA, ESA, CSA, I. Labbe/Swinburne University of Technology, R. Bezanson/University of Pittsburgh, A. Pagan/STScI

Justine Calma ~ A tech-backed mission to monitor methane pollution launches today

<https://www.theverge.com/2024/3/4/24090025/methanesat-satellite-launch-spacex-bezos-fund-google-map-methane-edf>

<https://www.methanesat.org/>

<https://earthengine.google.com/>

Credit: MethaneSAT via EDF



Carl Franzen ~ Anthropic's Claude 3 knew when researchers were testing it



<https://venturebeat.com/ai/anthropics-claude-3-knew-when-researchers-were-testing-it/>

<https://www.anthropic.com/news/claude-3-family>

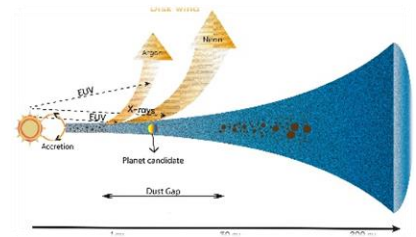
Credit: VentureBeat made with Midjourney V6

SETI Institute ~ James Webb Space Telescope captures the end of planet formation

<https://phys.org/news/2024-03-james-webb-space-telescope-captures.html>

<https://dx.doi.org/10.3847/1538-3881/ad22e1>

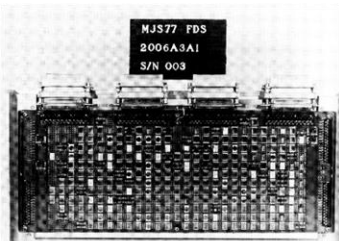
Credit: Naman S. Bajaj et al 2024 AJ 167 127



Stephen Clark ~ Humanity's most distant space probe jeopardized by computer glitch

<https://arstechnica.com/space/2024/02/humanitys-most-distant-space-probe-jeopardized-by-computer-glitch/>

Credit: [NASA Contractor Report 182505](#)



Nell Greenfieldboyce ~ NASA's Voyager 1 spacecraft is talking nonsense. Its friends on Earth are worried
<https://www.npr.org/2024/03/06/1236033493/nasas-voyager-1-spacecraft-is-talking-nonsense-its-friends-on-earth-are-worried>

Credit: NASA/JPL-Caltech



Robert Lea ~ NASA finds clue while solving Voyager 1's communication breakdown case
<https://www.space.com/voyager-1-communications-update-fds-memory-issue>

Credit: Caltech/NASA-JPL



Mark Kaufman ~ NASA scientist viewed first Voyager images. What he saw gave him chills.

<https://mashable.com/article/nasa-voyager-mission> Credit: Mashable composite / NASA / Nuamfolio / Shutterstock



Stephen Clark ~ NASA knows what knocked Voyager 1 offline, but it will take a while to fix
<https://arstechnica.com/space/2024/04/the-diagnosis-is-in-bad-memory-knocked-nasas-aging-voyager-1-offline/>
<https://blogs.nasa.gov/voyager/2024/04/04/engineers-pinpoint-cause-of-voyager-1-issue-are-working-on-solution/>

"Although it may take weeks or months, engineers are optimistic they can find a way for the FDS to operate normally without the unusable memory hardware, which would enable Voyager 1 to begin returning science and engineering data again," NASA said.

David L. Chandler ~ Tests show high-temperature superconducting magnets are ready for fusion

<https://phys.org/news/2024-03-high-temperature-superconducting-magnets-ready.html>

<https://ieeexplore.ieee.org/xpl/tocresult.jsp?isnumber=10348035&punumber=77>

Credit: Gretchen Ertl



Michelle Starr ~ 'Incredibly Rare' Astronomical Object Has Markings in Multiple Languages
<https://www.sciencealert.com/incredibly-rare-astronomical-object-has-markings-in-multiple-languages>
https://brill.com/view/journals/nun/39/1/article-p163_9.xml

Credit: Federica Gigante



Ethan Seigel ~ The future of US astronomy just dimmed by half

<https://bigthink.com/starts-with-a-bang/future-astronomy-dimmed-by-half/>
Credit: Giant Magellan Telescope/GMTO Corporation



Gareth Halfacree ~ Lime Micro Unveils the LimeNET Micro 2.0, a Raspberry Pi CM4-Powered LimeSDR XTRX Radio Powerhouse

<https://www.hackster.io/news/lime-micro-unveils-the-limenet-micro-2-0-a-raspberry-pi-cm4-powered-limesdr-xtrx-radio-powerhouse-03554f8bcc6f>

<https://www.crowdsupply.com/lime-micro/limenet-micro-2>

Credit: Lime Microsystems

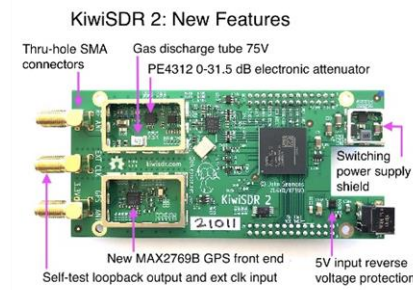


John Seamons ~ KiwiSDR: Wide-band SDR + GPS cape for the BeagleBone Black

<https://forum.kiwisdr.com/index.php?p=/discussion/2986/kiwisdr-2-production-status>

<https://kiwisdr.nz/products/kiwisdr2-1>

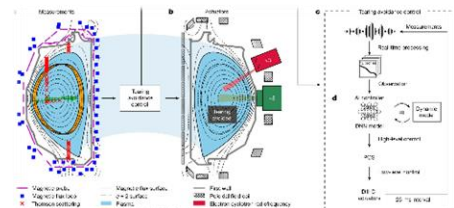
Credit: KiwiSDR



Jaemin Seo, et al. ~ Avoiding fusion plasma tearing instability with deep reinforcement learning

<https://doi.org/10.1038/s41586-024-07024-9>

Credit: Nature 626, 746–751 (2024)

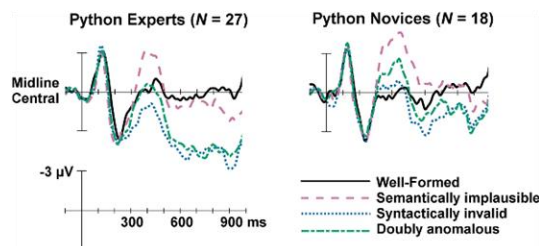


Chu-Hsuan Kuo & Chantel S. Prat ~ Computer programmers show

distinct, expertise-dependent brain responses to violations in form and meaning when reading code

<https://doi.org/10.1038/s41598-024-56090-6>

Credit: Sci Rep 14, 5404 (2024)



Nancy Atkinson ~ Now You Can See Exactly Where Hubble and JWST are Pointed

<https://www.universetoday.com/166046/now-you-can-see-exactly-where-hubble-and-jwst-are-pointed/>

<https://spacetelescopelive.org/>

<https://www.stsci.edu/contents/news/jwst/2024/updated-space-telescope-live-now-shows-jwst-observations>

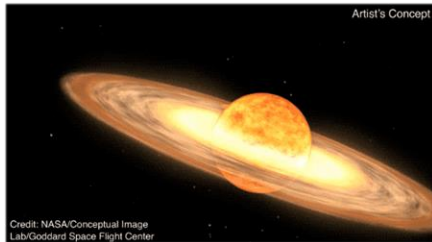
Credit: NASA/STScI



Stephen Luntz ~ A Medieval Manuscript Adds Credibility To Prediction Of A Nova Next Year

<https://www.iflscience.com/a-medieval-manuscript-adds-credibility-to-prediction-of-a-nova-next-year-70802>

<https://arxiv.org/abs/2308.13668>



Mia Taylor ~ Move over, solar eclipse: Scientists predict a once-in-a-lifetime nova explosion in the coming months

<https://www.bbc.com/future/article/20240322-visible-nova-explosion-is-coming>

https://blogs.nasa.gov/Watch_the_Skies/2024/02/27/view-nova-explosion-new-star-in-northern-crown/

Credit: NASA's Goddard Space Flight Center

Andrea Gianopoulos ~ NASA's Webb, Hubble Telescopes Affirm Universe's Expansion Rate, Puzzle Persists

<https://science.nasa.gov/missions/webb/nasas-webb-hubble-telescopes-affirm-universes-expansion-rate-puzzle-persists/>

<https://dx.doi.org/10.3847/2041-8213/ad1ddd>

Credit: NASA, ESA, CSA, STScI, Adam G. Riess (JHU, STScI)

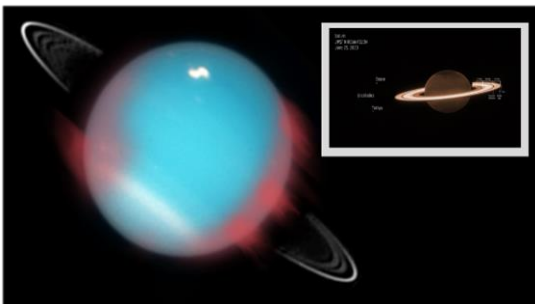


Robert Lea ~ Stunning light shows on Uranus and Saturn may soon draw James Webb Space Telescope's eye

<https://www.space.com/uranus-saturn-auroras-james-webb-space-telescope>

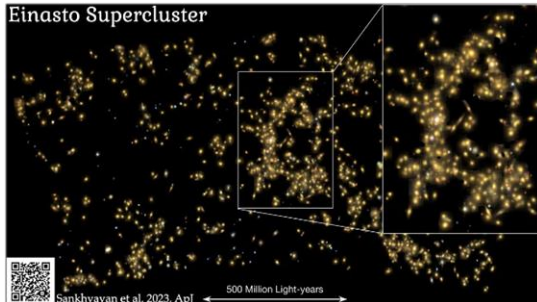
<https://doi.org/10.1038/s41550-023-02096-5>

Credit: NASA, ESA, CSA, STScI, M. Tiscareno (SETI Institute), M. Hedman (University of Idaho), M. El Moutamid (Cornell University), M. Showalter (SETI Institute), L. Fletcher (University of Leicester), H. Hammel (AURA); image processing by J. DePasquale (STScI)



Alex Baumhardt ~ Oregon State University scientists discover metal capable of removing carbon dioxide from air
<https://oregoncapitalchronicle.com/briefs/oregon-state-university-scientists-discover-metal-capable-of-removing-carbon-dioxide-from-air/>
<https://doi.org/10.1039/D3SC05381D>

Credit: U.S. Department of Energy



Mark Thompson ~ Astronomers Find the Most Massive Supercluster to Date

<https://www.universetoday.com/166228/astronomers-find-the-most-massive-supercluster-to-date/>

<https://arxiv.org/abs/2309.06251>

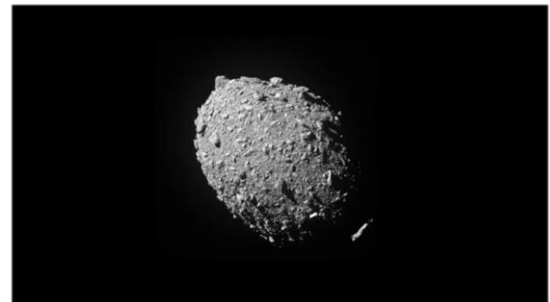
Credit: Einasto superparv (author: Shishir Sankhyayan)

Ian J. O'Neill, Karen Fox, Charles Blue ~ NASA study: Asteroid's orbit, shape changed after DART impact

<https://phys.org/news/2024-03-nasa-asteroid-orbit-dart-impact.html>

<https://dx.doi.org/10.3847/PSJ/ad26e7>

Credit: NASA/Johns Hopkins APL



Karmela Padavic-Callaghan ~ We've glimpsed something that behaves like a particle of gravity

<https://www.newscientist.com/article/2424426-weve-glimpsed-something-that-behaves-like-a-particle-of-gravity/>

<https://doi.org/10.1038/s41586-024-07201-w>

Credit: zf L/Getty Images

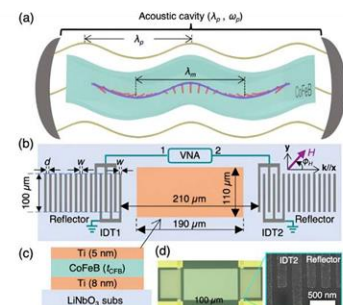
RIKEN ~ 'Shear sound waves' provide the magic for linking ultrasound and magnetic waves

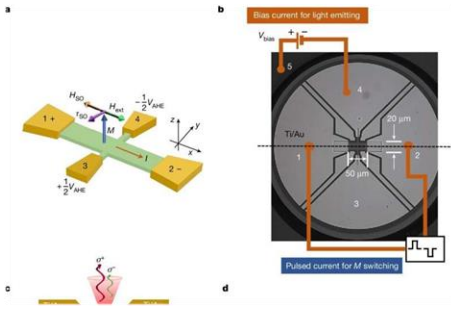
<https://phys.org/news/2024-03-magic-linking-ultrasound-magnetic.html>

<https://doi.org/10.1103/PhysRevLett.132.056704>

<https://dx.doi.org/10.48550/arxiv.2309.12690> (pre-print, open access)

Credit: Phys. Rev. Lett. 132, 056704





Tom Dinki and Christophe Cartier dit Moulin ~ From Earth to Mars: Transporting spin information at the speed of light
<https://phys.org/news/2024-03-earth-mars.html>
<https://dx.doi.org/10.1038/s41586-024-07125-5>
 Credit: Nature 627, 783–788 (2024)

Scott Alan Johnston ~ Astronomers Catch a Supernova Explode Almost in Realtime
<https://www.universetoday.com/166380/astronomers-catch-a-supernova-explode-almost-in-realtime/>
<https://doi.org/10.1038/s41586-024-07116-6>
 Credit: E. Zimmerman et al., Weizmann Institute of Science/Liverpool Telescope



Ryan Whitwam ~ James Webb Space Telescope Snaps Its First Image of a Protoplanetary Disk
<https://www.extremetech.com/science/james-webb-space-telescope-snaps-its-first-image-of-a-protoplanetary-disk>
<https://dx.doi.org/10.3847/1538-3881/ad2de9>
 Credit: NASA/JPL-Caltech



Andy Tomaswick ~ Astronomers only knew of a single binary Cepheid system—they just found nine more
<https://phys.org/news/2024-03-astronomers-knew-binary-cepheid.html>
<https://doi.org/10.48550/arXiv.2403.12390>
 Credit: NASA, ESA, and the Hubble Heritage Team



Jonathon Ramsey ~ Oak Ridge National Laboratory demonstrates 100-kW wireless charging from a parking space
<https://www.autoblog.com/2024/03/29/oak-ridge-national-laboratory-demonstrates-100-kw-wireless-charging-from-a-parking-space/>
<https://www.osti.gov/biblio/1871097>
<https://doi.org/10.1049/pel2.12624>
 Credit: ORNL



Mark Tyson ~ New open source GPU is free to all — FuryGPU runs Quake at 60fps, supports modern Windows software

<https://www.tomshardware.com/pc-components/gpus/new-open-source-gpu-is-free-to-all-supports-modern-windows-software-stack-runs-on-an-fpga-with-custom-pcb>

<https://www.furygpu.com/>

<https://news.ycombinator.com/item?id=39836745>

Rebecca Sohn ~ What are the true colors of images from the James Webb Space Telescope?



<https://www.space.com/what-are-true-colors-image-james-webb-space-telescope-jwst>

Credit: NASA, ESA, CSA, STScI; Joseph DePasquale (STScI), Anton M. Koekemoer (STScI), Alyssa Pagan (STScI)

Let us take a walk on the Wild Side

Piotr Ogonowski ~ A method to straighten curved space-time

<https://phys.org/news/2024-01-method-straighten-space.html>

<https://dx.doi.org/10.3389/fphy.2023.1264925>

Credit: AI-generated image [disclaimer](#)



Eric Ralls ~ Scientist: Dark matter does not exist and the universe is 27 billion years old

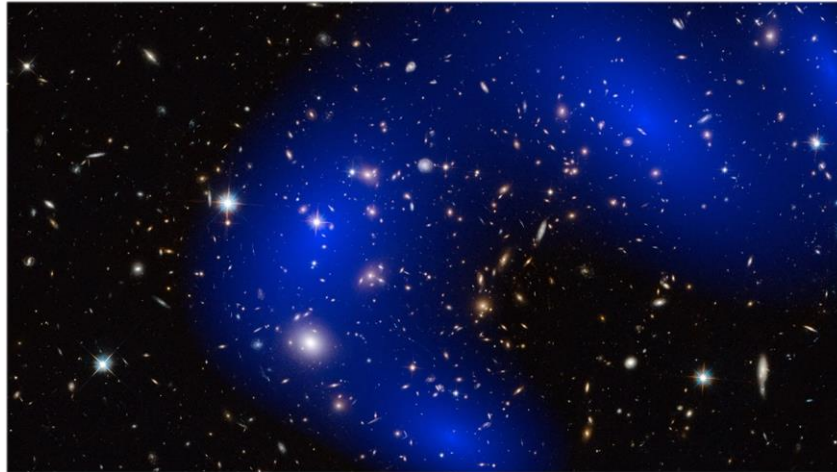


<https://www.earth.com/news/dark-matter-does-not-exist-universe-27-billion-years-old-study/>

Rajendra P. Gupta, "Testing CCC+TL Cosmology with Observed Baryon Acoustic Oscillation Features", 2024 ApJ 964 55, available=<https://dx.doi.org/10.3847/1538-4357/ad1bc6>

Credit: Earth.com

Ethan Siegel ~ Ask Ethan: Has a new study disproven dark matter and dark energy?
<https://bigthink.com/starts-with-a-bang/new-study-disprove-dark-matter-dark-energy/>



Credit: NASA, ESA, D. Harvey (École Polytechnique Fédérale de Lausanne, Switzerland), R. Massey (Durham University, UK), Harald Ebeling (University of Hawaii at Manoa) & Jean-Paul Kneib (LAM)

Technical Knowledge and Education: (March-April 2024)

Richard P. Feynman ~ Cargo Cult Science
<https://calteches.library.caltech.edu/51/2/CargoCult.pdf>

It is not a book, rather an article, but it deserves to be read...



Tobias Mann ~ How to run an LLM on your PC, not in the cloud, in less than 10 minutes

https://www.theregister.com/2024/03/17/ai_pc_local_llm/
<https://github.com/ollama/ollama>

SARA ~ ezRA – Easy Radio Astronomy Analysis Tutorials:

- ⚙ Simple Overview: <https://youtu.be/sqid9zn9KkY>
- ⚙ Analysis 1- Introduction and Data Collectors: https://youtu.be/ig_iPTuS8ZA
- ⚙ Analysis 2- Spreadsheet Analysis: <https://youtu.be/HkriN9d6Hd8>
- ⚙ Analysis 3- Signal Progression: <https://youtu.be/Vlp7L6glZPY>
- ⚙ Analysis 4- More Plots and ezB file: <https://youtu.be/K02MADafOhc>
- ⚙ Analysis 5- Interference Filters: <https://youtu.be/FeFk9EvITtc>
- ⚙ Analysis 6- ezSky: <https://youtu.be/UNwS0f9X7kE>

- ⚙ Analysis 7- AntXTVT and VLSR : <https://youtu.be/0ezig90GNBc>
- ⚙ Analysis 8- ezGal: <https://youtu.be/i0St2X7ODKM>

SARA ~ Radio Astronomy Video Series: Constants, Variables and Formulas, Radio Astronomy Formulas:

- ⚙ Introduction to Radio Astronomy: <https://youtu.be/AOqvjRXnins>
- ⚙ Lesson 1- Parabolic Dish Gain: https://www.youtube.com/watch?v=2bx5K9jUc_w
- ⚙ Lesson 2 -Parabolic Dish Half Power Beamwidth: <https://www.youtube.com/watch?v=XWOMRrwwjk18>
- ⚙ Lesson 3 -Thermal Noise: <https://youtu.be/MMJ6Xvapt10>
- ⚙ Lesson 4 -Focal Length and f/D : <https://youtu.be/Am6t06KqFPE>
- ⚙ Lesson 5 -Feed Illumination Angle: <https://youtu.be/4RZzPzVBSJ4>
- ⚙ Lesson 6 -Pointing Offset Gain Loss: <https://youtu.be/dQ8wAaTtm40>
- ⚙ Lesson 7 -Measuring System Temperature (T_{Sys}): <https://youtu.be/4gVUFFxra-U>
- ⚙ Lesson 8 -Coax Attenuation Interpolation: <https://youtu.be/3B8hV6vFyo8>
- ⚙ Lesson 9 -Pulsar math including electron density, distance, and age: https://youtu.be/Bymdp--_3JU
- ⚙ Lesson 10 -Distance Math - AU, Parallax, Parsecs and Light Years: <https://youtu.be/6fo0y3fDOZs>
- ⚙ Lesson 11 -Doppler Frequency and Relative Velocity Calculations: <https://youtu.be/8zKloAVpnJc>
- ⚙ Lesson 12 -Pointing to the Milky Way using a Compass and Protractor: <https://youtu.be/33xeUSji94U>
- ⚙ Lesson 13 -Radiometer Equation Basics: <https://youtu.be/vAyypJ8f2z8>
- ⚙ Lesson 14 -Noise Figure and Noise Factor Calculations: <https://youtu.be/GD6wZhW5NPA>
- ⚙ Lesson 15 -Interpreting Stokes Parameters: <https://youtu.be/wUVsbfURIsq>
- ⚙ Lesson 16 -Velocity Factor, Speed of Light in a Coax Cable: <https://youtu.be/WWuqRyb4Ad8>
- ⚙ Lesson 17 -Interferometry Fringe Spacing: <https://youtu.be/rYhUKFn7IWq>

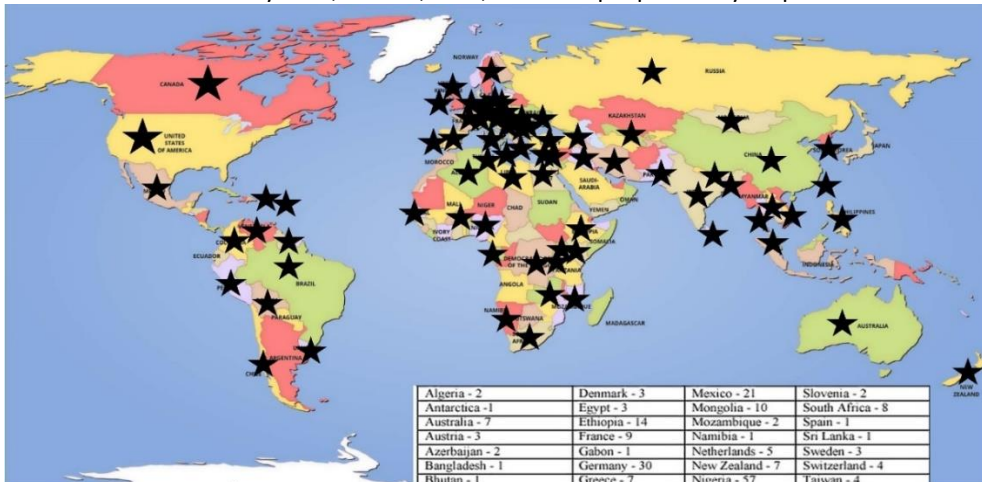
SuperSID



SuperSID
*Collaboration of Society
of Amateur Radio
Astronomers and
Stanford Solar Center*



- Stanford provides data hosting, database programming, and maintains the SuperSID website
- Society of Amateur Radio Astronomers (SARA) sells the SuperSID monitors for 48 USD to amateur radio astronomers and the funds are then used to support free distribution to students all over the world (image below as of Fall 2017)
- Jonathan Pettingale at SARA is responsible for building and shipping the SuperSID monitor kits: SuperSID@radio-astronomy.org
- SuperSID kits may be ordered through the SARA SuperSID webpage: <http://radio-astronomy.org/node/210>
- Questions about the SuperSID project may be directed to Steve Berl at Stanford: steveberl@gmail.com
- Jaap Akkerhuis at Stanford is responsible for the SuperSID software and SARA has provided financial support for his efforts
- SuperSID website hosted by Stanford: <http://solar-center.stanford.edu/SID/sidmonitor/>
- SuperSID database: <http://sid.stanford.edu/database-browser/>
- The data is searchable by time, station, date, and multiple plots may be placed on the same graph for comparison.



**SID Monitor
Distribution**
1078 instruments
82 countries
7 continents

Algeria - 2	Denmark - 3	Mexico - 21	Slovenia - 2
Antarctica - 1	Egypt - 3	Mongolia - 10	South Africa - 8
Australia - 7	Ethiopia - 14	Mozambique - 2	Spain - 1
Austria - 3	France - 9	Namibia - 1	Sri Lanka - 1
Azerbaijan - 2	Gabon - 1	Netherlands - 5	Sweden - 3
Bangladesh - 1	Germany - 30	New Zealand - 7	Switzerland - 4
Bhutan - 1	Greece - 7	Nigeria - 57	Taiwan - 4
Bolivia - 1	Guyana - 1	Pakistan - 4	Thailand - 5
Bosnia-Herzegovina - 2	Hungary - 1	Peru - 10	Tunisia - 9
Brazil - 11	India - 33	Philippines - 3	Turkey - 2
British Virgin Islands - 1	Indonesia - 2	Poland - 2	Uganda - 5
Bulgaria - 2	Iran - 4	Portugal - 3	UK - 32
Burkina Faso - 1	Iraq - 1	Rep of Congo - 3	Uruguay - 9
Canada - 33	Ireland - 9	Romania - 4	US Virgin Islands - 2
Chile - 1	Italy - 42	Russia - 3	USA - 491
China - 38	Kenya - 23	Rwanda - 1	Uzbekistan - 2
Columbia - 9	Korea (South) - 2	S Africa - 4	Venezuela - 2
Croatia - 7	Lebanon - 11	Senegal - 1	Vietnam - 1
Cyprus - 1	Libya - 1	Serbia - 1	Zambia - 2
Czech Republic - 1	Malaysia - 19	Singapore - 3	
D Rep of Congo - 4	Malta - 1	Slovak Repub - 2	

For official use only
 Monitor assigned: _____
 Site name: _____
 Country: _____

SuperSID Space Weather Monitor Request Form

<i>Your information here</i>				
Name of site/school (if an institution):				
Choose a site name: (3-6 characters) No Spaces				
Primary contact person:				
Email:				
Phone(s):				
Primary Address:	Name School or Business Street Street City State/Province Country Postal Code			
Shipping address, if different:	Name School or Business Street Street City State/Province Country Postal Code			
Shipping phone number:	<table border="1" style="width: 100%; border-collapse: collapse;"> <tr> <td style="width: 33%; height: 20px;"></td> <td style="width: 33%; height: 20px;"></td> <td style="width: 33%; height: 20px;"></td> </tr> </table>			
Latitude & longitude of site:	Latitude: _____ Longitude: _____			

I understand that neither Stanford nor the Society of Amateur Radio Astronomers is responsible for accidents or injuries related to monitor use. I will assure that a surge protector and other lightning protection devices are installed if necessary.

Signature: _____ **Date:** _____

I will need:

<i>What</i>	<i>Cost</i>	<i>How many?</i>
SuperSID distribution USB Power	\$48 (assembled)	
USB Sound card 96 kHz sample rate (or provide this yourself)	\$40 (optional)	
Antenna wire (120 meters) (or you can provide this yourself)	\$23 (optional) with connectors attached and tested	
RG 58 Coax Cable (9 meters) (or provide this yourself)	\$14 (optional) with connectors attached and tested	
Shipping	US \$12 Canada & Mexico \$40 all other \$60	
	TOTAL	\$

_____ I have included a \$_____ check (payable to SARA)

_____ I will make payment thru www.paypal.com to treas@radio-astronomy.org

or

_____ If you are a Minority-serving institution, in a Developing or economically deprived nation, and/or you are using the monitor with students for educational purposes, you may qualify for obtaining a monitor at reduced or no cost. Check here if you wish to apply for this designation. Then tell us how you want to use the SuperSID monitor. Include type of site, number of students involved, whether public or private school, grade levels, etc. and describe your program. The goal of the SuperSID project is to provide as many students with systems as possible. If you are able to pay for a system, even if you qualify for a free one, please do so and help support our goal.

For more details on the Space Weather Monitor project, see: <http://sid.stanford.edu>

To set up a SuperSID monitor you will need:

¹ Access to power and an antenna location that is relatively free of electric interference (could be indoors or out)

² A **PC**** with the following minimal specifications:

- a. A sound card that can record (sample) up to 96 kHz, or a USB port to connect such a sound card (for North and South America)
 - i. All other countries can use AC97 sound card with 48 kHz record (sample) rate. Most computers made after 1997 will have AC97.
- b. Windows 2000 or more recent operating system
- c. 1 GHz Processor with 128 mb RAM
- d. Ethernet connection & internet browser (desirable, but not required)
- e. Standard keyboard, mouse, monitor, etc.

³ An inexpensive antenna that you build yourself. You'll need about 120 meters (400 feet) of **insulated** wire. Solid wire is easier to wind than stranded. Magnet wire will work but be more fragile. You can use anything from #18 to #26 size wire. The antenna frame can be made of wood, PVC pipe, or similar materials. We'll provide instructions. You can purchase the wire from us or obtain your own.

⁴ RG58 coax cable with a BNC connector at one end to run from the antenna to the SuperSID receiver. 9 meters is recommended, but the length will depend on where you place the antenna. You can purchase the coax from us or obtain your own.

⁵ Surge protector and other protection against a lightning strike

Return this form to: SuperSID@radio-astronomy.org

or mail to:

SARA Treasurer
c/o Thomas Jacobs
P. O. Box 4245
Wilmington, NC 28406.

Announcing Radio JOVE 2.0

The Radio JOVE Team



Radio JOVE students and amateur scientists from around the world observe and analyze natural radio emissions of Jupiter, the Sun, and our galaxy using their own easy to construct radio telescopes.

Our Project announces Radio JOVE 2.0, where participants assemble a 16-24 MHz radio spectrograph to observe solar, Jupiter, Galactic, and Earth-based natural radio emissions and share their observations with fellow participants.

In the Beginning

Radio JOVE started as a NASA sponsored educational outreach project in 1999. We developed a radio telescope kit suitable for receiving signals from Jupiter, the Sun, the Galaxy, and Earth-based radio emissions. The original kit comprised a radio receiver (RJ1.1) and a dual dipole antenna for 20.1 MHz. An important goal was to teach electronic principles including how to build, solder, and assemble the radio receiver and antenna.

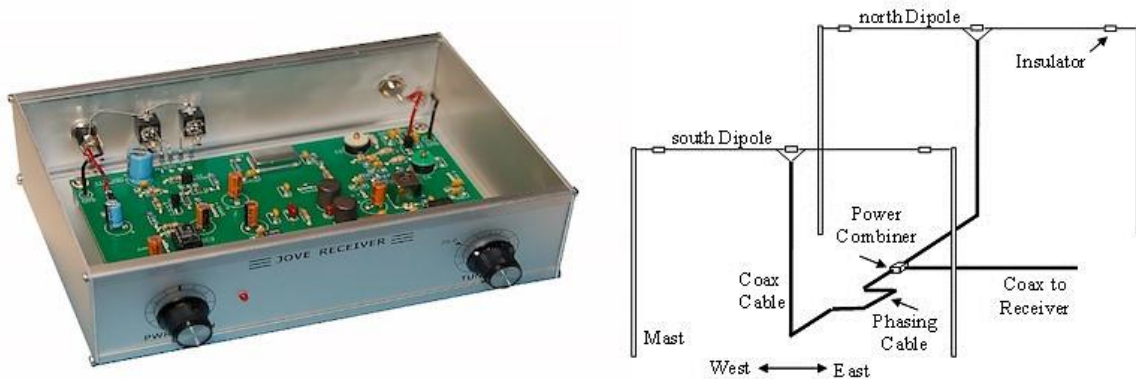


Figure 1. A Radio JOVE RJ1.1 receiver and a schematic of the dual-dipole antenna.

In addition to the hardware, three software packages were developed. These were Radio Jupiter Pro (Jupiter emission prediction program), Radio-SkyPipe (strip chart program) and Radio Sky Spectrograph (control and display of radio spectrograph data).

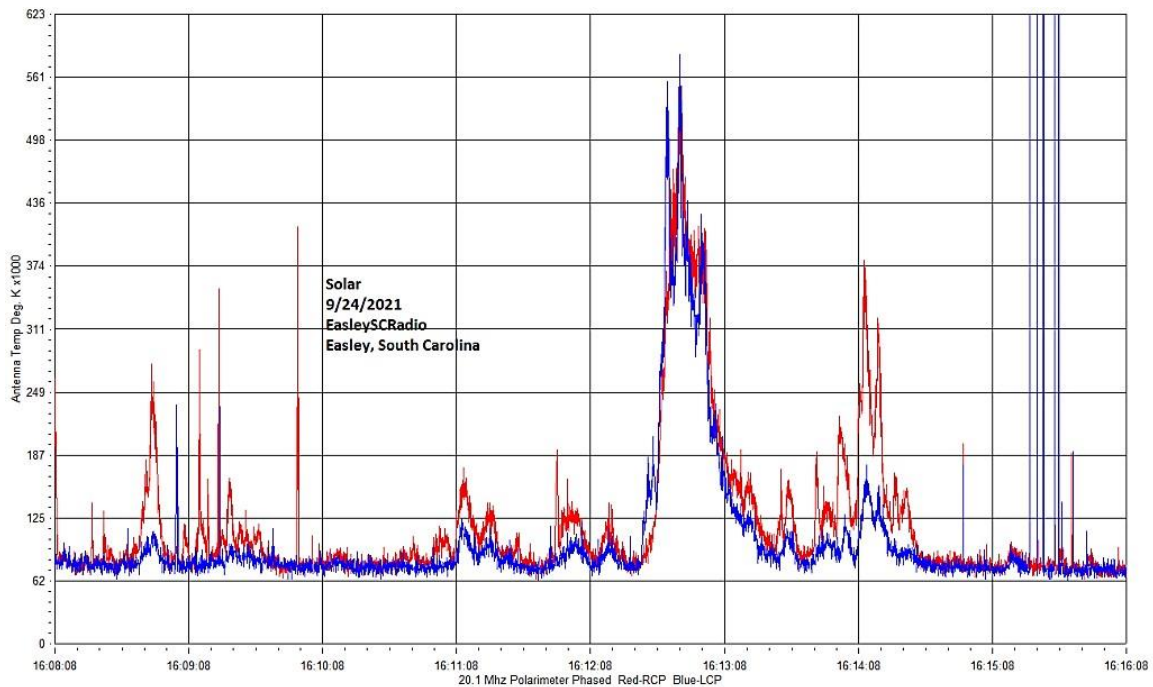


Figure 2. A SkyPipe strip chart showing multiple solar bursts using a JOVE receiver. John Cox, SC.

The Growth of Radio JOVE

As of Autumn 2021, over 2,500 kits have been sold at cost to schools and individuals around the world. Thousands of data submissions from observers have been made to the Radio JOVE data archive.

The Radio JOVE web site has always provided a wealth of information describing observation methods and various educational materials intended to teach radio astronomy techniques and scientific methods. Biannual newsletters are produced, and several telephone help sessions are held each year.

A sub-group of experienced observers known as the Spectrograph Users Group (SUG) evolved from the core JOVE group. These observers developed data collection and analysis techniques using more advanced equipment and techniques. SUG members have contributed to articles published in peer-reviewed scientific journals. This group remains active under the Radio JOVE listserv at <https://groups.io/g/radio-jove/>.

Moving Forward with New Technology

In the past, Radio JOVE provided the hands-on experience of building a radio kit. We have many RJ1.1 receivers in operation successfully contributing scientifically valuable data. It has, however, become increasingly difficult to obtain parts for the RJ1.1 receiver kits and we therefore decided to replace the RJ1.1 receiver with a new SDR-based design for the receiver portion of our radio telescope kits. While we continue to support the hardware and software for the original RJ1.1 receivers, the only kits now available for purchase from Radio JOVE contain this newly designed system.

In recent years, new technologies have made software defined radios (SDRs) ever more affordable. These radios can operate on a single frequency like the original JOVE receiver but can also generate spectrograms which depict radio activity as a function of both time and frequency. Such displays offer new insights into our studies of the Sun, Jupiter, the Galaxy, and both natural and artificial Earth-based radio emissions.

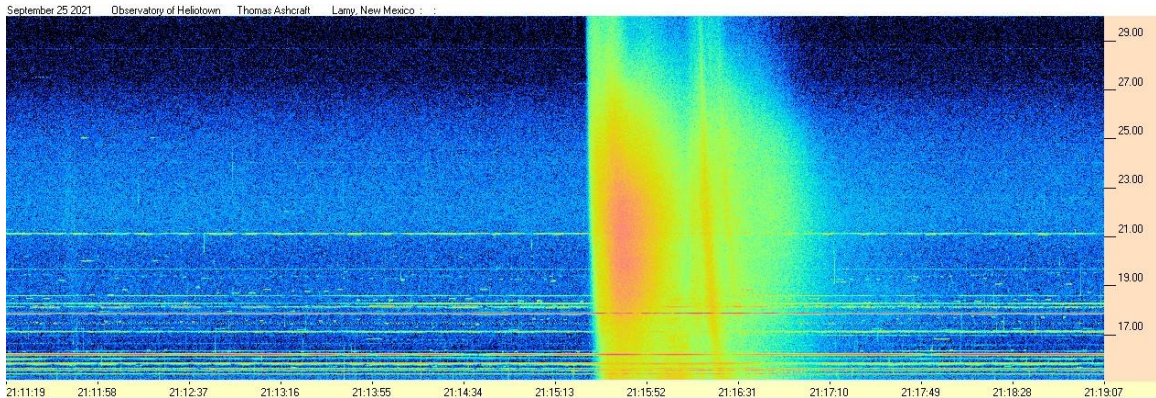


Figure 3. Radio spectrogram showing multiple solar bursts received by Tom Ashcraft in New Mexico. Horizontal scale is time, and the vertical scale is frequency. Amplitude is displayed using different colors corresponding to the strength of signals.

Radio JOVE continues to sell radio telescope packages including an antenna, receiver, and software; however, the receiver is now a commercially built SDR.



Figure 4. The JOVE team has had considerable success with the SDRPlay RSP1A unit and will provide support for using this instrument for our radio astronomy program. Not all SDR types can be supported, but it is our intent to provide support for some other SDRs as they become available during this period of rapid SDR development.

It continues to be our goal to introduce new observers to the scientific method and help them experience the thrill of receiving cosmic radio signals. Through a series of educational training modules and observing and analysis projects we aim to guide new observers to levels where they can contribute to Citizen Science projects.

We continue to support our large user base that uses JOVE RJ1.1 receivers – both in terms of technical support for the receivers but also with new and exciting observing projects for both RJ1.1 and SDR users.

We welcome both new and experienced observers to the JOVE 2.0 program as we share the excitement of receiving, studying, and understanding radio signals from our corner of the galaxy.

Please see the Radio JOVE web site at <https://radiojove.gsfc.nasa.gov> for more information.



RADIO JOVE 2.0 RADIO TELESCOPE KIT ORDER FORM

Order Online using PayPal™

* * * Please allow 2 to 3 weeks for delivery. * * *

IMPORTANT: Before you order the Jove receiver kit and/or the antenna kit, we suggest that you read the on-line manuals. You will need to provide additional materials and tools to complete the antenna. The cost of additional materials for the antenna support structure (masts, etc.) may be in the range of US\$75 to US\$100. Also note that the optimal antenna height can be up to 20ft, depending upon your latitude.

<p>Item # RJK2u – Complete 2.0 Kit: Receiver + Unbuilt Antenna Kit + Software</p> <p>This kit includes an SDRplay RSP1A, USB Cable, SMA/BNC cable, F-adapter, unbuilt Antenna Kit (RJA), printed assembly manuals, and Radio-Sky Spectrograph (RSS) software.</p> <p>Note: Kit does not include antenna support structure.</p> <p>Price: \$215 + Shipping (See reverse for shipping)</p>	<p>Item # RJK2p – Complete 2.0 Kit: Receiver + Professionally Built Antenna Kit + Software</p> <p>This kit includes an SDRplay RSP1A, USB Cable, SMA/BNC cable, F-adapter, Professionally Built Antenna Kit (RJA2), printed assembly manuals, and Radio-Sky Spectrograph (RSS) software.</p> <p>Note: Kit does not include antenna support structure.</p> <p>Price: \$384 + Shipping (See reverse for shipping)</p>
<p>Item # RJA – Unbuilt Antenna Kit</p> <p>The RJA Radio JOVE Antenna Kit includes a printed construction manual, stranded copper easy-to-solder antenna wire, ceramic insulators, RG-59 easy-to-solder coax cable, screw-on F connectors, and a power combiner.</p> <p>Note: Kit does not include antenna support structure. Assembly requires a soldering gun and other tools.</p> <p>Price: \$90 + Shipping (See reverse for shipping)</p>	<p>Item # RJA2 – Professionally Built Antenna Kit</p> <p>The RJA2 Radio JOVE Antenna Kit includes a printed installation manual, two professionally assembled dipole antennas constructed of #14 Copperweld wire with Budwig center insulators and center support rope attachment points, high quality RG-6 coax with pre-installed commercial grade connectors, and a power combiner.</p> <p>Note: Kit does not include antenna support structure.</p> <p>Price: \$249 + Shipping (See reverse for shipping)</p>
<p>Item # LTJ2 – Listening to Jupiter, 2nd Ed. by R. S. Flagg</p> <p>PDF download of Richard Flagg's book "Listening to Jupiter, 2nd Ed., 2005". The file is downloaded from a secure website.</p> <p>Price: \$10 + \$0 shipping (PDF file download)</p>	<p>Item # RJR2 – Radio JOVE 2.0 Receiver-Only Kit</p> <p>This kit includes one SDRplay RSP1A SDR receiver, USB Cable, SMA/BNC cable, and F-adapter, printed assembly manuals, and Radio-Sky Spectrograph (RSS) software.</p> <p>Price: \$135 + Shipping (See reverse for shipping)</p>

RADIO JOVE 2.0 RADIO TELESCOPE KIT ORDER FORM (continued)

Order Online at https://radiojove.net/kit/order_form.html OR
 Complete this form and mail with payment

Payment may be made by Credit Card via PayPal™, U.S. Check, U.S. Money Order, International Money Order in U.S. funds drawn on a U.S. bank, or Western Union Money Transfer made payable to **The Radio JOVE Project**. No bank-to-bank wire transfers are accepted. Purchase Orders are accepted from U.S. Institutions.

Send to: The Radio JOVE Project
 1301 East Main St
 MTSU Box 412
 Murfreesboro, TN 37132, USA
 email: chiggins@mtsu.edu
 FEIN: 20-5239863

Item	Description	Quantity	Item Price	Shipping (see below)	Subtotal
RJK2u	Complete Radio JOVE 2.0 Kit Receiver + unbuilt Antenna		\$215		
RJK2p	Complete Radio JOVE 2.0 Kit Receiver + Professionally Built Antenna		\$384		
RJA2	Professionally Built Antenna-Only Kit		\$249		
RJA	Unbuilt Antenna-Only Kit		\$90		
RJR2	Receiver-Only Kit		\$135		
LTJ2	Listening to Jupiter, 2 nd Ed., by R.S. Flagg (PDF download)		\$10	\$0	
Total:					

Shipping Fees for Radio JOVE: We ship all packages using USPS Priority Mail flat rate boxes.
 U.S.A.: \$17.00
 Canada: \$57.00
 All Other International Shipping: \$85.00

Ship to: (Please print clearly)

Name: _____
 Address: _____
 City, State, Postal Code: _____
 Province, Country: _____
 Email: _____

Visit the Radio JOVE web site and fill out the team application form at https://radiojove.net/sign_up_form.php even if you are just an interested individual so that you can receive important information about kit updates, online services, and activities within the project as they occur!



Please send questions, reports, and observations to John Cook: jacook@jacook.plus.com

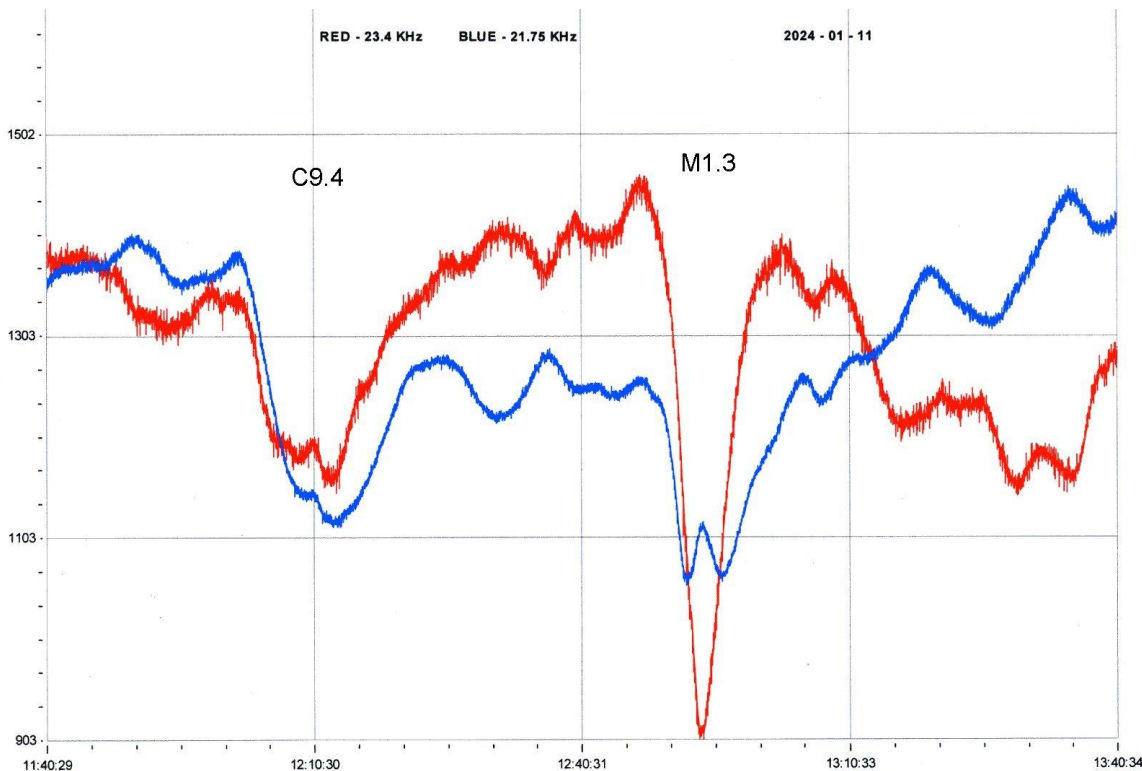
BAA Radio Astronomy Section, Director: Paul Hearn

RADIO SKY NEWS

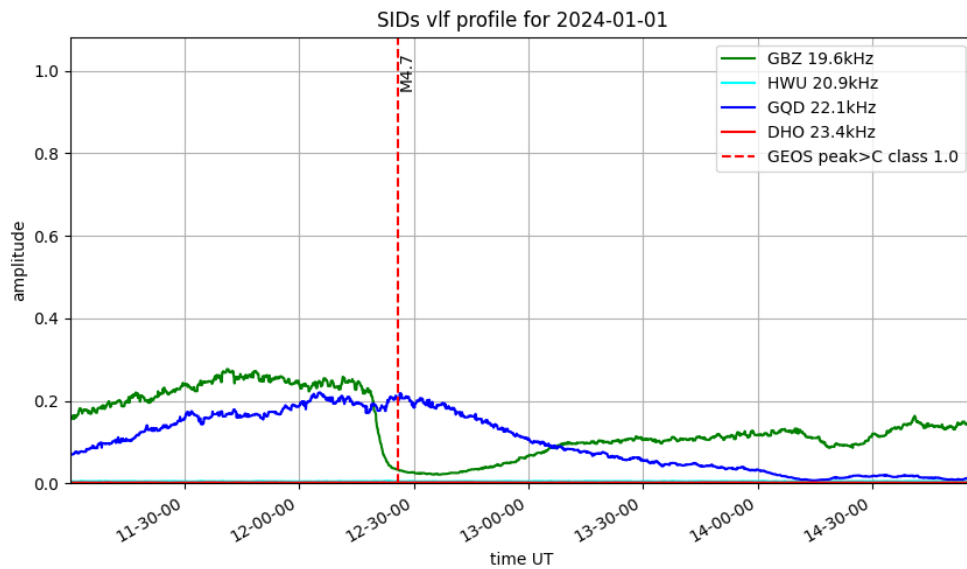
2024 JANUARY

VLF SID OBSERVATIONS

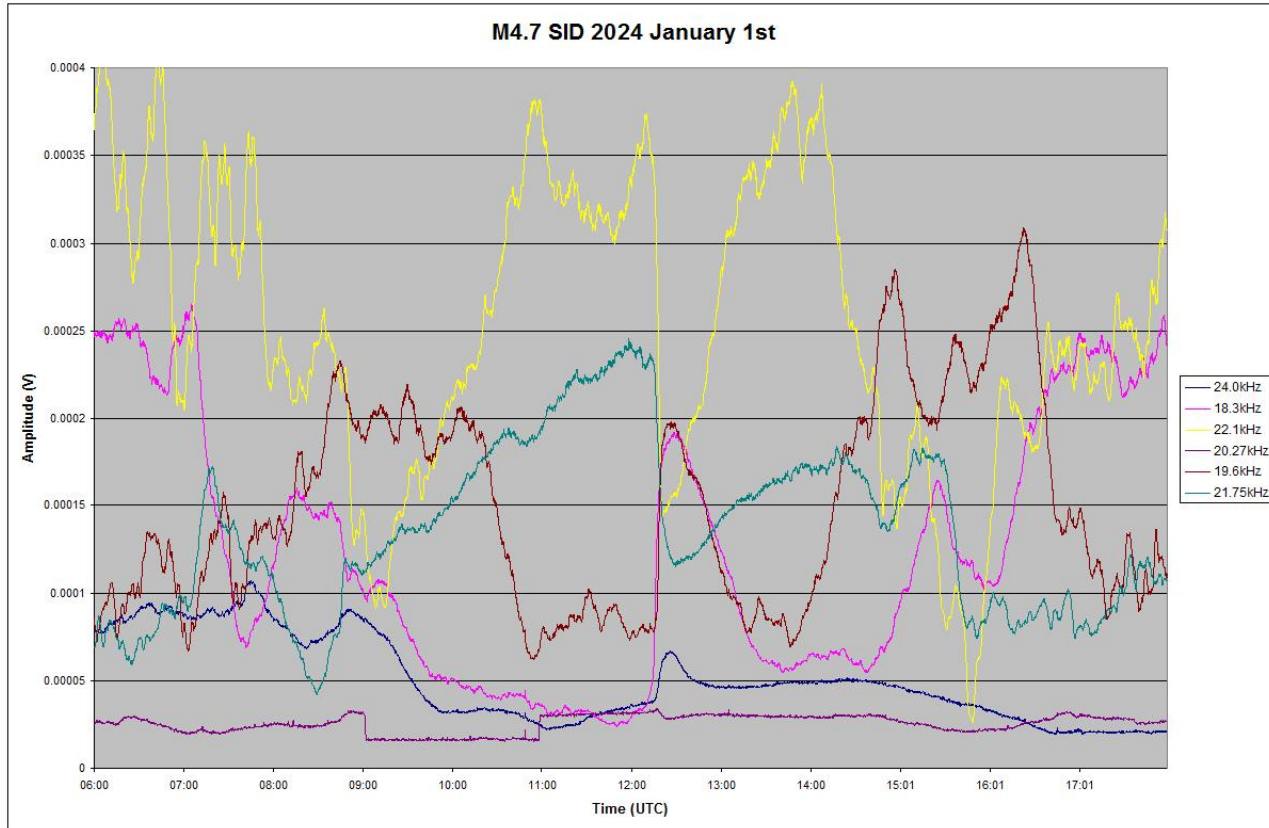
Solar flare activity has been at similar levels to the last few months, although the flare magnitudes have been much higher. Many of the weaker flares have not produced SIDs due to the low altitude of the sun and ionosphere instability. We did record a C2.8 flare on the 28th, although it has been a puzzle to analyse. The SWPC bulletin gives a start time of 11:49, maximum at 11:57, ending at 12:54UT. Our SID recordings are fairly consistent with a start around 12:40 and a peak between 12:44 and 12:50UT. These are over several frequencies, and so do seem to be genuine SID timings.



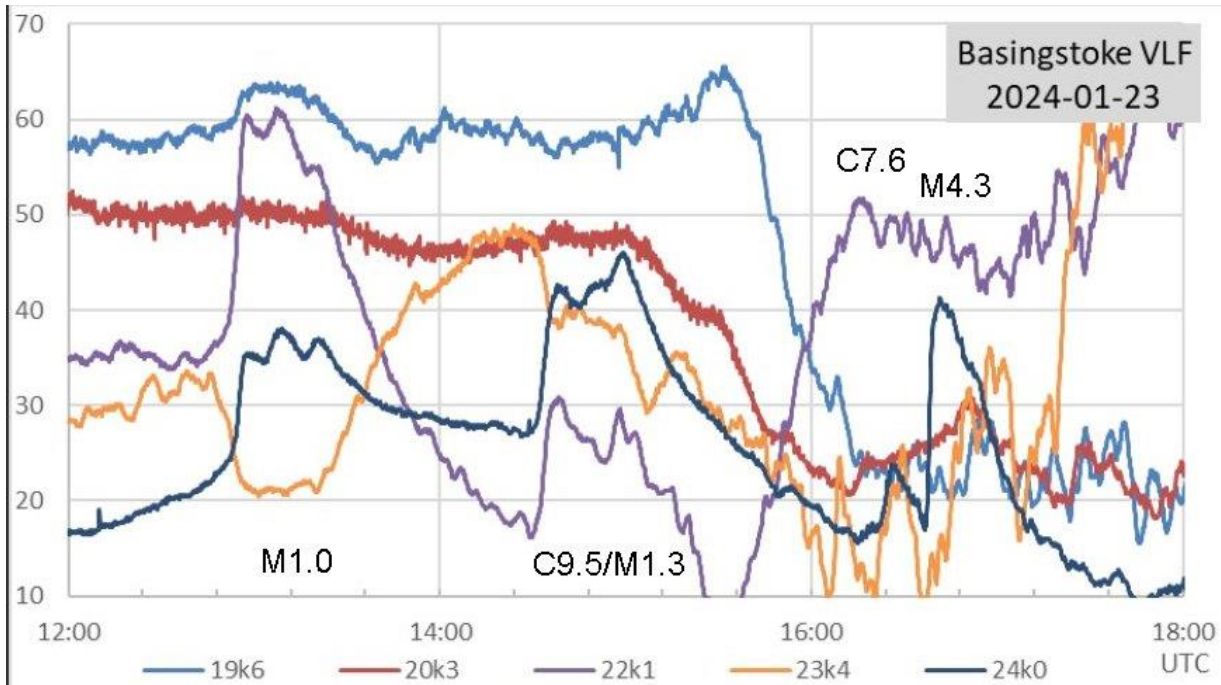
This recording by Colin Clements shows two of the stronger flares on the 11th. The M1.3 flare has produced a clean negative going SID at 23.4kHz, with a spike and wave type SID at 21.75kHz. The slightly smaller C9.4 flare appears to have produced spike and waves on both signals, although this could be from two peaks in the flare. Paul Hyde's recording showed a similar response. Most spike and wave SIDs have a much 'sharper' spike compared to the more symmetrical shape seen here. The background shows some gentle instability, expected at this time of year.



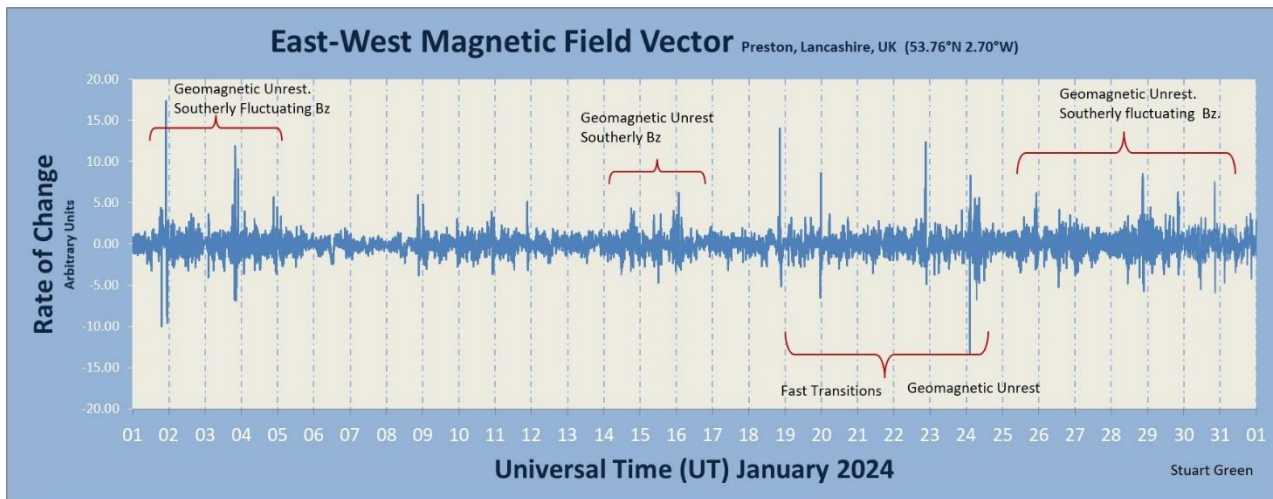
The M4.7 flare on the 1st was the strongest that we recorded in January. This recording by Mark Prescott shows a slow recovery after the peak on both signals. The start of the SID at 19.6kHz is very obvious, but barely visible at 22.1kHz. The recording by Mark Edwards shows a similar slow recovery at 21.75kHz (green trace), although other signals are much faster.



January 23rd was the most active day, with nine individual peaks identified. Many of these have merged to give multiple-peaked SIDs. The recording by Paul Hyde on the next page shows the details. I have attempted to label them based on the SWPC X-ray satellite data. 24kHz (dark blue) shows the two later SIDs, while the European signals have gone into sunset.

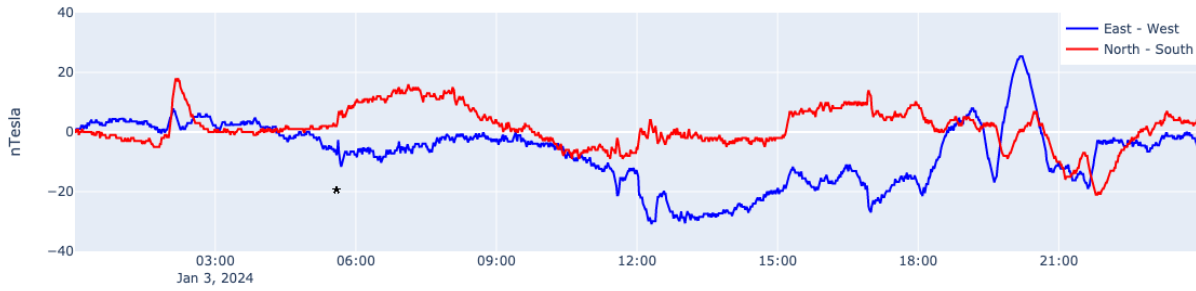


MAGNETIC OBSERVATIONS

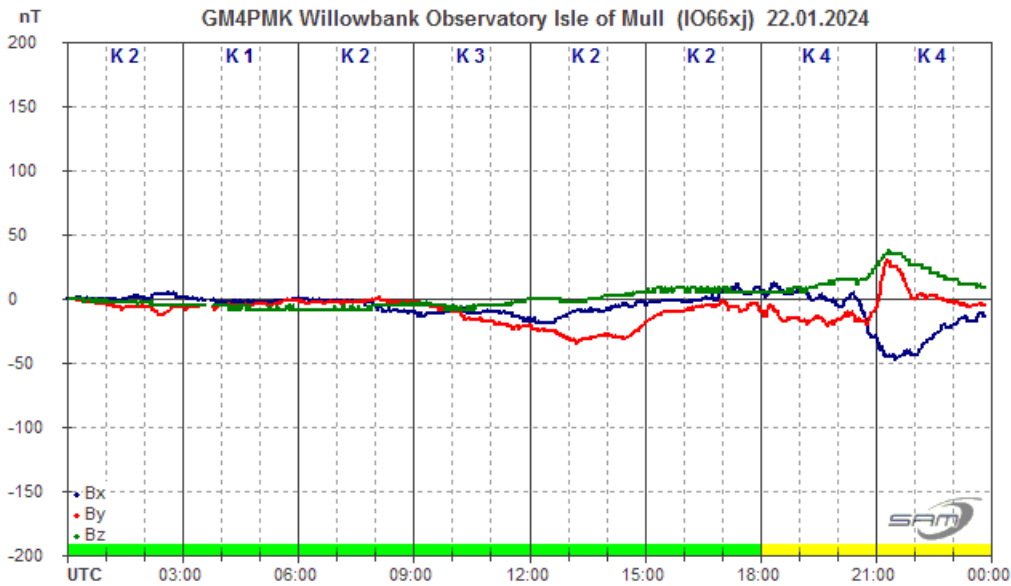


Stuart Green’s monthly summary of magnetic activity shows a fairly quiet period, with some mild disturbance from solar wind. The STCE bulletin does mention that a pair of CMEs from the end of December were recorded on January 3rd, with impacts at 04:50 and 14:25UT.

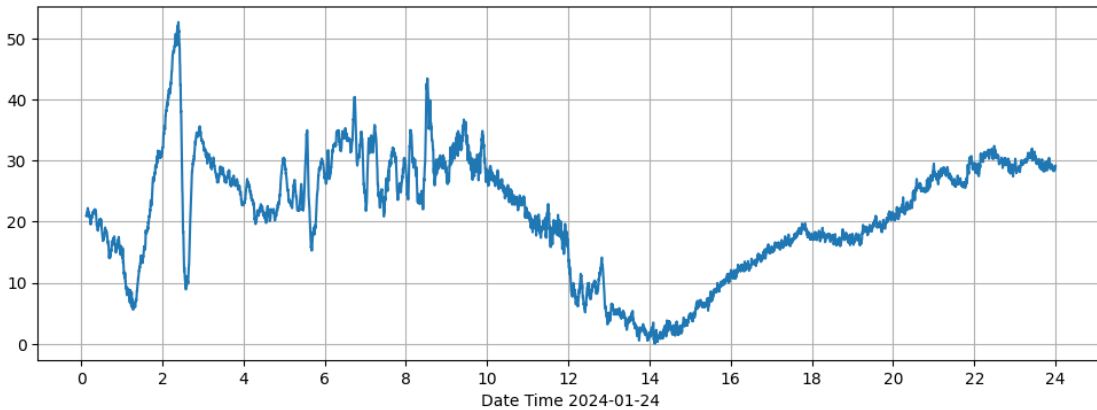
Steyning Magnetometer (50.8 North, 0.3 West)



The first impact is marked ‘*’ on this recording by Nick Quinn, rather later than reported, the second being much less clear. Recordings by Callum Potter also show the earlier impact but not the later one.



Wasbister Magnetometer (59.17N,3.06W)



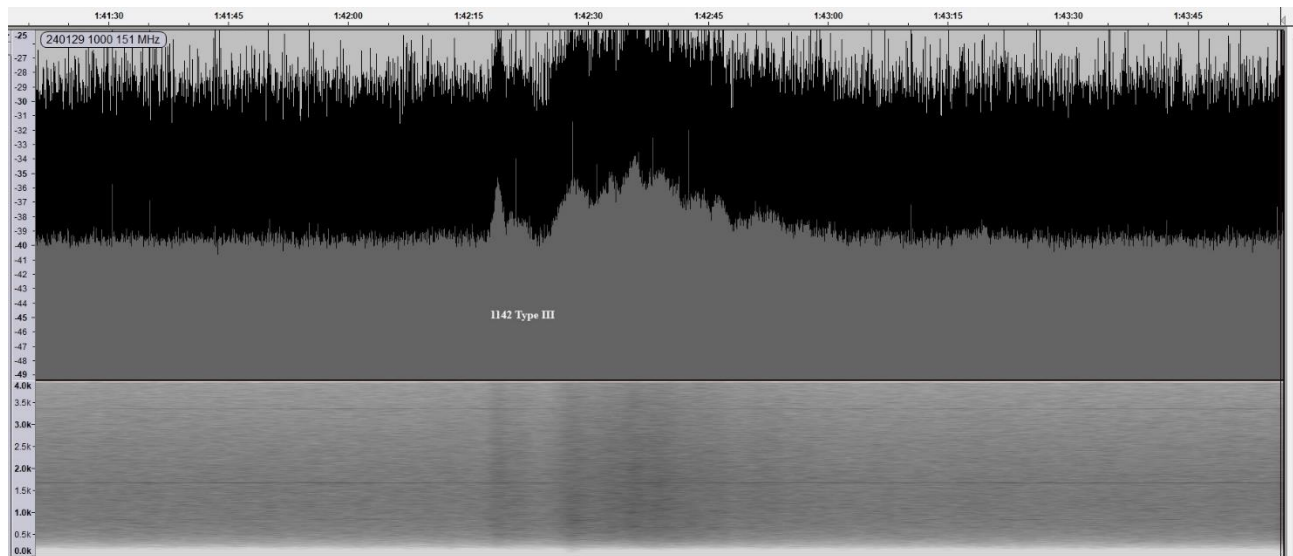
There was a very mild disturbance through the last week of January, starting in the evening of the 22nd. Roger Blackwell's recording (top) shows less than ± 50 nT, fading out after midnight. The lower chart from Callum Potter shows the disturbance continuing in the morning of the 24th, again very mild.



I have included my own recording from January 21st to show just how bad local magnetic interference can be. The grey line is the average though the day, the sensor recording $+40 / -130$ nT, greater than the genuine activity recorded through the month. I have no idea what caused the problem, and just assume that it was from large vehicles in the road outside.

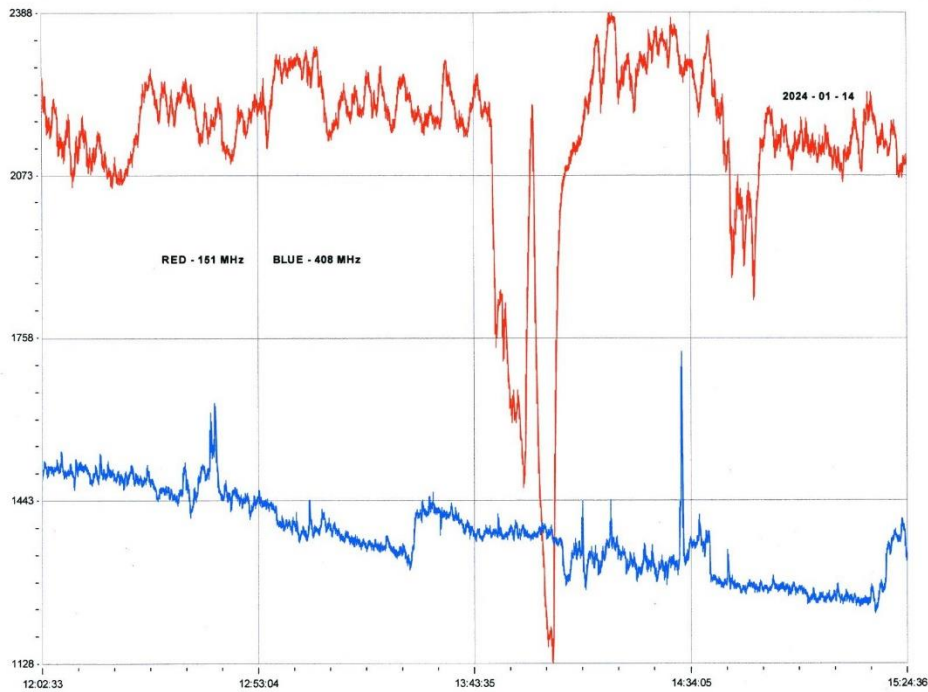
Magnetic observations received from Roger Blackwell, Stuart Green, Callum Potter, Nick Quinn, and John Cook.

SOLAR EMISSIONS



Colin Briden made this recording of a type III emission at 151MHz on the 29th. Timed at 11:42UT it lasted just under a minute with a peak amplitude 6dB above the noise floor. This matches the timing of a C2.8 flare listed in the SWPC bulletin, but not recorded as a SID. The

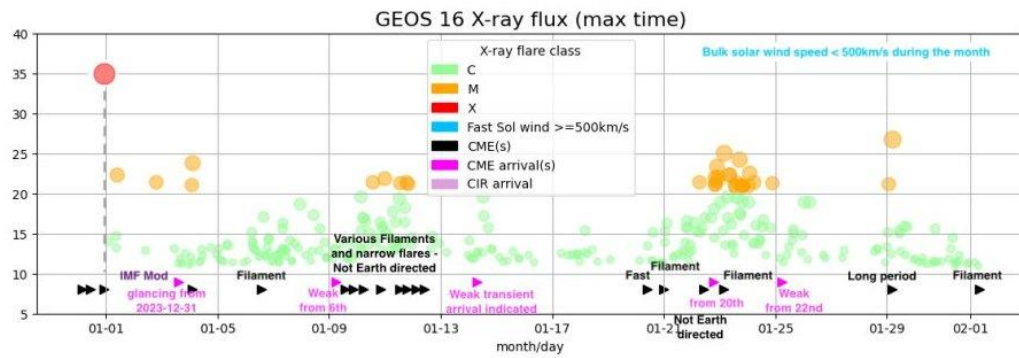
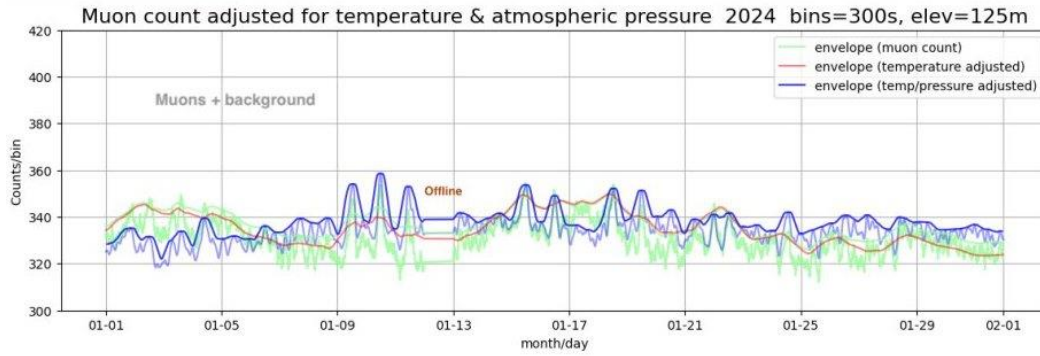
very low winter altitude of the sun is probably responsible for the weak signal. Colin Clements recorded some unusual 151MHz behaviour on the 14th:



The sharp dip in 151MHz (red) occurs shortly after the C7.2 flare, with a rise at 408MHz over the same period. There may well also be some effects from the low sun causing the deep 151MHz dip.

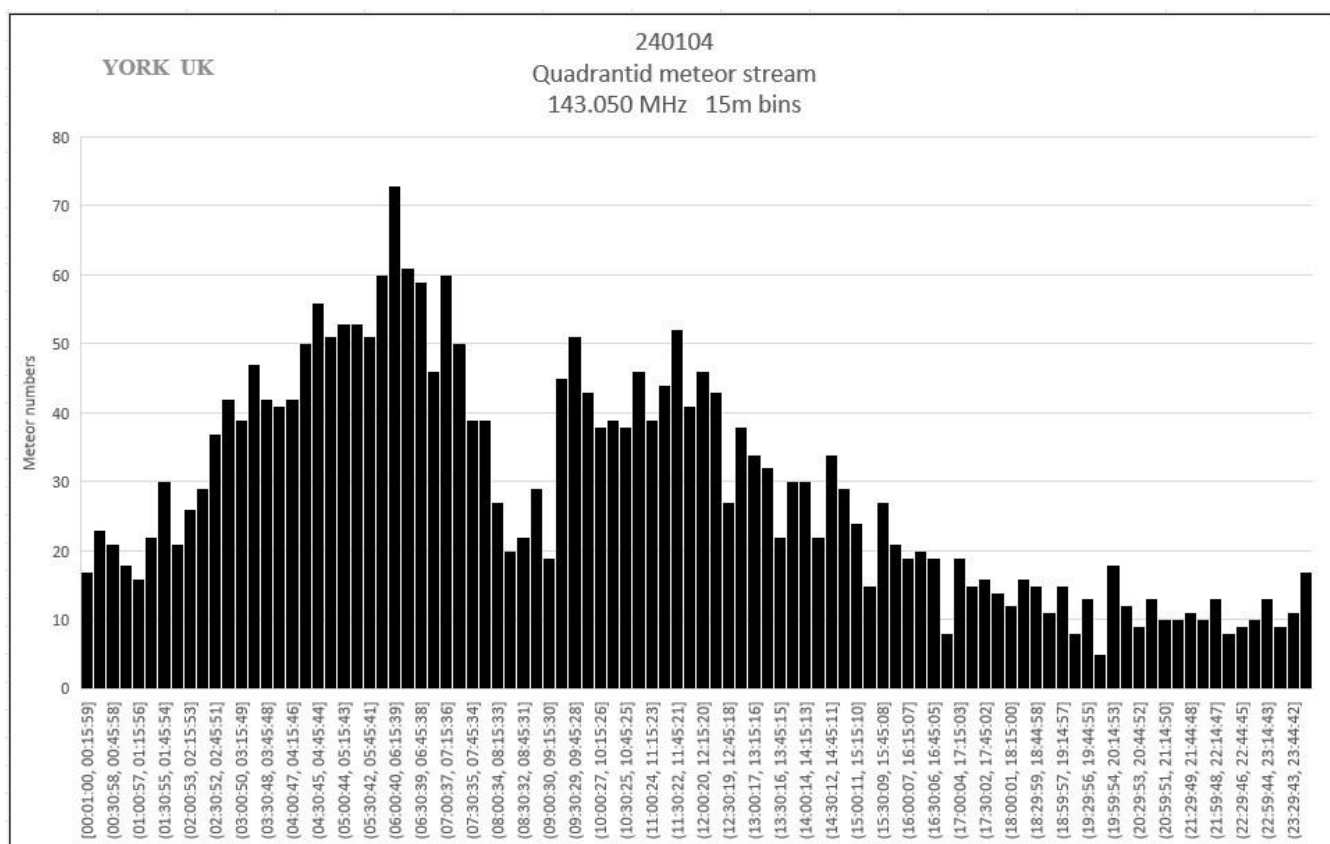
MUONS

Mark Prescott's recording of Muons shows increased levels during mid-month. These match similar behaviour in the Oulu cosmic-ray monitor.



The connection is not clear but does seem to indicate a rise in counts as the solar wind speed drops.

QUADRANTIDS



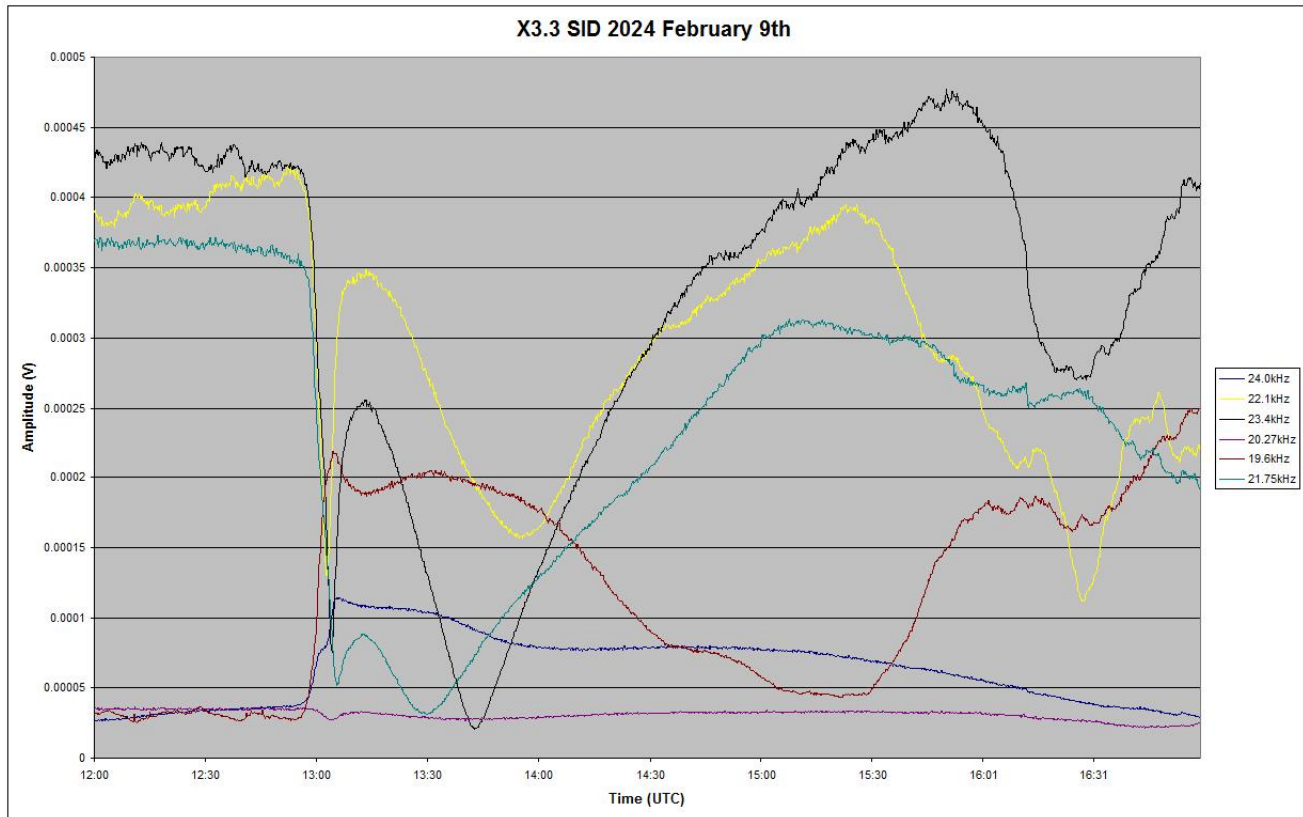
Colin Briden made recordings of the Quadrantid meteor shower using the GRAVES 143MHz signal. There is a clear peak in activity around 05:30 to 07:00UT, followed by a dip and secondary peak between 09:00 and mid-day on January 4th. The decay after this peak lasts through the afternoon, much slower than the rise in activity. The gap between the peaks matches the time when the shower radiant azimuth is in the same direction as the GRAVES aerial, so reducing its effectiveness. Unfortunately I have not received any other reports of Quadrantid activity.

Colin also reported some quite dramatic consequences of the severe storms in January. A trampoline from a neighbour's garden was launched over the fence and a garden shed, landing on his 38MHz aerial system. The aerial was wrecked, but has now been re-built, and the offending trampoline returned to its owner. I am glad that all my own aerials are safely indoors.

Finally, a reminder that the Radio Astronomy Section’s programme of zoom meetings can be found on the BAA web site. Follow the link to the [Radio Astronomy Section](#) where there is another link to the [programme list](#).

VLF SID OBSERVATIONS

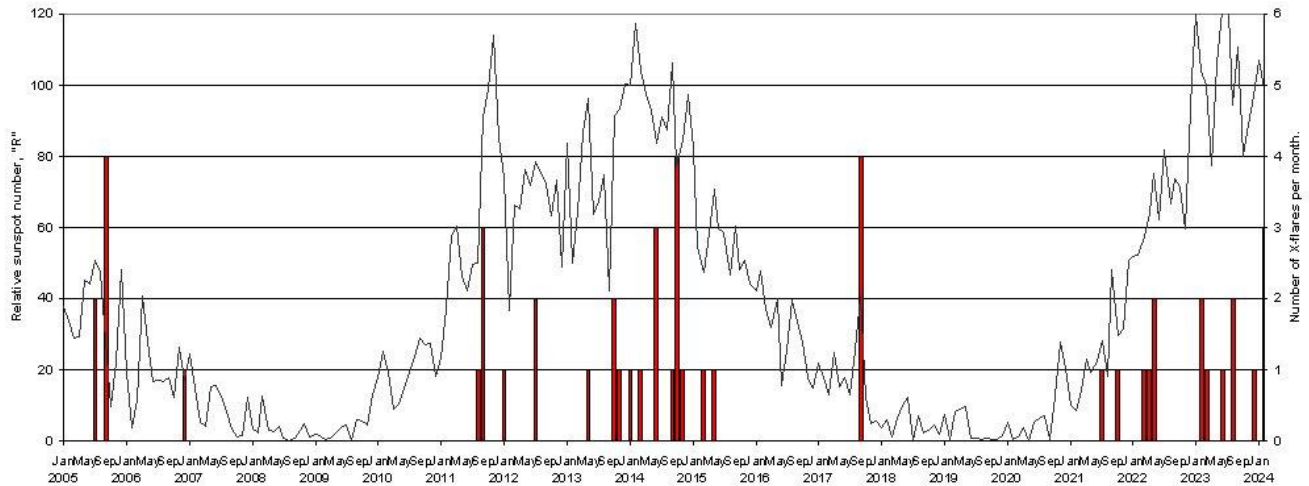
Solar activity in February was very strong, with a number of X-class flares produced by several large and complex active regions. We managed to record three of these as SIDs, including a strong X3.3 flare well timed at 13:00UT on the 9th. Mark Edwards’ recording shows the event on multiple frequencies:



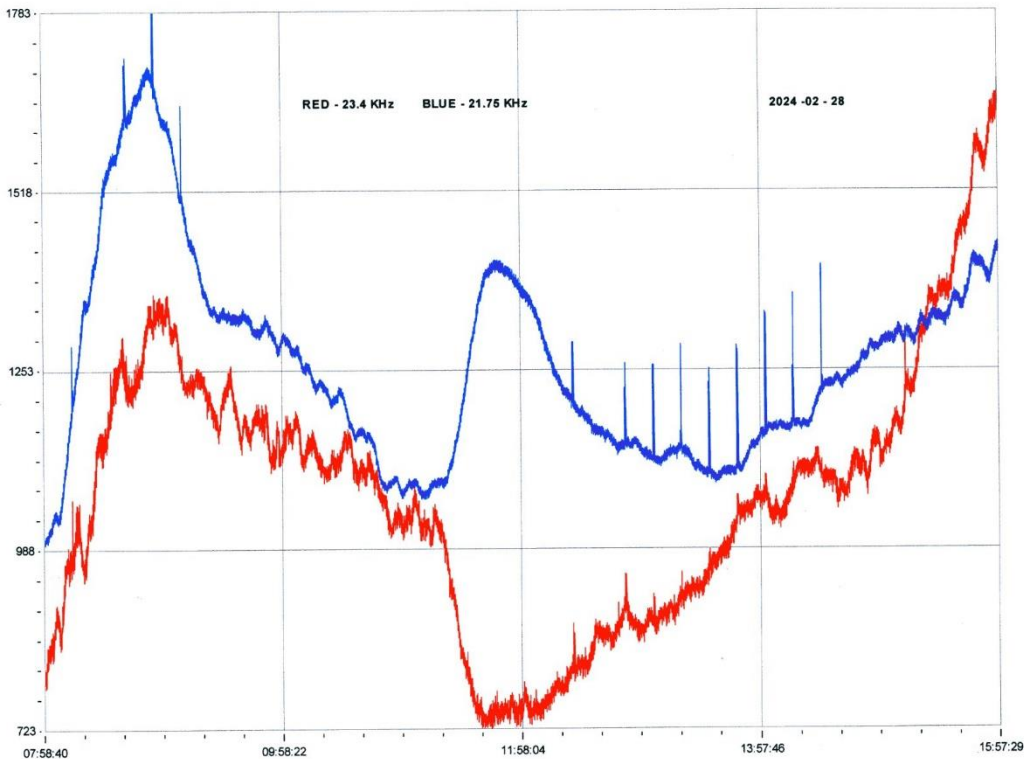
Most of the European signals have produced clear ‘spike and wave’ SIDs, while 24kHz shows a more unusual shape. The SID at 20.27kHz is very weak, barely noticeable at the bottom of the chart. Mark’s timings for the peaks are all within 90 seconds. We have recorded a total of 16 X-flares so far in solar cycle 25, compared with a total of 28 in cycle 24. The chart below shows

how these compare. We only have the tail-end of cycle 23 in our archive, but it is interesting that both cycles 23 and 24 show a burst of activity later in the cycle.

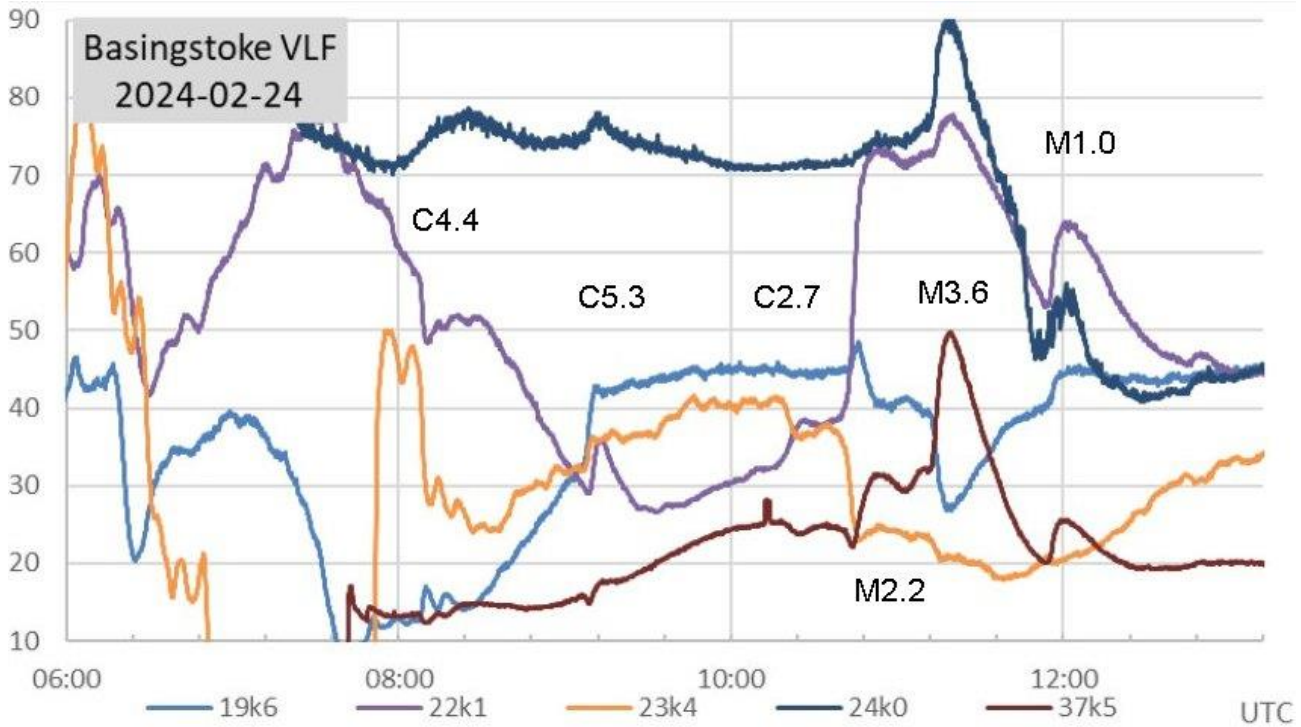
X-class flares 2005-24.



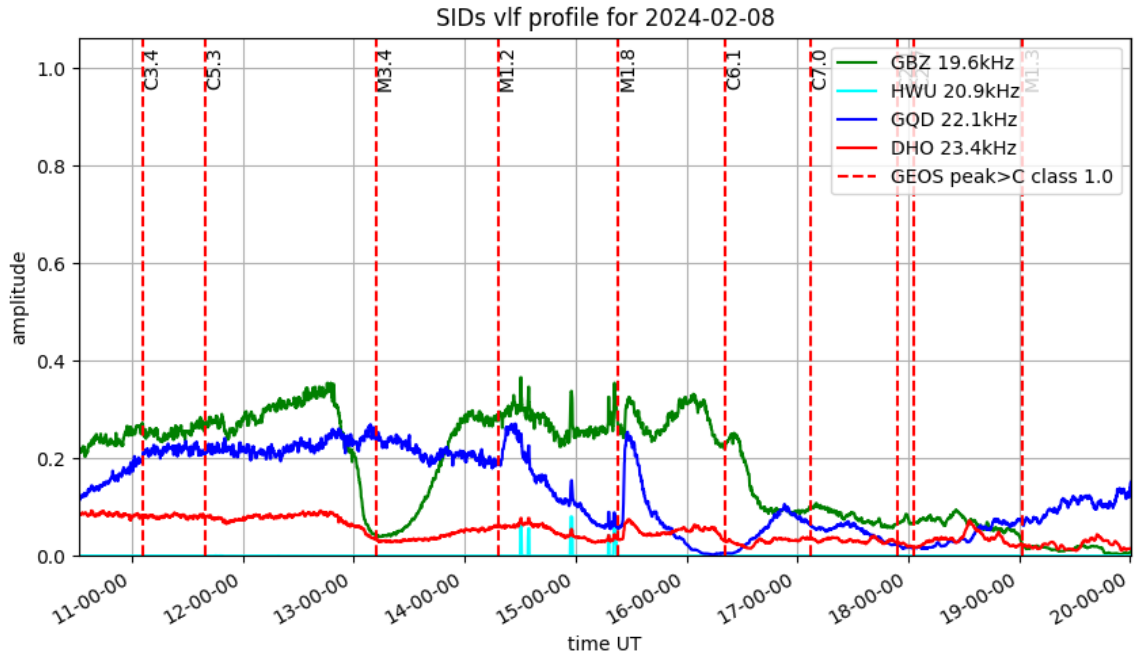
We also recorded a very unusual slow disturbance around midday on the 28th, with nothing shown in the SWPC GOES–satellite X–ray data. It was recorded on most of the signals monitored, and so cannot simply be a transmitter effect.



This recording by Colin Clements shows a very slow start and end, with nearly mirror-image responses on 23.4kHz and 21.75kHz. There was an earlier C5.1 flare from a filament eruption, but that peaked around 09UT and had ended well before this event started. The STCE bulletin recorded a small increase in its LYRA data covering 6 to 80nm matching this event, while the GOES data covering 0.1 to 0.8nm showed no flaring.

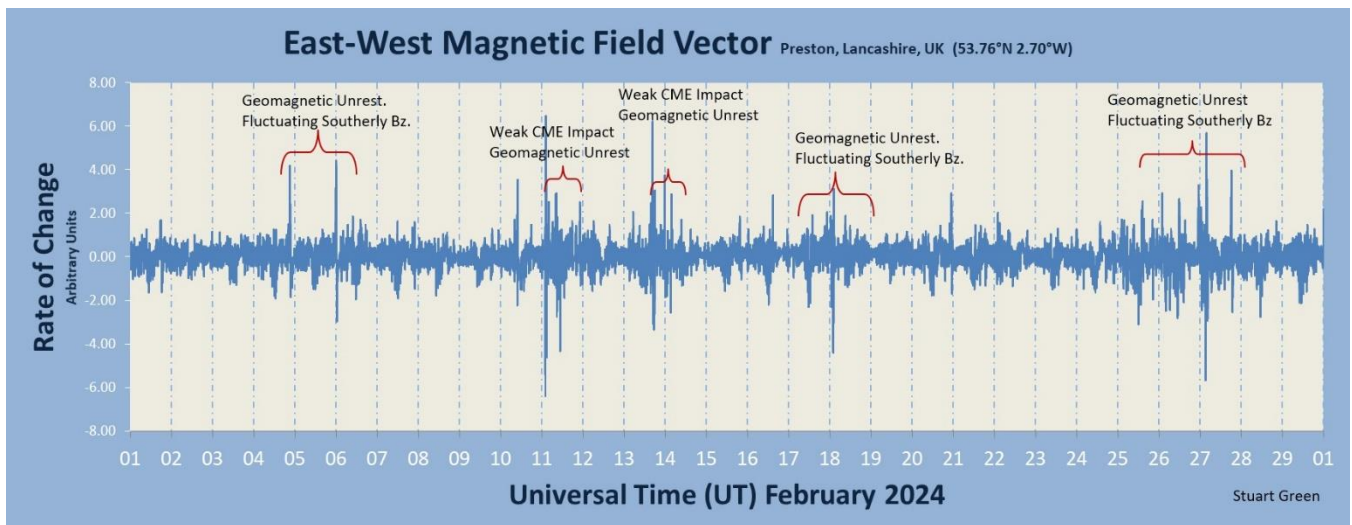


February 24th was very active, with four M-class flares as well as seven C-class and a number of smaller unclassified peaks. The recording by Paul Hyde shows activity during the morning, including the complexity of peaks from the three M-flares around midday. They are best identified at 37.5kHz, while 23.4kHz has merged them all into one SID.



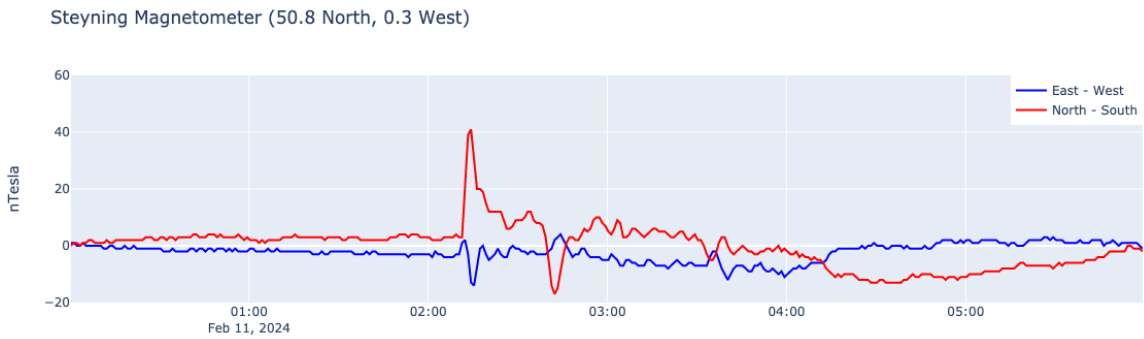
February 8th was also quite busy, shown in Mark Prescott’s recording. The series of three M-class flares during the afternoon have left very different SIDs on the three signals active on this recording. 22.1kHz shows clear SIDs for the M1.2 and M1.8 flares, but the earlier (and stronger) M3.4 is barely visible. This flare had a slow rise time, SWPC listing the start at 12:41, and is well recorded at 19.6kHz. The C6.1 flare has merged into the sunset, and not visible.

MAGNETIC OBSERVATIONS

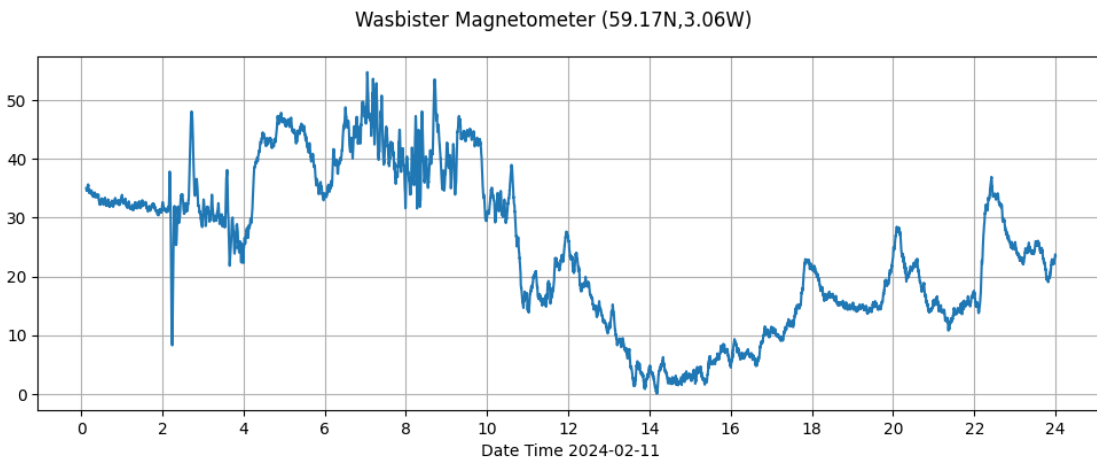


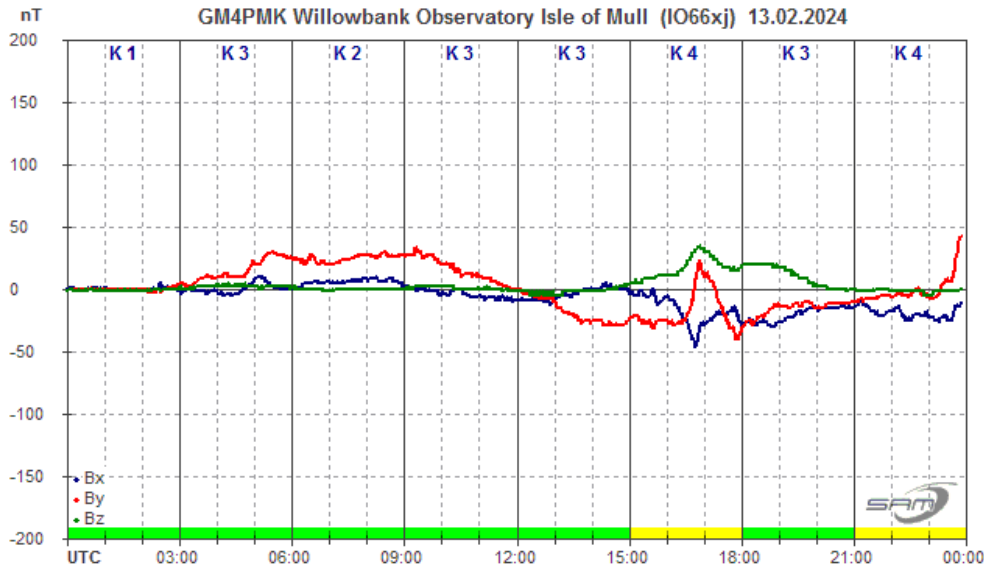
Stuart Green’s monthly summary shows plenty of magnetic activity. Many of the flares that we recorded did produce CMEs, but most seem to have managed to avoid a direct impact

with Earth's magnetosphere. We did record one very clear CME impact around 02:15UT on the 11th:

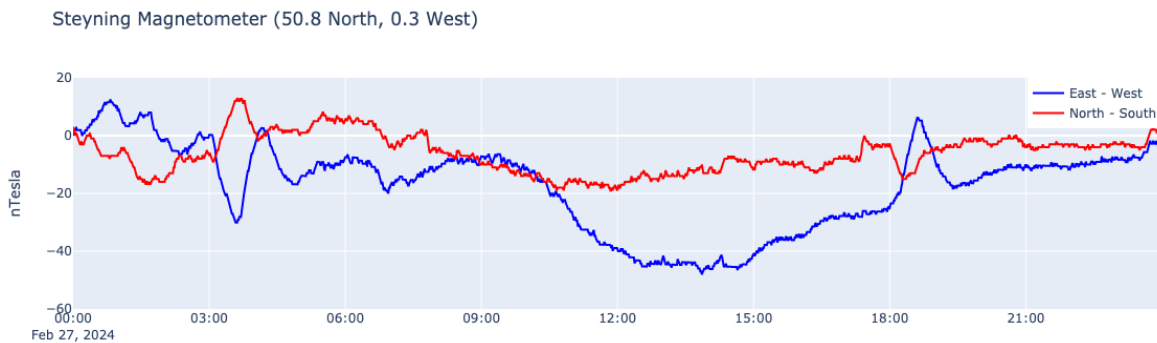


Nick Quinn's recording shows a very quiet period over the first 2 hours, with a distinct Sudden Impulse followed by a mild disturbance. Callum Potter's chart shows the disturbance continuing through the rest of the day. It faded out by midday on the 12th.





Roger Blackwell's recording from the 13th shows a hint of a possible mild CME impact at 02:30, followed by some mild disturbance. This also faded out over the next day with a few short periods of disturbance. The last few days of February showed some more periods of mild disturbance, but without any clear evidence of CMEs. Our VLF SID recordings shows that flare activity was much weaker compared to earlier in the month. Nick Quinn's chart shows activity on the 27th:

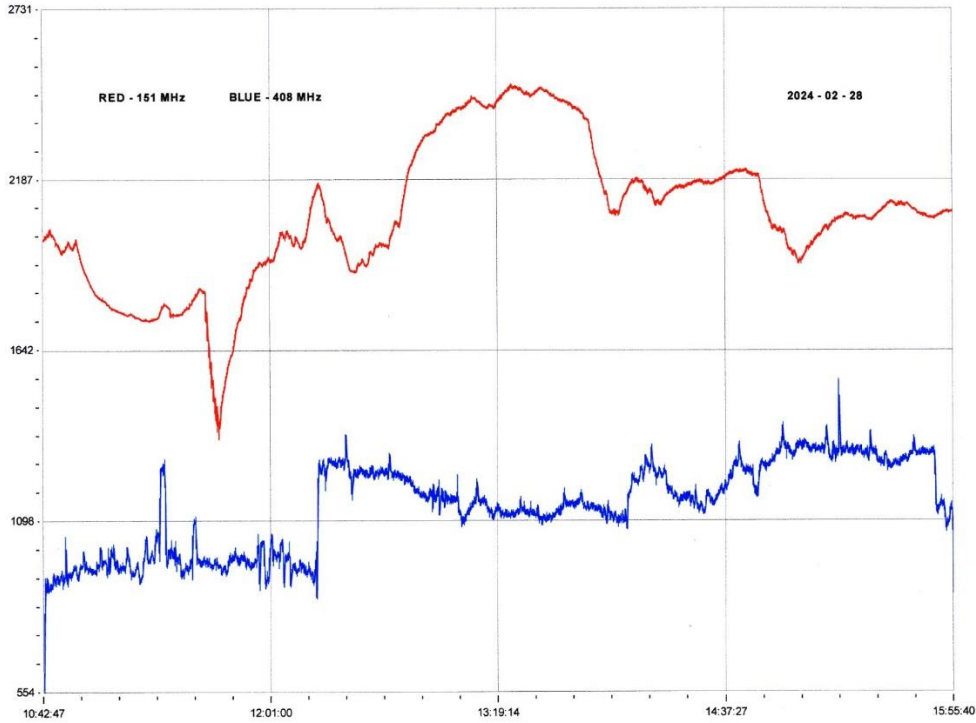


Magnetic observations received from Roger Blackwell, Stuart Green, Callum Potter, Nick Quinn, and John Cook.

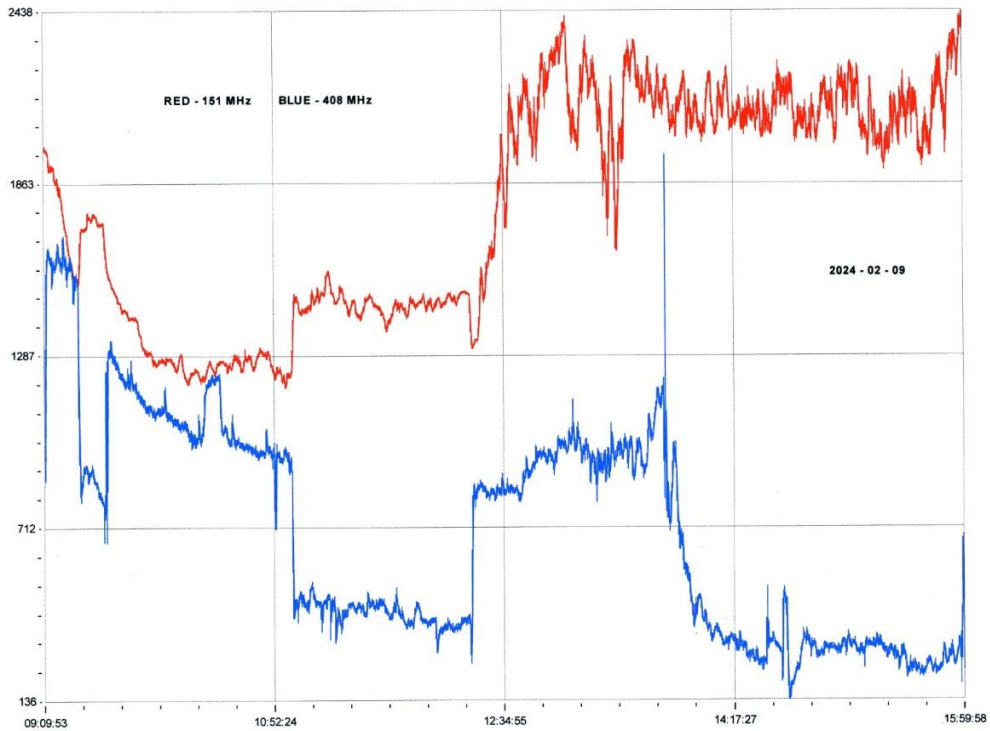
SOLAR EMISSIONS



Colin Briden has recorded a type III and V 38MHz emission starting at 09:48UT on the 26th. The small spike on the left of the chart lasts about 30 seconds, with an amplitude of 4dB above the background. It is followed by a flat-topped pulse starting at 09:50, together with a train of smaller spikes lasting about two minutes. The peak amplitude is about 6dB. These bursts are confirmed by the SWPC data, although no flares are listed during the morning of the 26th. A similar set of emissions were seen on the 28th, matching the timing of the long SID reported earlier in the summary. Colin Clements recorded 151MHz and 408MHz emissions that also seem to be related to this event:



151Mhz (blue) in particular shows a very smooth rise in strength during the decay phase of this event. Colin did have an increased time-constant in use at the time, accounting for the unusually smooth curve. Colin Clements also reported significant 151MHz activity following the X3.3 flare on the 9th, with a shorter burst on 408Mhz. 151MHz activity was also high throughout the afternoon of the 8th, matching the string of M-flares recorded.



BARTELS CHART

ROTATION	KEY:	DISTURBED.	ACTIVE	SFE	B, C, M, X = FLARE MAGNITUDE:	Synodic rotation start (carrington's).																									
2570	6	7	8	9	10	11	12	13	14	15	16	17	18	19	20	21	22	23	24	25	26	27	28	29	30	31	1				
	F	CC	CC	CC	CC	CC	CC	CC	CC	CC	CC	CC	CC	CC	CC	CC	CC	CC	CC	CC	CC	CC	CC	CC	CC	CC	CC				
2571	2022 February							2253	8	9	10	11	12	13	14	15	16	17	18	19	20	21	22	23	24	25	26	27	28		
	F	CC	CC	CC	CC	CC	CC	CC	CC	CC	CC	CC	CC	CC	CC	CC	CC	CC	CC	CC	CC	CC	CC	CC	CC	CC	CC	CC			
2572	2022 March							2254	1	2	3	4	5	6	7	8	9	10	11	12	13	14	15	16	17	18	19	20	21	22	
	F	CM	CC	CC	CC	CC	CC	CC	CC	CC	CC	CC	CC	CC	CC	CC	CC	CC	CC	CC	CC	CC	CC	CC	CC	CC	CC	CC			
2573	2022 April							2255	28	29	30	31	1	2	3	4	5	6	7	8	9	10	11	12	13	14	15	16	17	18	
	F	CMC	MCCC	CCCC	CCXC	CCXC	CCMM	CC																							
2574	2022 May							2256	24	25	26	27	28	29	30	1	2	3	4	5	6	7	8	9	10	11	12	13	14	15	
	F	MCCC	CCCC	CC	CC	MCCM	MMXM	CC	CC																						
2575	2022 June							2257	21	22	23	24	25	26	27	28	29	30	31	1	2	3	4	5	6	7	8	9	10	11	12
	F	CCC	CC	CC	CC	CC	CC	CC	CC	CC	CC	CC	CC	CC	CC	CC	CC	CC	CC	CC	CC	CC	CC	CC	CC	CC	CC	CC	CC		
2576	2022 July							2258	17	18	19	20	21	22	23	24	25	26	27	28	29	30	1	2	3	4	5	6	7	8	9
	F	CCCC	CC	C	CC	C	CC	C	CC	C	CC	C	CC	C	CC	C	CC	C	CC	C	CC	C	CC	C	CC	C	CC	C			
2577	2022 August							2259	14	15	16	17	18	19	20	21	22	23	24	25	26	27	28	29	30	31	1	2	3	4	5
	F	CMCM	CC	MCM	CCCC	C	CCCC	C	CCCC	C	CCCC	C	CCCC	C	CCCC	C	CCCC	C	CCCC	C	CCCC	C	CCCC	C	CCCC	C	CCCC	C			
2578	2022 September							2260	10	11	12	13	14	15	16	17	18	19	20	21	22	23	24	25	26	27	28	29	30	31	1
	F	C	CC	CC	CC	CC	CC	CC	CC	CC	CC	CC	CC	CC	CC	CC	CC	CC	CC	CC	CC	CC	CC	CC	CC	CC	CC	CC			
2579	2022 October							2261	6	7	8	9	10	11	12	13	14	15	16	17	18	19	20	21	22	23	24	25	26	27	28
	F	CC	C	CCCC	CCCC	CCCC	CCCC	CCCC	CCCC	CCCC	CCCC	CCCC	CCCC	CCCC	CCCC	CCCC	CCCC	CCCC	CCCC	CCCC	CCCC	CCCC	CCCC	CCCC	CCCC	CCCC	CCCC	CCCC			
2580	2022 November							2262	3	4	5	6	7	8	9	10	11	12	13	14	15	16	17	18	19	20	21	22	23	24	25
	F	CM	M	C	CC	CC	CC	CC	CC	CC	CC	CC	CC	CC	CC	CC	CC	CC	CC	CC	CC	CC	CC	CC	CC	CC	CC	CC			
2581	2022 December							2263	30	31	1	2	3	4	5	6	7	8	9	10	11	12	13	14	15	16	17	18	19	20	21
	F	C	C	CC	CC	CC	CC	CC	CC	CC	CC	CC	CC	CC	CC	CC	CC	CC	CC	CC	CC	CC	CC	CC	CC	CC	CC	CC			
2582	2023 January							2264	26	27	28	29	30	1	2	3	4	5	6	7	8	9	10	11	12	13	14	15	16	17	18
	F	C	C	CC	CC	CC	CC	CC	CC	CC	CC	CC	CC	CC	CC	CC	CC	CC	CC	CC	CC	CC	CC	CC	CC	CC	CC	CC			
2583	2023 February							2265	23	24	25	26	27	28	29	30	31	1	2	3	4	5	6	7	8	9	10	11	12	13	
	F	CC	C	CCC	CM	CM	CCCM	C	CC																						
2584	2023 March							2266	19	20	21	22	23	24	25	26	27	28	29	30	31	1	2	3	4	5	6	7	8	9	10
	F	MMC	CC	CC	CMCM	C	CCC	MCM	CMCC	C	CC																				
2585	2023 April							2267	15	16	17	18	19	20	21	22	23	24	25	26	27	28	29	30	31	1	2	3	4	5	6
	F	CCCC	C	CX	CC	CC	CMCC	MCCM	CCCM	CCMC	CCM	CC																			
2586	2023 May							2268	14	15	16	17	18	19	20	21	22	23	24	25	26	27	28	29	30	31	1	2	3	4	5
	F	C	C	CC	CC	CC	CC	CC	CC	CC	CC	CC	CC	CC	CC	CC	CC	CC	CC	CC	CC	CC	CC	CC	CC	CC	CC	CC			
2587	2023 June							2269	10	11	12	13	14	15	16	17	18	19	20	21	22	23	24	25	26	27	28	29	30	31	1
	F	MCCC	MC	CCC	CCCC	CCMC	CCCC	C	CC																						
2588	2023 July							2270	7	8	9	10	11	12	13	14	15	16	17	18	19	20	21	22	23	24	25	26	27	28	29
	F	C	CCCM	MCM	MCCC	MCCM	CCCC	CCCC	C	CC																					
2589	2023 August							2271	3	4	5	6	7	8	9	10	11	12	13	14	15	16	17	18	19	20	21	22	23	24	25
	F	CC	CC	CC	CC	CC	CC	CC	CC	CC	CC	CC	CC	CC	CC	CC	CC	CC	CC	CC	CC	CC	CC	CC	CC	CC	CC	CC			
2590	2023 September							2272	30	31	1	2	3	4	5	6	7	8	9	10	11	12	13	14	15	16	17	18	19	20	21
	F	CCCC	CCCC	CCCC	MCCC	MC	CCCM	CCM	MC	C	CC																				
2591	2023 October							2273	27	28	29	30	31	1	2	3	4	5	6	7	8	9	10	11	12	13	14	15	16	17	
	F	CMCC	CMCC	CCCM	MC	CMCC	MMMM	MMMM	CMCC	CC																					
2592	2023 November							2274	23	24	25	26	27	28	29	30	31	1	2	3	4	5	6	7	8	9	10	11	12	13	
	F	CCC	C	C	C	C	MC	MCC																							
2593	2023 December							2275	19	20	21	22	23	24	25	26	27	28	29	30	31	1	2	3	4	5	6	7	8	9	10
	F	MCCC	CMCC	M	CCMM	CCCC	CCMC	C	CC																						
2594	2024 January							2276	16	17	18	19	20	21	22	23	24	25	26	27	28	29	30	31	1	2	3	4	5	6	7
	F	CCC	C	C	C	C	CC																								
2595	2024 February							2277	13	14	15	16	17	18	19	20	21	22	23	24	25	26	27	28	29	30	31	1	2	3	4
	F	C	CCCC	C	CM	CC	MCCC	CCCC	CCMC	MC	C	CC																			
2596	2024 March							2278	10	11	12	13	14	15	16	17	18	19	20	21	22	23	24	25	26	27	28	29	30	31	1
	F	CCC	CCCC	CC	C	MMX	MCCM	CC	C	C	C	C	C	C	C	C	C	C	C	C	C	C	C	C	C	C	C	C			
2597	2024 April							2279	6	7	8	9	10	11	12	13	14	15	16	17	18	19	20	21	22	23	24	25	26	27	
	F	C	CC	CC	CC	CC	CC	CC	CC	CC	CC	CC	CC	CC	CC	CC	CC	CC	CC	CC	CC	CC	CC	CC	CC	CC	CC	CC			
2598	2024 May							2280	2	3	4	5	6	7	8	9	10	11	12	13	14	15	16	17	18	19	20	21	22	23	24
	F	CCCC	CCCC	MMMM	CC	CC	CCM	MMMM	CXM	C	C	CMCM	CC	CC	CC	CC															



British Astronomical Association

Supporting amateur astronomers since 1890

Radio Astronomy Section

BAA RA Section programme 2024

Fri. Jun. 7th. 19:30 GMT (19:30 UTC)	Professor Roger Deane Director: Wits Centre for Astrophysics; Professor/SKA Chair in Radio Astronomy · University of the Witwatersrand	What next for Very Long Baseline observations
---	--	---

Paul Hearn
BAA Radio Astronomy Section Director
UKRAA Trustee

Featured Articles

Run GNU Radio on a Windows 11 PC with Windows Subsystem for Linux, ver. 2 (WSL 2)

By Tom Hagen

Introduction

I've been experimenting with GNU Radio; here's a quick definition: "GNU Radio is a free and open-source software development toolkit that provides signal processing blocks to implement software radios." [\[1\]](#)

GNU Radio (GR) can be used with readily-available cheap external RF hardware such as the ever-popular RTL-SDR USB dongle to create software-defined radios for radio astronomy.

GR was developed for the Linux operating system and runs best on Linux. Although there is a Windows version of GR, I have had difficulties using this version and since I've had past success running GR in Linux, I decided to have a whack at running it in WSL 2. As for my preferred version of Linux, I like Ubuntu since I've had the most experience with it.

Here's a quote from Microsoft describing WSL 2: "Developers can access the power of both Windows and Linux at the same time on a Windows machine. The Windows Subsystem for Linux (WSL) lets developers install a Linux distribution (such as Ubuntu, OpenSUSE, Kali, Debian, etc.) and use Linux applications, utilities, and Bash command-line tools directly on Windows, unmodified, without the overhead of a traditional virtual machine or dualboot setup." [\[2\]](#)

Another great resource I take advantage of is the Digital Signal Processing in Radio Astronomy (DSPIRA) project. [\[3\]](#) This project is a part of the West Virginia University Radio Astronomy Instrumentation Laboratory (WVU RAIL) group. I can't say enough about DSPIRA as an excellent resource for amateurs learning to work HI.

In the past I have run GR on Raspberry Pi 4 and Odroid XU4 single board computers. I've also run GR on Windows/Ubuntu dual-boot PC's both from bootable USB drives and partitioned hard drives. Getting GR to work on WSL 2 will simplify my setup and let me run GR on my Win11 laptop without the bother of dual booting. It's also possible to run GR sketches using different versions of GR using Docker containers running on top of WSL 2 that are set up to run specific versions of GR such as versions 3.8, 3.10, etc.

These instructions were proved out on my Win 11 Dell laptop (64-bit operating system, x64-based processor). If you're running Win 10 the process should be similar, but I don't believe USBIPD-WIN will work for you; you may have to use rtl_tcp instead.

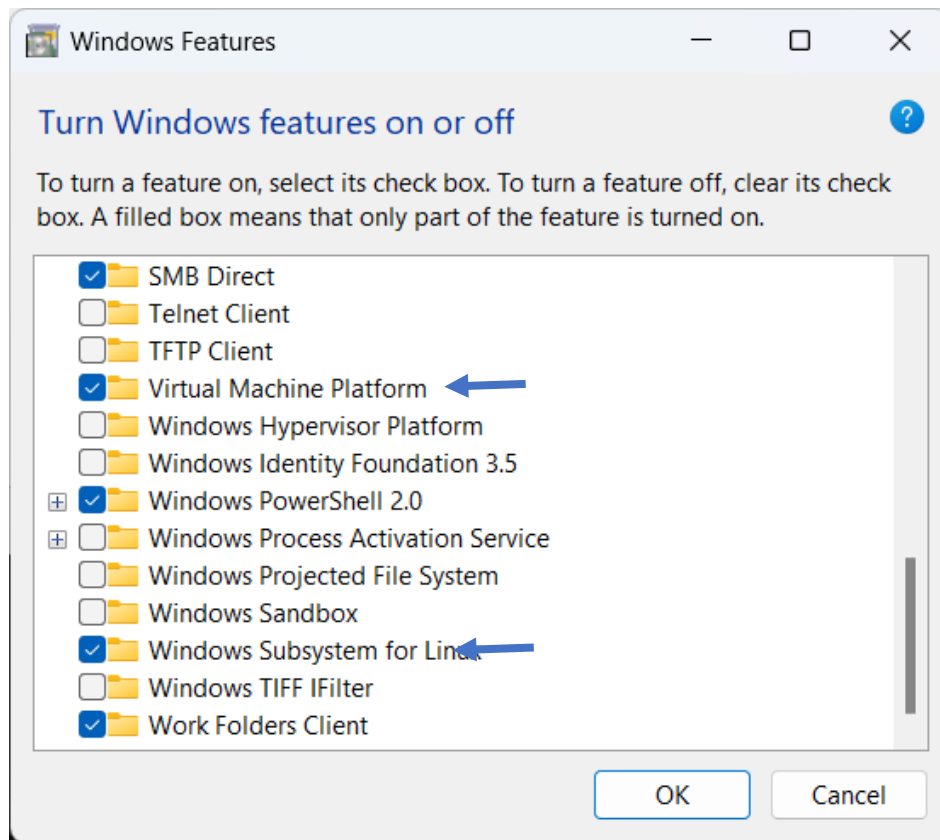
The setup described in this article is pretty simple, there are just three steps to it:

- Activate the WSL 2 feature in Windows 11
- Install the USBIPD-WIN software that lets you connect your USB SDR dongle to Linux running on WSL 2
- Install GNU Radio on the Linux distribution you're running on WSL 2

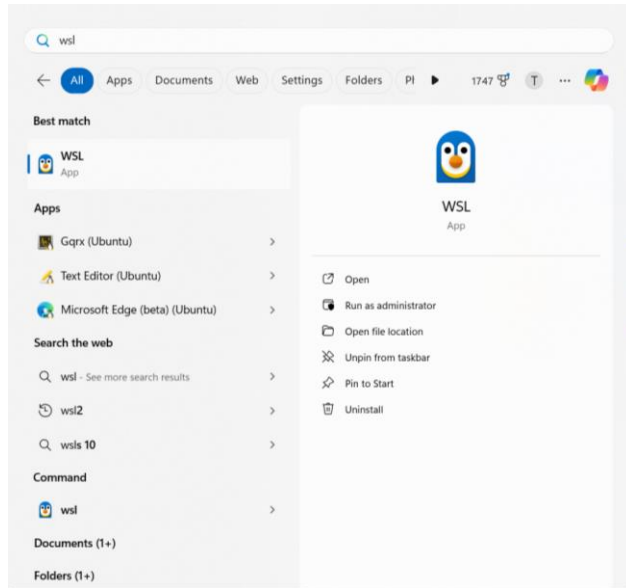
Activate WSL 2 in Windows 11

WSL 2 is a clever Microsoft product that lets you run Linux on your Windows PC just as you would run any other application such as Word or Excel. WSL allows developers to run a Linux environment directly on Windows without the need for a separate virtual machine or dual-boot setup. In the past if you wanted to run Linux on your PC one way to do it would be to use a virtual machine such as Hyper V. I have used virtual machines and they're a bit more difficult to set up as compared to WSL 2 and so far, I haven't run into anything I couldn't do on WSL 2 that I could do on a virtual machine. Memory access is faster running WSL 2 vs. a traditional virtual machine. WSL 2 uses virtualization technology to run a Linux kernel inside a lightweight utility virtual machine (VM). The Linux distribution within WSL2 runs as an isolated container.

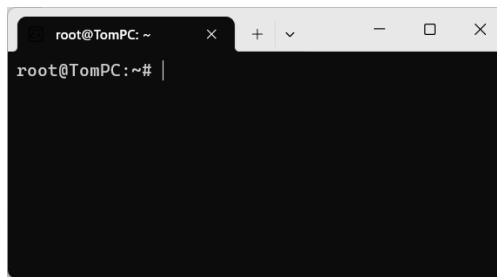
WSL 2 is already installed on your Windows 10/11 distribution and you only have to turn on a couple of Windows features to start using it. Click on the Windows button on the far left of your toolbar and type "turn windows feature on or off" in the search text box. Then click on the "Turn Windows features on or off" icon that pops up to get the window below. Select the "Virtual Machine Platform" and "Windows Subsystem for Linux" check boxes. Hit the OK button and reboot Windows.



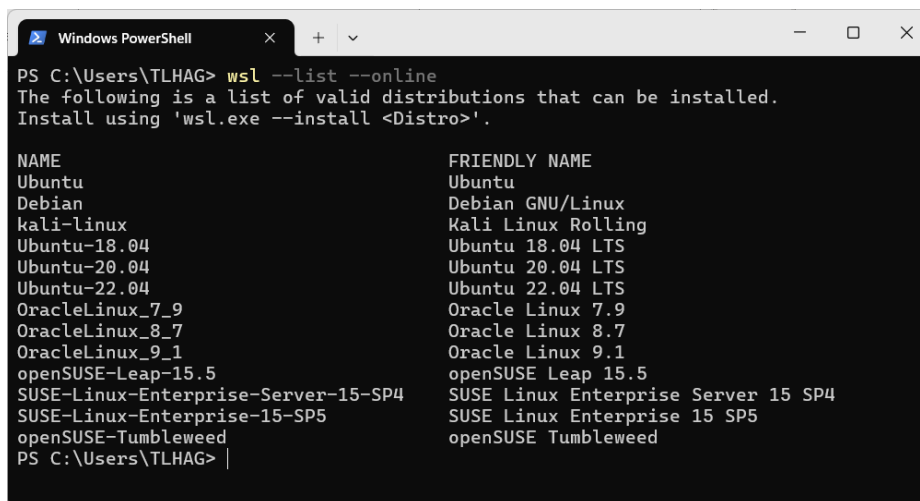
To check that WSL 2 is available, click on the Windows button at the far left of the toolbar and type wsl in the search bar. You should see the window below.



Click on the Open button to start WSL 2 and you'll get the WSL 2 terminal window as seen below.

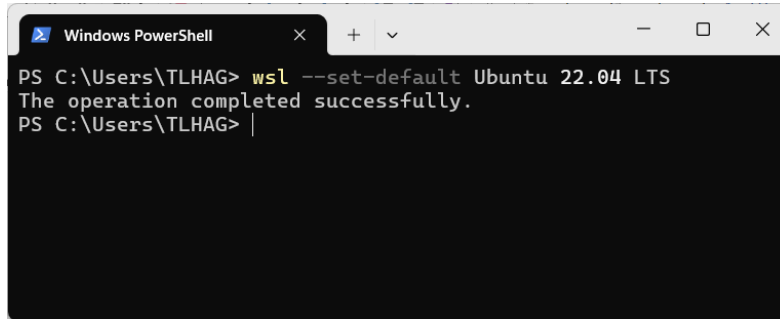


WSL 2 comes with the latest distribution of Ubuntu installed as the default OS. If you need to install a different distribution, you can find out which ones are available by `wsl --list --online`. Open a Windows PowerShell or Command Line terminal and enter the command: `wsl --list --online`



If you need a specific distro for your project, use the following command to install the desired Linux distro (in this case I installed Ubuntu 22.04 LTS):

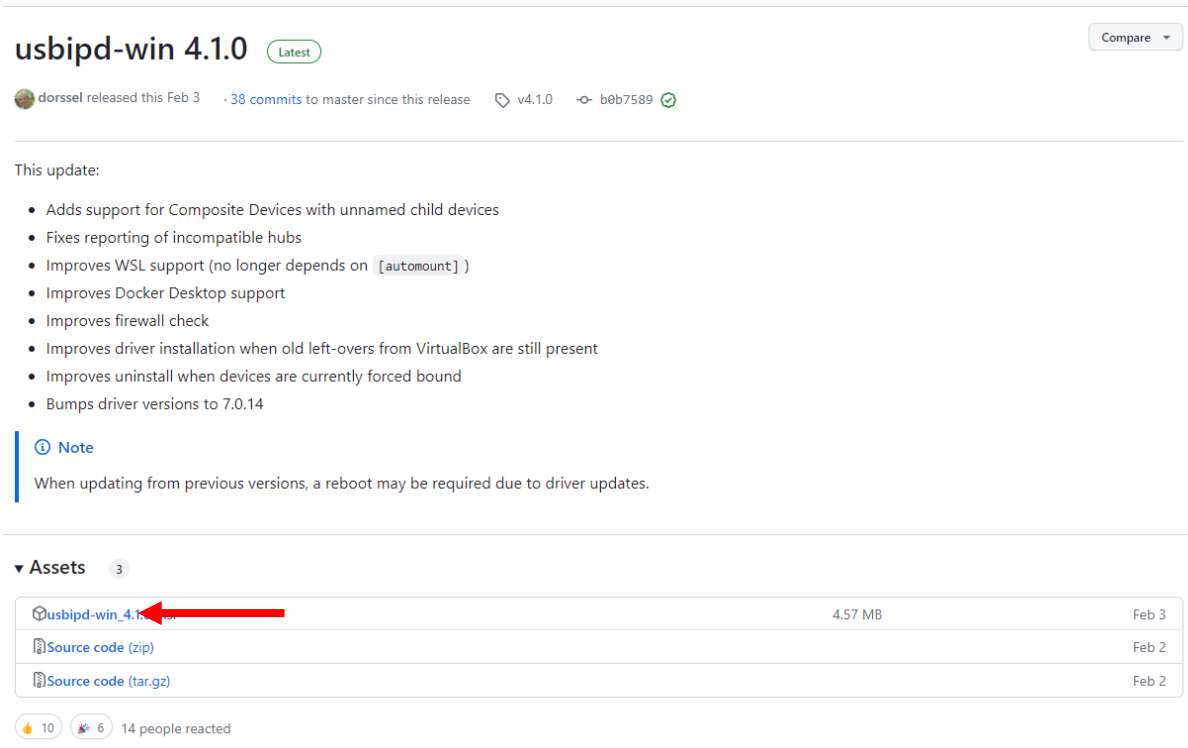
```
wsl --set-default Ubuntu 22.04 LTS
```



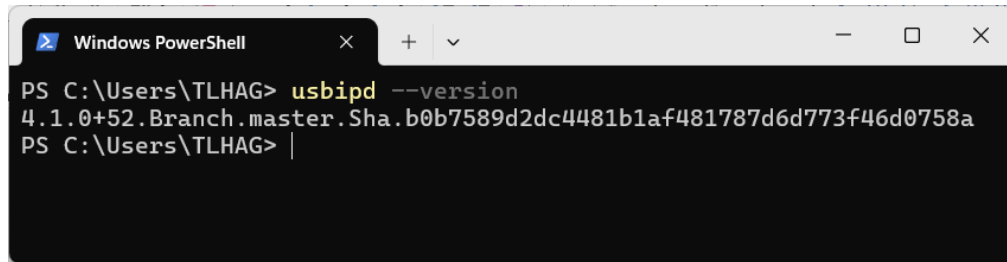
Install the USBIPD-WIN Software

When operating in the WSL 2 environment, your USB dongle will not work because there is no direct connection from WSL2 to the USB port that the dongle is plugged into. To solve this problem, there is the `usbipb-win` project. The `usbipb-win` software uses TCP/IP protocol to forward the USB device traffic over a virtual network interface between WSL and Windows. Note: `usbipd-win` only works for Windows 11. There is another workaround called `rtl_tcp` that can be used as an alternative to `usbipb-win`. I have not tried this method.

To install `usbipb-win` [5], first go to the `usbipd-win` GitHub site and locate the *.msi file as seen below. <https://github.com/dorsel/usbipd-win/releases/tag/v4.1.0>

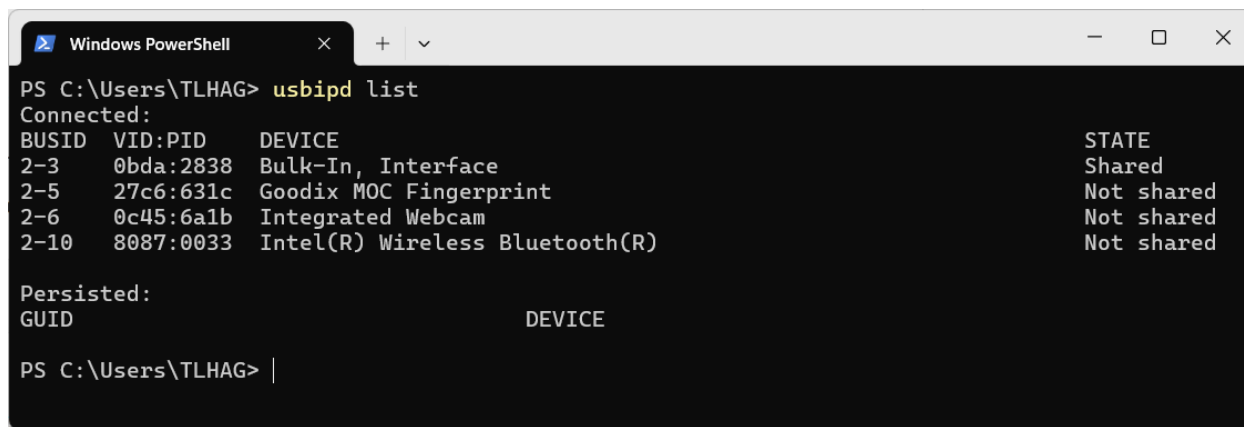


Click on the file and it will automatically download to your PC. When the download has completed, simply click on the msi file and it will install using the familiar MS process. Verify installation with the `usbipd --version` command in your Windows terminal window as seen below.



```
Windows PowerShell
PS C:\Users\TLHAG> usbipd --version
4.1.0+52.Branch.master.Sha.b0b7589d2dc4481b1af481787d6d773f46d0758a
PS C:\Users\TLHAG> |
```

Plug your SDR into a USB port, then run this command in your Windows terminal: `usbipd list`



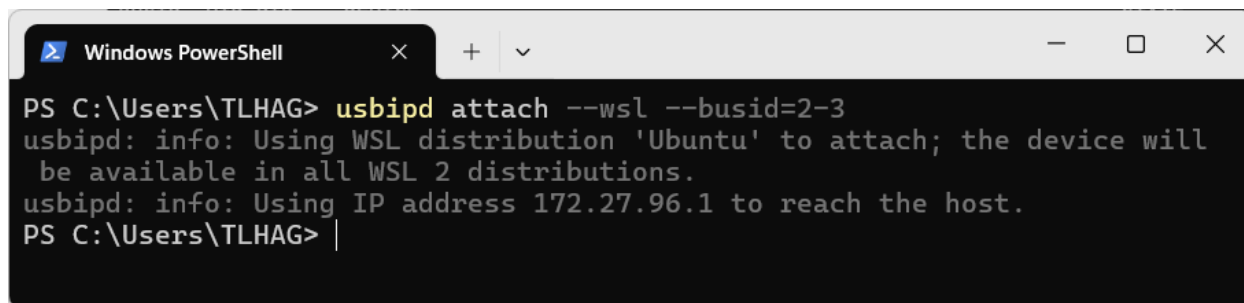
```
Windows PowerShell
PS C:\Users\TLHAG> usbipd list
Connected:
BUSID  VID:PID  DEVICE                                STATE
-----
2-3    0bda:2838 Bulk-In, Interface                    Shared
2-5    27c6:631c Goodix MOC Fingerprint                Not shared
2-6    0c45:6a1b Integrated Webcam                     Not shared
2-10   8087:0033 Intel(R) Wireless Bluetooth(R)        Not shared

Persisted:
GUID                                DEVICE

PS C:\Users\TLHAG> |
```

My RTL-SDR dongle shows up as BUSID 2-3. The PID 2838 is the standard PID for this dongle, and as far as I know it's common for all RTL-SDR makes. If you're not sure which PID your device has, unplug it and run the command again to see which device disappears from the list.

Next, start WSL 2 in Windows and then attach the SDR to WSL using this command in the Windows terminal: `usbipd attach --wsl --busid=<busid>`



```
Windows PowerShell
PS C:\Users\TLHAG> usbipd attach --wsl --busid=2-3
usbipd: info: Using WSL distribution 'Ubuntu' to attach; the device will
be available in all WSL 2 distributions.
usbipd: info: Using IP address 172.27.96.1 to reach the host.
PS C:\Users\TLHAG> |
```

My busid for the dongle is 2-3, yours will probably be different. Observe that WSL is using the IP address of 172.27.96.1 in my case.

Note though, that every time you boot WSL you will have to use `usbipd` to list and attach the SDR dongle to WSL. The dongle will also disconnect from WSL if you unplug it, so you'll have to run these commands again when you unplug when running WSL.

In your WSL terminal you can use the `lsusb` command to see connected USB devices, below you see that the SDR is indeed connected.

```
hagent@TomPC: ~  
hagent@TomPC:~$ lsusb  
Bus 002 Device 001: ID 1d6b:0003 Linux Foundation 3.0 root hub  
Bus 001 Device 002: ID 0bda:2838 Realtek Semiconductor Corp. RTL2838 DVB-T  
Bus 001 Device 001: ID 1d6b:0002 Linux Foundation 2.0 root hub  
hagent@TomPC:~$ |
```

Install GNU Radio

From the GR site [2]: “GR is a free & open-source software development toolkit that provides signal processing blocks to implement software radios. It can be used with readily-available low-cost external RF hardware to create software-defined radios, or without hardware in a simulation-like environment. It is widely used in research, industry, academia, government, and hobbyist environments to support both wireless communications research and real-world radio systems.”

To install GNU Radio, you will do it from the WSL terminal window and there is plenty of help online on how to do this. I chose however to install GR and a number of prepared GR setup files from the Digital Signal Processing In Radio Astronomy (DSPIRA) site. A very good calibrated hydrogen line setup file is provided and I have been using it with good results.

The website [3] of The Digital Signal Processing In Radio Astronomy group states: “(DSPIRA) is an NSF Research Experiences for Teachers (RET) in Engineering and Computer Science Site at the West Virginia University Lane Department of Computer Science and Engineering”.



DSPIRA Horn with Base (Courtesy DSPIRA)

“(DSPIRA) was designed to provide teachers the training and materials in the field of Radio Astronomy. This acts as a stepping stone for an eclectic journey through science and engineering with the given Core context in Astronomy. The culmination of this program are lessons and exercises designed by the participating cohort of teachers themselves. These lessons involve all aspects of Radio astronomy from building a radio telescope to its operation.” DSPIRA provides six-week summer sessions for high school science teachers desiring to learn about radio astronomy, digital signal processing, GR, and radio telescope construction and operation. DSPIRA has a unique horn design using an F-style metal gallon container (typically used for paint solvents) and ½” foil backed foam insulation board. I’ve built a couple of these and they work well.

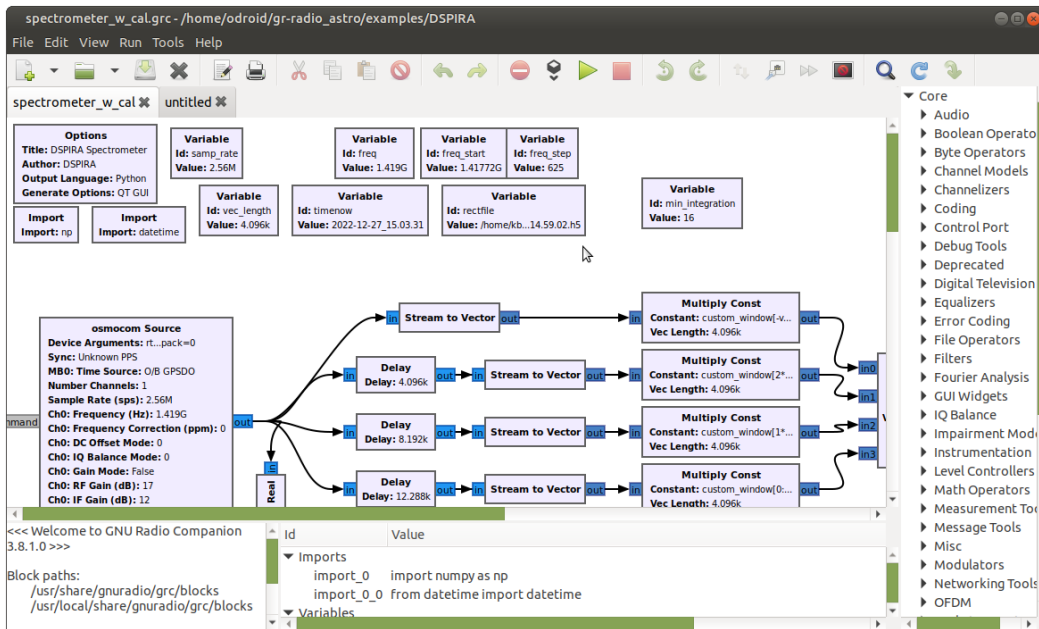
In addition, DSPIRA provides excellent tutorials and other resources that you can use to learn more about software defined radio, GNU Radio, and hydrogen line work.

To install the DSPIRA setup for Ubuntu 22.04, go to this link and follow the instructions. Instructions are also listed in the Appendix at the end of this paper:

https://wvurail.org/dspira-lessons/gr_radio_astro_Installation

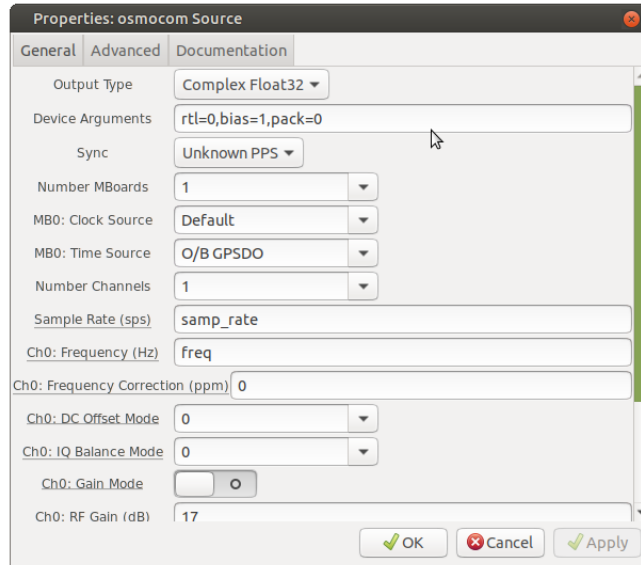
Observing With the DSPIRA GNU Radio Package

The spectrometer_w_cal.grc from the DSPIRA group is seen below. This is the setup I used to observe HI in the galactic plane. The only change I made was to change the default SDR to my RTL-SDR SDR dongle and to turn on 5 VDC from the dongle to power the Nooelec H1 filtered preamp I use.



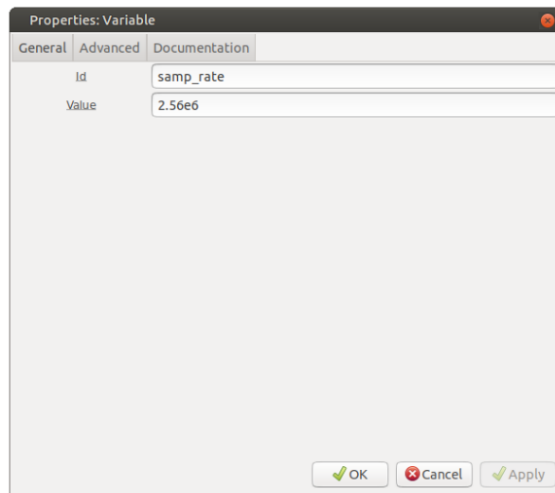
GNU Radio Companion Setup from DSPIRA

The default setup is configured for an Airspy R2 SDR and since I’m using an RTL-SDR dongle (RTL2832U), I had to change the “Device Arguments” settings in the osmocom Source to “rtl=0” from “airspy=0”. The “bias=1” setting supplies 5VDC to the external preamp from the RTL-SDR, and the “pack=0” setting is an option for the Airspy source referring to packed/unpacked USB transmission and appears to have no effect on RTL-SDR dongle operation. Access these settings by double clicking on the osmocom Source block as seen below.



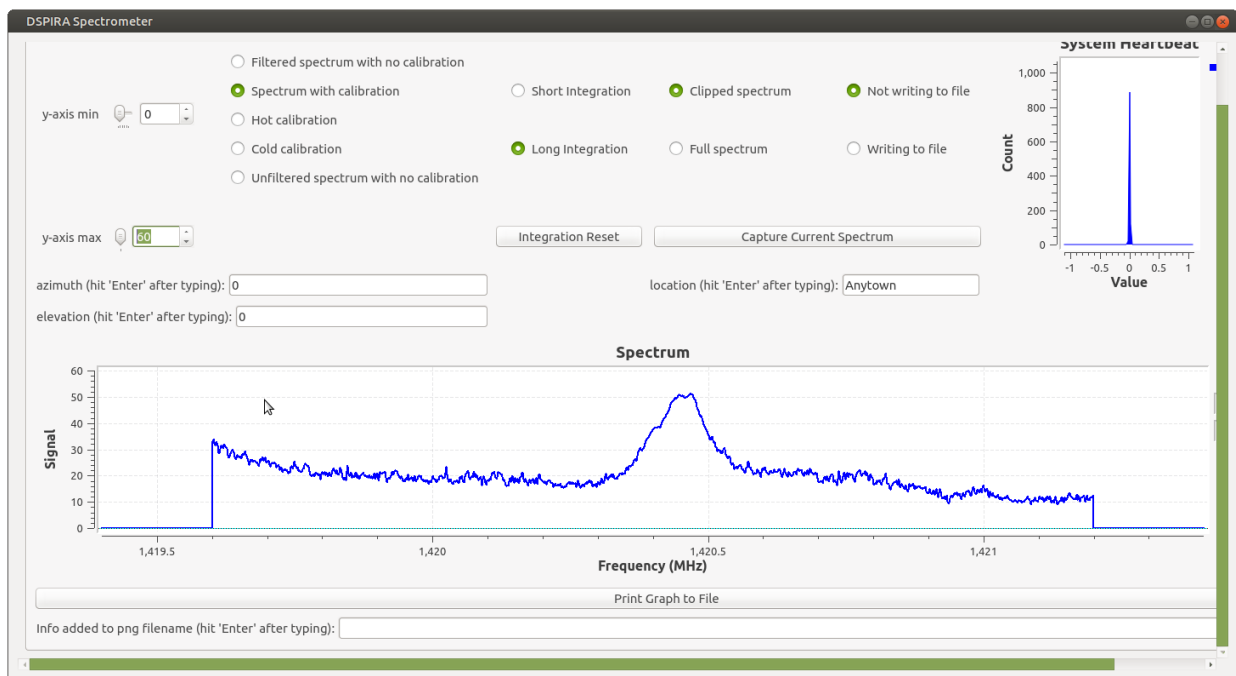
Setup for the RTL-SDR Dongle

You'll also need to set the sample rate variable in the upper left corner to 2-3 MHz or so. Click on the Variable box "samp_rate" and set the rate to 2.56 MS/s for example, enter the "Value" as 2.56e6.



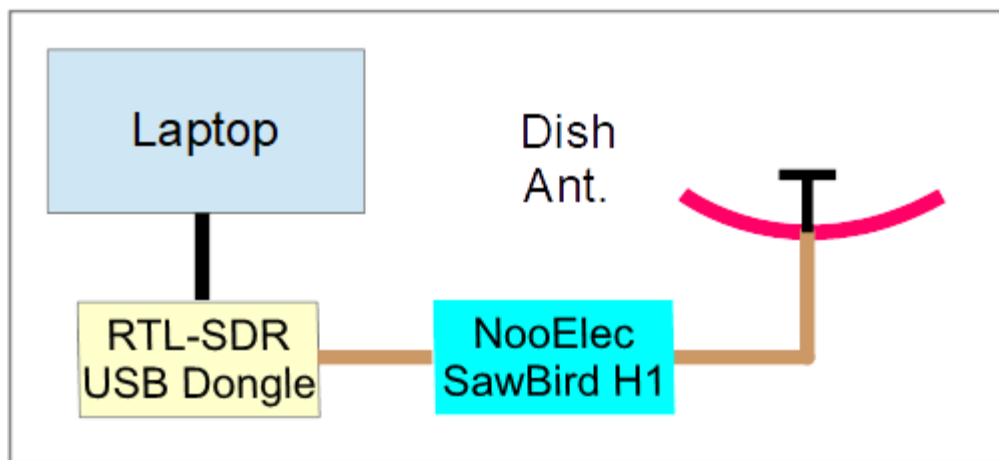
Sample Rate Setup for the RTL2832U Dongle (2.56 MS/s)

To start the sketch, press the little triangle on the top menu bar and the triangle changes to a square. Pressing the square stops the setup. The running setup window appears in the following figure. It's important to follow the hot/cold procedure for calibrating the telescope too, because otherwise you will not get a clear view of the HI spectrum.



DSPIRA “spectrometer_w_cal.grc” Sketch in Operation

Observing HI on the Setup



Setup Diagram

The setup for HI observing is shown in the above diagram. The band-passed Nooelec SAWbird+H1 40dB, 0.7 dB noise figure (50 K noise temperature) preamp works well with the RTL-SDR. There’s a male-male SMA barrel adapter between the RTL-SDR and the preamp. I have used USB cables as long as 20 feet and I haven’t noticed any problems with signals. RFI doesn’t seem to be an issue either in my suburban location. Power to the preamp is supplied through a bias-T supply from the RTL-SDR and is configured to turn on in the GR setup.

I like to point the dish straight up and let the Milky Way roll over my site. The plane of the Milky Way in Cygnus is straight overhead at my latitude and this gives me a strong signal that shows up well on the display. I receive no observable signal when the galaxy is out of the antenna beam. I modified the dish by extending the little

reflector at the feed out another 1" and this improves the SWR from around 3.5 to 1.5 at 1.42 GHz, the H1 frequency.



WiFi Antenna Used for H1

Conclusions and Future Plans

It's definitely feasible to run GNU Radio on WSL 2 on a Windows 11 PC and the performance is quite adequate for my purposes. Running WSL 2 simplifies my setup in that I don't have to run Ubuntu on an external USB stick or on a partitioned hard drive. The only catch is that you have to run the USBIPD-WIN "attach" command in the Windows terminal window to reconnect the SDR dongle every time you restart the WSL 2 setup.

Future work may be to install Docker on Ubuntu in WSL 2. Docker allows the use of different Linux versions of Linux distributions or even different Linux distributions altogether. Docker runs the different versions in separate containers. This will help in running GR setups developed in older releases, for example, in Ubuntu 20.04, 18.04, etc. GR can be ornery when you try to run a setup developed in an older GR version in a newer GR version. For example, I had problems running the DSPIRA GR 3.8 setups in GR 3.10.

Hope you found this useful and interesting, I'm happy to answer any questions and to help out any way I can!

References:

- [1] GR Wiki: [GR](#)
- [2] Microsoft WSL 2 Website: [Install WSL | Microsoft Learn](#)
- [3] DSPIRA Website: <https://wvurail.org/dspira-lessons/>
- [4] Ubuntu 22.04 DSPIRA Software Setup: https://wvurail.org/dspira-lessons/gr_radio_astro_Installation
- [5] USBIPB-WIN Software: <https://github.com/dorsse/usbipd-win/releases/tag/v4.1.0>

APPENDIX

Installing GR and the gr-radio_astro Package onto WSL 2 Running Ubuntu 22.04

These terminal commands are from the DSPIRA “Telescope Software Setup” page [4]. Copy and paste these commands into the terminal window (explanations for what the commands do are given on the DSPIRA page):

```
$ sudo apt install gnuradio gr-osmosdr airspy python3-h5py python3-ephem git cmake liborc-0.4-dev -y
$ git clone https://github.com/WVURAIL/gr-radio_astro.git
$ cd gr-radio_astro
$ git branch
$ mkdir build
$ cd build
$ cmake ..
$ make
$ make install
$ cd~
```

Start GNU Radio Companion:

```
$ gnuradio-companion
```

When GR Companion opens, use the menu bar buttons to navigate to the spectrometer_w_cal.grc file and start the file.

File→Open →gr-radio_astro→examples →DSPIRA→spectrometer_w_cal.grc and press the Start triangle in the top menu bar. If everything’s ok, you will see the graphic spectrometer window open up and run.

Some Folding Algorithm Variants for Optimizing Pulsar SNR for Small Apertures

Peter W. East

Abstract

Pulsar hunting is not always successful due to system noise, RFI, scintillation, drift scan under-illumination or just plain acquisition limitations of small antenna apertures. Some folding algorithm tweaks are described in this article to ensure that the best possible pulse fidelity is extracted from a pulsar present in a data record.

Introduction

The basic folding algorithm involves dividing the detected data record into intervals exactly equal to the expected pulsar period and parallel-adding these coherently. This ensures that any pulsar pulse present occurs at the same point in each interval so adds linearly. The detected system noise, assumed random, sums as the amplitude square-root, ensuring the pulse data signal-to-noise ratio (SNR) increases, providing each interval's pulse exceeds a certain positive level. If the interval or section SNR falls below this level, then the potential final SNR is reduced. This critical level is given by SNR_{final}/\sqrt{N} , where N is the number of intervals/sections summed.

Six folding algorithm variants are described to process some real observation data without any RFI modification, but still allows the best possible final data SNR to be obtained. The algorithms' functions and operation are demonstrated using data from an extended drift scan observation.

Note, the algorithm equations 1 to 6 in the following 'Folding Algorithms' section are in a pseudo-descriptive form for information but have been implemented in 'C' for this analysis.

Example Observation Data File

16800 seconds of drift scan data was collected with a small twin-Yagi antenna with elevation and azimuth beam widths of 14 and 28 degrees. The target was B0329+54 and the antenna 3dB half-width beam dwell was around 3 hours. The extended trial dwell allowed for periods at the beginning and end where low target signal levels were expected to better visualize and accentuate pulsar detection over the azimuth beam maximum response. The data record contained some minor RFI and the only RFI reduction feature included was for any spikes greater than 3.5 times each band rms to be reduced by a third.

Folding Algorithms

1. **Basic Fold** - finds pulsar but poor resolution

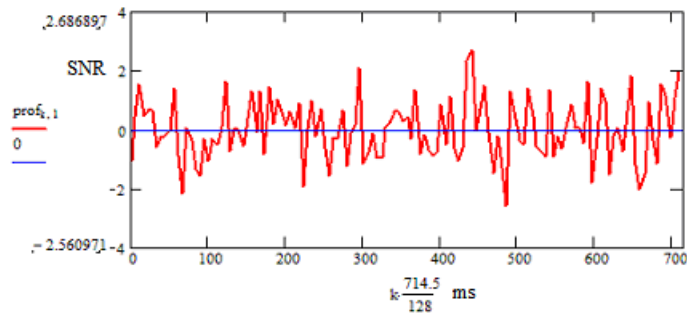


Figure 1 Basic folding, 128 bins, resolution ~ 5.6 ms. Target Pulsar SNR = 2.7:1 (at bin No: 79 \sim 441ms/714.5ms)

The basic folding algorithm limits the number of fold bins, and final time resolution, to numerically equal the pulsar period divided by the average pulse half-height width (for B0329, 714.5/6.5 \sim 110). In this way, the folding

averaging process reduces the data bandwidth to effectively just pass the pulsar pulse duration so maximizing the potential SNR.

Unfortunately, unless the pulse peak happens to lie in the center of a fold resolution bin, this is not so, as shown in Figure 1 with 128 bins, where the indicated target SNR = 2.7:1.

With this estimation alone, the probability of confirming pulsar detection is very low.

If, $p_{b,n}$ is the n^{th} period in the data record, each period sampled into B bins, where $b = 0 \rightarrow B-1$, the basic folding (summing) of N coherent periods can be described by,

$$F1_b = snr \left(\sum_{n=0}^{N-1} p_{b,n} \right) \quad (1)$$

where, $F1_b$ defines the folded equivalent data SNR at bin ' b '; for basic folding the optimum number of fold bins $B = P/W$.

The function $snr()$, calculates the folded data SNR. The summation term coherently sums the N discrete pulsar periods $p_{b,n}$, where $n \rightarrow 0$ to $N-1$.

If the folding bin resolution is simply increased to around 0.7 ms (1024 bins), higher frequency noise is allowed in and the target pulsar pulse is further obscured as typically shown in Figure 2.

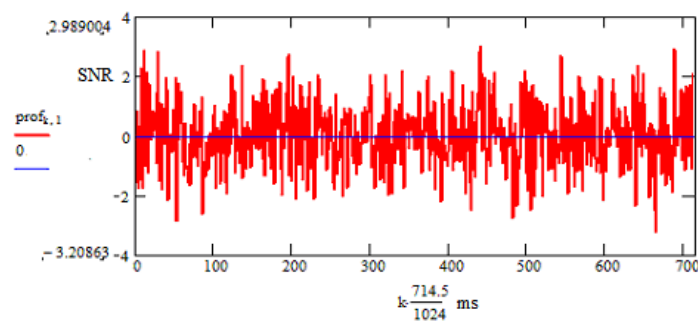


Figure 2 Basic folding, 1024 bins, bin resolution ~ 0.7 ms

2. Matched-filter Fold - optimizes SNR and resolution

An obvious alternative to basic folding is to low-pass filter the data to achieve the pulse-matched data bandwidth. In this case there is no restriction on bin numbers and much better resolution is possible to more accurately identify the pulse peak. Figures 2 and 3 show increased target detectability between without and with band limiting. The indicated SNR increases to 4.1:1 and is slightly more credible as a B0329 pulsar acquisition.

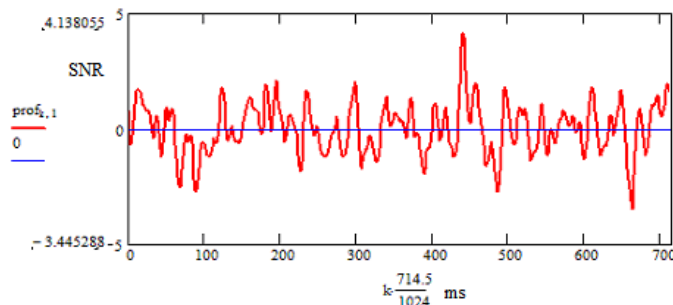


Figure 3 Matched-filter folding, bin resolution ~ 0.7 ms. Target Pulsar SNR = 4.1:1 at bin 631 ~ 441ms/714.5ms

Also, the improved resolution allows checking the pulsar target pulse width adding some detection confidence.

This matched-filter process SNR at bin 'b' is now described by,

$$F2_b = snr \left(\sum_{n=0}^{N-1} p_{b,n} \right)_{Fil} \quad (2)$$

where now, the number of resolution bins B , can be much greater than P/W .

The suffix addition Fil indicates the data is pre-filtered to just pass the pulsar pulse bandwidth. The filtering can be implemented by low-pass data filtering or FFT convolution with a pulse width matching Gaussian pulse.

3. Partial Folding - simplifies further analysis

In partial folding, the data is folded into a number of period-synchronized blocks or sections and each are matched-filter folded. This process partially averages and compresses the data, making it easier and quicker to analyze further. No information is lost.

In Figure 4, the 16800 seconds of drift scan data from the 28 degree beamwidth antenna is coherently divided and folded into 128 sections or equivalent periods. The measured target SNR in each section is plotted against section number.

These sections data can be processed in several ways but summing folds from all sections and calculating the final SNR produces exactly the same result as Figure 3 indicating that no information is lost.

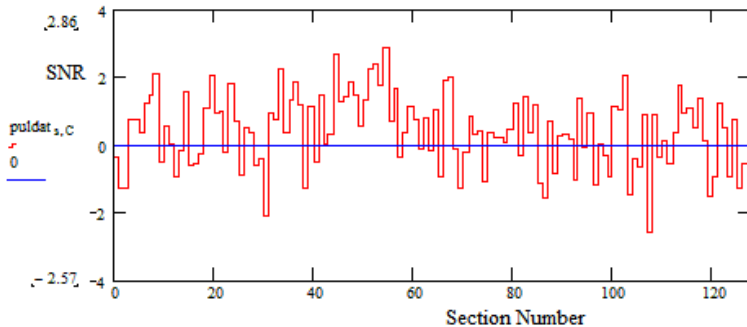


Figure 4 Matched-filter partial folding into 128 sections - target pulse bin SNR

The partial folding algorithm is described by,

$$F3_{b,s} = snr \left(\sum_{n=\frac{N}{S}s}^{(s+1)\frac{N}{S}-1} p_{b,n} \right)_{Fil} \quad (3)$$

$F3_{b,s}$ specifies the match-filtered fold SNR at bin number 'b' of the folded section 's', where S is the total number of sections and $s = 0 \rightarrow S - 1$.

Each section synchronously folds N/S consecutive pulsar periods.

As expected for this weak signal, the section target signal SNRs are low and comparable to the folded noise level. If the example data were just random noise, the mean should be zero with the SNR peaks around $\pm 3:1$ SNR. It is noted that in Figure 4, that there is a region between sections 40 and 60 that is largely positive, (signifying the possibility of a strong target signal) but towards the end of the observation the data appears closer to zero mean (target exiting the antenna beam?).

The estimated antenna 3dB dwell on target for this example is between sections 10 an 90.

4. Cumulative Folding - finds best SNR in full data

With cumulative folding, first the target folded SNR of section 0 is plotted relative to the x-axis section 0. Then sections 0 and 1 folds are summed and the combined SNR plotted relative to x-axis section 1. And so on until all sections are summed and plotted relative to section 127. In this way the growth of the target SNR is visualized, indicating strong (steep rise) and weak (falling SNR) scintillating or target acquisition sections.

The cumulative folding algorithm operates on the partially folded and filtered section data, $F3_{b,s}$ and is described by,

$$F4_{b,s} = snr\left(\sum_{a=0}^s F3_{b,a}\right) \quad (4)$$

$F4_{b,s}$ specifies the cumulative fold SNR at bin number 'b' of the sum of all sections numbers less than and including section 's'.

The example data cumulative result at the target bin peak position is plotted in Figure 5.

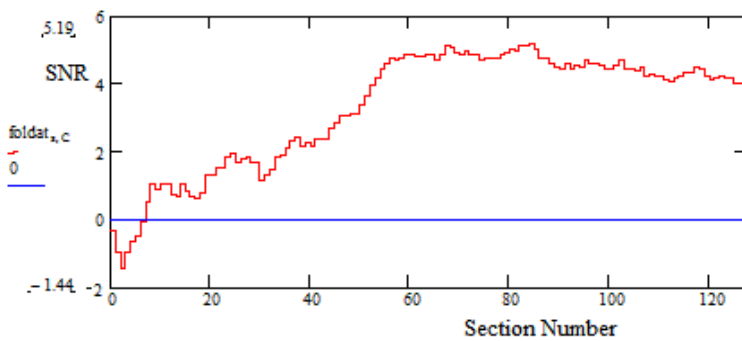


Figure 5 Matched-filter section cumulative target folding - Best Target Pulsar SNR = 5.2:1

The obvious conclusion from cumulative SNR plot is that there is a significant SNR increase between sections 30 and 60, but the trend is to a reduction in SNR towards higher section numbers. A maximum cumulative SNR of 5.2:1 is indicated around section 85, reducing to 4.1:1 when all the sections are accumulated, the final figure agreeing with all the data folded at section 127 as in Figure 3.

An immediate suggestion might be to trim the data file at a point equivalent to section 85, but maybe we can do better!

Figure 6 plots the target bin peak together with all noise-containing bins outside the target pulse showing that the noise typically lies within $\pm 3 \times$ rms level (SNR $\equiv 3:1$) and indicates no significant or long-term growth with the accumulating sections.

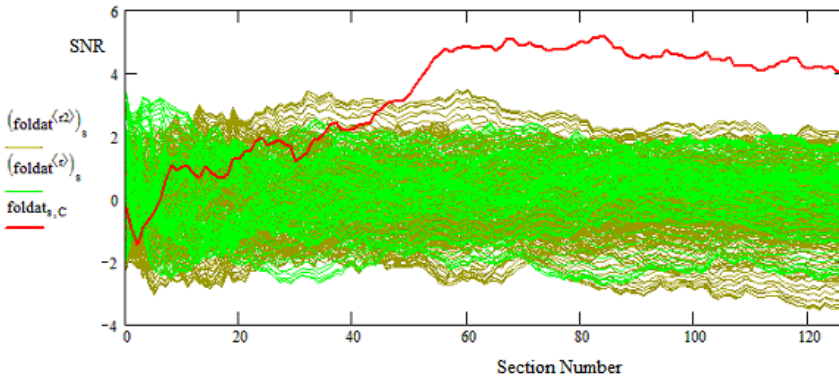


Figure 6 Matched-filter section cumulative folding - target + noise bins outside target

The obvious rise and fall of the accumulated target SNR suggests that there is a continuous portion of the data that maximizes the target SNR and the following algorithm variants identify and locate this optimum range.

5. Rolling Block Average Folding - finds optimum SNR extent

For this rolling average block fold algorithm, first the maximum SNR (target or noise) of all single section folds is plotted relative to x-axis section 0 in Figure 7. Then the maximum SNR of all adjacent section sums is plotted relative to x-axis section 1. Similarly the maximum SNR of all 3 adjacent section sums is plotted relative to section 2 and so on to all 128 sections folded together and summed with the SNR plotted relative to section 127; this final SNR figure again agreeing with the original all data fold result.

This algorithm effectively does a variable section block scan across all sections and reports the maximum SNR observed within each scan-block range. Assuming a constant amplitude pulsar pulse is present then a rising square-root curve would be expected. For a scintillating pulse, the plotted curve maximum indicates the optimum extent of the densest target region in the observation.

The rolling average block folding algorithm is described by,

$$F5_s = \left| \max_b \left(snr \left(\sum_{x=y}^{x=s+y} F3_{b,x} \right) \right) \right|_{y=0}^{y=S-s-1} \quad (5)$$

where, the $\max_b(\)$ function records the maximum of each variable summation/fold bin 'b' data SNR maximum.

Figure 7 plot maximum shows the minimum number of adjacent summed sections needed to ensure maximum target signal amplitude or scintillation optimum SNR. In this case, just 36 sections folded together (approximately 80 minutes) out of the total 16800 seconds observation would generate an increased target SNR of 6.8:1. In fact, just 14 sections generates an SNR of 6.5:1 (approximately 31 minute observation time).

Note that in some early blocks containing only a few sections, these could report a noise or RFI spike peak - this can be checked by reporting the corresponding peak bin number in parallel since once the accumulating target dominates the bin report number will stabilize at the target final value.

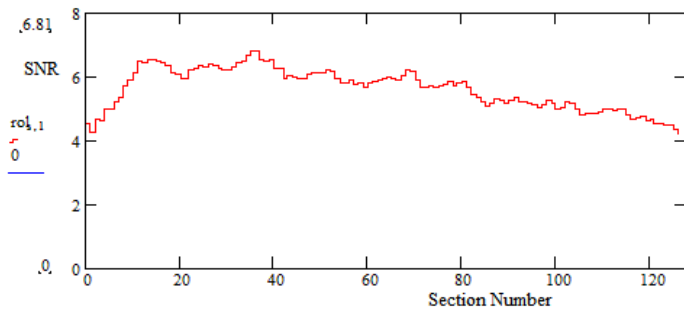


Figure 7 Rolling Block Average Peak Plot - Target Pulsar Best Maximum SNR = 6.8:1

Whilst this algorithm indicates the optimum wanted data block extent, it does not identify the optimum position in the data, which is left to algorithm 6 below.

6. Optimum Block Fold - finds best SNR data range center

This final fold algorithm locates the section center that produces the indicated optimum section block from Algorithm 5, above. With the optimum extent, in this example, 36 sections, the sections (0 to 35) are summed and the peak SNR plotted relative to the halfway x-axis section 18 in Figure 8. Then the next 36 sections 2 to 37 are summed and the SNR result is plotted relative to section 19 etc.:. Until the final data plot at section 109, summing sections 91 to 127. The result is shown in Figure 8 from which several conclusions can be drawn, not the least being the obvious received signal strength tracking the static antenna beam pattern.

The optimum block center search algorithm is written,

$$F6_{y+\frac{S^*}{2}} = \left| \max_b \left(snr \left(\sum_{x=y}^{x=y+S^*-1} F3_{b,x} \right) \right) \right|_{y=0}^{y=S-S^*-1} \quad (6)$$

where, S^* is the optimum range identified by the peak position plot of Algorithm $F5$.

Plotting $F6_{y+S^*/2}$ over the variable 'y' range $0 \rightarrow (S - S^* - 1)$ generates a plot as in Figure 8.

The maximum occurring at SNR 6.8:1, identifying the optimum center section for the 36-section fold as section 50.

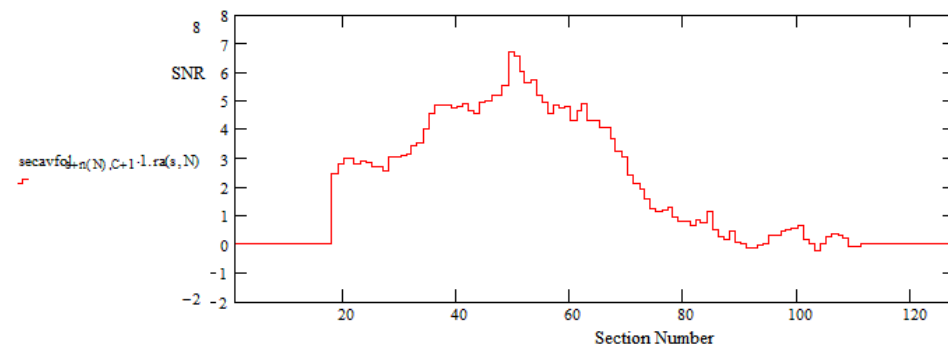


Figure 8 Optimum 36-Section Fold ($S^* = 36$), Target Pulse bin SNR Peaking at Section 50

The extended observation (above section 90) as the target drifts out of the antenna beam confirms the expectation of zero mean system noise.

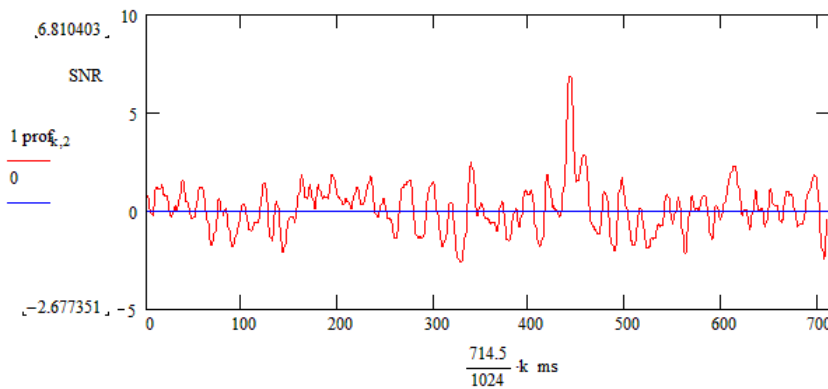


Figure 9 Optimum 36-Section Fold, Centered on Section 50, SNR = 6.8:1.

Figure 9 shows the target bin SNR result with the optimum 36-section range, centered on section 50 when the peak target SNR indicates an SNR of 6.8:1.

Finally, Figure 10 plots the optimum 36-section sum SNR after de-dispersion, indicating a further improvement of SNR from 6.8:1 to 7.4:1.

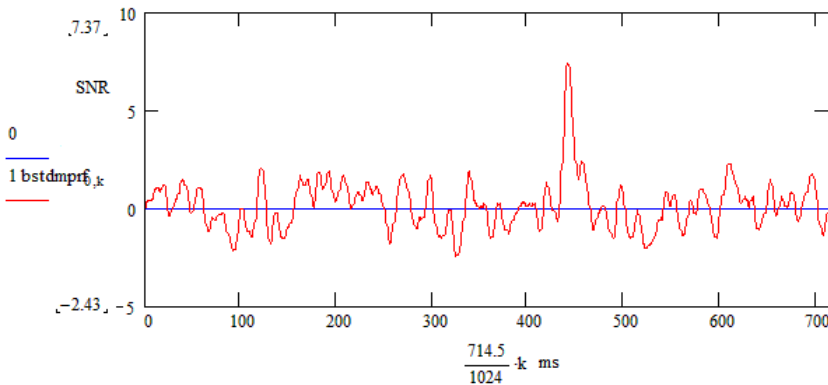


Figure 10 Optimum 36 -Section Fold, De-dispersed Result. SNR = 7.4:1

Conclusions

With drift-scan pulsar observations, due to target scintillation and/or antenna beam pointing accuracy, it is not always advisable to rely on restricting the observation time to be controlled by the antenna 3dB beam-width. On the other hand by extending the observation time, it allows target confirmation by noting the target is rejected out of beam whereas any repetitive pulse-type RFI masquerades might be relatively unaffected.

This article has shown that by adapting the standard folding algorithm the optimum region for maximizing the final measured target SNR can be found. An important message here is that no data was rejected, although with the tools described, weak and low contribution data sections and/or sub-bands within this range are easily identified and could have been rejected.

From the original basic fold SNR estimate of 2.7:1, by choosing the optimum reception region the final estimate of 7.4:1 is much more convincing.

The key aspect of the fold algorithm adaptations described is that they allow detailed investigation and tracking of scintillation and amplitude/time variations in collected data and provide improved evidence of genuine intercepts.

By extracting and fully analyzing the optimum SNR data range, it has been found that other pulsar parameter search indicators, such as period/p-dot correlation and dispersion, become more convincing.

Caution - So what can be learned from this exercise?

Automatic software analysis of B0329+54 strongly scintillating data is unlikely to offer the best SNR result. Data manipulation/selection/rejection schemes intended for RFI suppression should be well understood to ensure confidence in the final SNR result.

Two confidence criteria were applied in this exercise, the first to note the amplitude tracking the antenna beam pattern and the second to closely track the de-dispersion theoretical response. Both were positive. However, it is recognized that at relatively low final SNRs, the influence of system noise is still evident. For example, if sn is the actual SNR, there is a significant probability that the measured value is in the range $sn \pm 1$. This means that at low SNRs this noise uncertainty can still affect the accuracy of period, pdot and dispersion measure (DM) searches. Period search accuracy is dependent upon valid pulsar intercept duration and for dispersion search, be aware that the residual base noise adds a zero DM component which can affect DM estimation accuracy.

PWEast, March 2024



Peter East, pe@y1pwe.co.uk is retired from a Defense Electronics career in radar and electronic warfare system design. He has authored a book on Microwave System Design Tools, is a member of the British Astronomical Association since the early '70s and joined SARA in 2013. He is presently active in amateur detection of pulsars using SDRs, and researching low SNR pulsar recognition and analysis. He has recently written two other books, 'Galactic Hydrogen and Pulsars' and 'Small Aperture Pulsar Detection', both describing his work in Radio Astronomy. He maintains an active RA website at <http://www.y1pwe.co.uk/RAProgs/>

Notes on building a maser receiver

by Dimitry Fedorov UA3AVR

This paper is about building receivers optimized for astronomic masers detection. Subjects of consideration are receiver parameters and tunings, the radiometer equation for maser lines, Software Defined Radios (SDR) usage for spectral observations, processing of samples, and data postprocessing. I would also share some details of my experience on receiver building using Ettus USRP SDRs. It is supposed that the maser receiver is equipped with a parabolic reflector antenna; they are together is a single dish maser telescope considered here. Discussed issues are concerned on small dish telescopes; some of issues are general for observations with spectral line analysis.

General notes on maser receivers

As expected a maser receiving system provides:

- Enough receiving bandwidth for the maser spectrum with all its features; it may be as wide as up to several MHz.
- Rather small resolution bandwidth (RBW) to distinguish narrow maser lines or narrow features of maser spectrums;
- Averaging (integration) procedures to pick out a maser spectrum from the background noise. It is assumed the telescope antenna looks to observed maser all the integration time;
- Performing the integration on-fly without storing intermediate data in the computer memory;
- Possibility for several day observations combining obtained data in one result;
- Tools of correction the receiver frequency response (FR), which can be significantly uneven and distort weak received spectrums when the integration time is rather long;
- Recalculation scales of spectrum axes to get a plot in Jy versus velocity (VLSR).

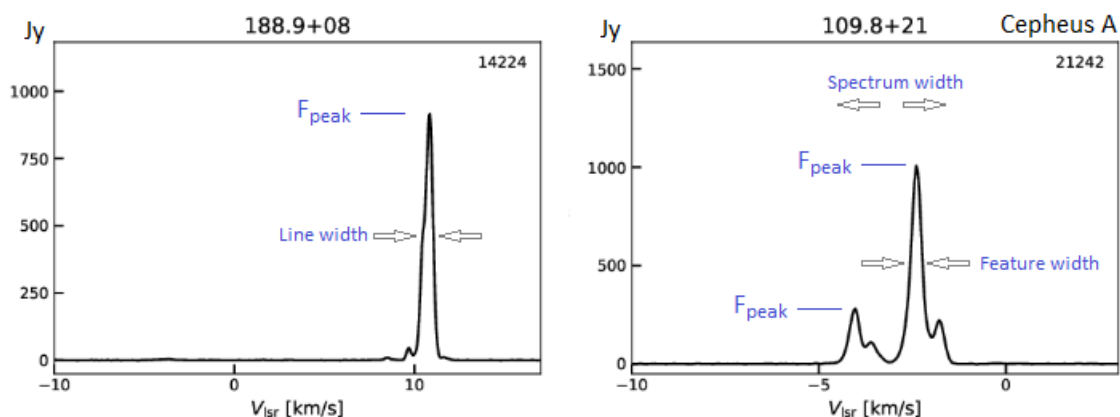


Figure 1. Examples of maser lines and spectrums form Ibaraki iMet [1] for methanol 6.7 GHz masers.

Maser spectrums are usually drawn in plots versus Velocity in Local Standard of Rest (VLSR), see Figure 1. It reminds that a maser cloud is a moving object, and one observes a line at the Earth with the Doppler shift. Moreover, different parts of this cloud may move differently leading to the multiline or broadened spectrum. Needed minimal receiving bandwidth Δf can be obtained from expected width of a maser spectrum Δv in velocity units,

$$\Delta f = f_{\text{line}} \Delta v / c, \quad (1)$$

where f_{line} – the frequency of observed molecular line, c – the speed of light $\approx 300\,000$ km/s. Let's consider W49 H₂O 22 GHz maser spectrum for example. According [2] one can anticipate the width of W49 spectrum Δv about 40 km/s; the line frequency $f_{\text{line}} \approx 22\,235$ MHz. Minimal receiving bandwidth will be $22\,235 \text{ MHz} \cdot 40 / 300\,000 \approx 3$ MHz. This is rather wide spectrum and receiving bandwidth; for methanol maser lines 6.7 and 12 GHz the receiving band up to 1-2 MHz would be enough [3,4]. For 1.6 GHz OH lines the receiver bandwidth can be even narrower.

Formula (1) could be applied for resolution bandwidth (RBW) estimations. Let's suppose a hunted maser line has 1 km/s in width. One need the resolution at least 0.2 km/s (5 times narrower the line width) for possibility to draw the line shape on the spectrum screen. This is so called "5 times rule". Now Δf from (1) has to be understood as RBW, Δv as a resolution in the maser spectrum versus VLSR. So, the RBW for H₂O spectrum 22 GHz will be $22\,235 \cdot 0.2 / 300\,000 \approx 0.015$ MHz=15 kHz, for 6.7 GHz methanol spectrum RBW ≈ 4.5 kHz, for 12 GHz methanol spectrum RBW ≈ 8 kHz.

The resolution bandwidth RBW defines needed average (integration) time for picking out the line from the background noise. An expected peak flux in Jy of the maser spectrum F_{peak} is needed for time estimations. The integration time Δt can be extracted from the radiometer equation (see its general form ch. 4.2.1 in [5]),

$$\Delta T_{\text{ant}} = K T_{\text{sys}} / (\Delta t \text{ RBW})^{1/2}, \quad K=3 \text{ or more.} \quad (2)$$

Here ΔT_{ant} means the added antenna temperature from the maser peak flux F_{peak} , which can be discerned after the integration time Δt , T_{sys} – the system temperature of the telescope (has to be known *a priori*), RBW – is needed resolution bandwidth. The coefficient $K=3$ (the peak factor) is inserted in (2) keeping in mind that the line peak in received spectrum has to be at least 3 times higher than RMS of the background noise after averaging. The added antenna temperature ΔT_{ant} can be calculated also from the antenna sensitivity (forward gain) G using formulas (see ch. 7.1.4 in [5])

$$\Delta T_{\text{ant}} = G F_{\text{peak}}, \quad G = \eta_A \pi D^2 / (8 k). \quad (3)$$

Here η_A – the Aperture Efficiency of the dish antenna (to be known *a priori* too), D – the reflector diameter, $k=1.380649 \cdot 10^{-23}$ J/K – the Boltzmann constant. The antenna sensitivity (forward gain) G is measured in K/Jy. It can be measured immediately (see details in [6]), but one should care for choosing the cold sky point in measurements and for recalculations the known solar flux to needed frequency. Equations (2) and (3) give the same ΔT_{ant} ; combining them one can get the integration time

$$\Delta t = (K \text{ SEFD} / F_{\text{peak}})^2 \text{ RBW}^{-1}, \quad \text{SEFD} = T_{\text{sys}} / G, \quad (4)$$

and vice versa, the estimation of minimal detectable peak flux F_{peak} for given integration time Δt can be calculated by

$$F_{\text{peak}} = K \text{ SEFD} / (\Delta t \text{ RBW})^{1/2}. \quad (4a)$$

Here $\text{SEFD} = T_{\text{sys}} / G$ is the System Equivalent Flux Density usually expressed in Jy; it is a kind of measure of the telescope sensitivity and means a flux density which gives the same added antenna temperature as T_{sys} (see ch. 7.3 in [5] or [6]). Equation (4a) can be considered as a radiometer equation for maser telescopes.

Let's consider my methanol maser telescope 6.7 GHz, Figure 2, for example of calculations by (4), (4a). The telescope characteristics was following:

- Dish size $D = 1.8$ m, linear polarization feed, downconverter with LO=5.7 GHz, IF ≈ 969 MHz.
- Sensitivity (forward gain) $G = 0.0006$ K/Jy [7];
- Aperture efficiency $\eta_A = 0.65$;
- System temperature:
- $T_{sys} \approx 150$ K, by Y-factor method with brickwall as a hot source [4];
- $T_{sys} \approx 115$ K, estimated by lunar noise measurements in the end of September 2023 [7];
- Maser automatic tracking during all the integration time.



Figure 2. Methanol maser telescope 6.7 GHz.

The worst value of $T_{sys} = 150$ K is taken for SEFD, integration time $\Delta t = 2$ hours = 7200 s, resolution bandwidth RBW=4.5 kHz = 4500 Hz, peak factor $K=3$. For SEFD value we have $150/0.0006 = 2.5 \cdot 10^5$ Jy. Minimal peak flux for the line detection will be by (4a) $F_{peak} = 3 \cdot 2.5 \cdot 10^5 / (7200 \cdot 4500)^{1/2} \approx 132$ Jy. Lines with higher F_{peak} would be identified on the spectrum screen more fairly.

Similarly, for line with peak flux density $F_{peak} = 500$ Jy one need the averaging time by (4) $\Delta t = (3 \cdot 2.5 \cdot 10^5 / 500)^2 / 4500 = 500$ s ≈ 8 min, but further averaging would help to recognize the line better.

One can sacrifice the "5 times rule" choosing the RBW size about a maser line width. Then the integration time could be 5 times shorter for quick detection, but the line shape will be lost. Wider RBWs are not recommended.

SDR for a maser receiver

Here we consider the structure of SDR maser receiver and some issues in its building. General schematic of receiving system is shown on Figure 3 and consist of hardware and software parts presented by groups of blocks. It is supposed the first stage (LNA and downconverter) on the schematic gives rather high amplification of antenna signal for well work of the telescope at all. Our main attention will be concentrated around following stages. Next is the SDR receiver module based on quadrature (IQ) receiver. Inside this receiver we have two mixers fed by one local oscillator (LO) but with phases shifted by 90° . These mixers convert the input signal to zero frequency in both I and Q channels, i.e. they realize so called quadrature direct conversion receiver. Hence, frequency of the local oscillator F_{LO} defines the central frequency of the receiver as a whole. The receiving band will be defined next by the sample rate F_s for Analog-to-Digital Converters (ADC); it is measured in frequency units or in samples per second.

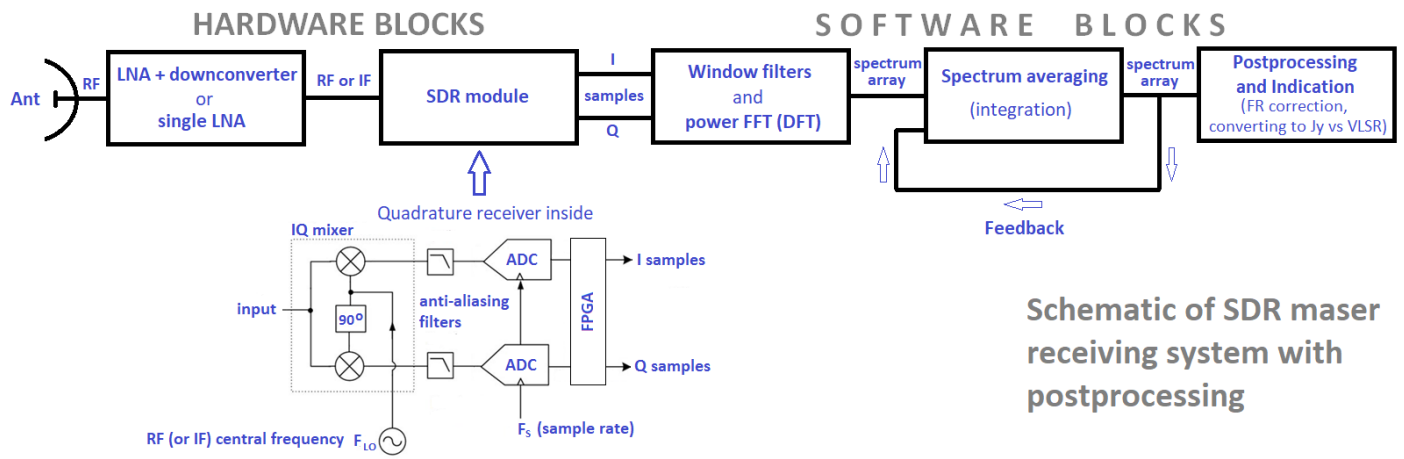


Figure 3. General schematic of SDR maser receiving system.

Full width of the receiving band is exactly F_s , i.e. it is equal to the sample rate and lays in bounds from $F_{LO} - F_s/2$ to $F_{LO} + F_s/2$. Anti-aliasing filters limit the receiver band in these bounds; in real receivers anti-aliasing filters may even make the receiver band lesser than F_s , see Figure 4. Frequency $F_s/2$ is called the Nyquist frequency. Necessity of anti-aliasing filters is forced by the Nyquist sampling theorem, ch. 1.3 [8], which limits the receiving band by F_s in quadrature IQ receivers. There are input signals (aliases) outside the range $[F_{LO} - F_s/2, F_{LO} + F_s/2]$, and they will be indistinguishable from similar signals inside after sampling by ADCs with the rate F_s . Anti-aliasing filters suppresses the signals outside the range $[F_{LO} - F_s/2, F_{LO} + F_s/2]$, but may distort the frequency response of receiver noticeably.

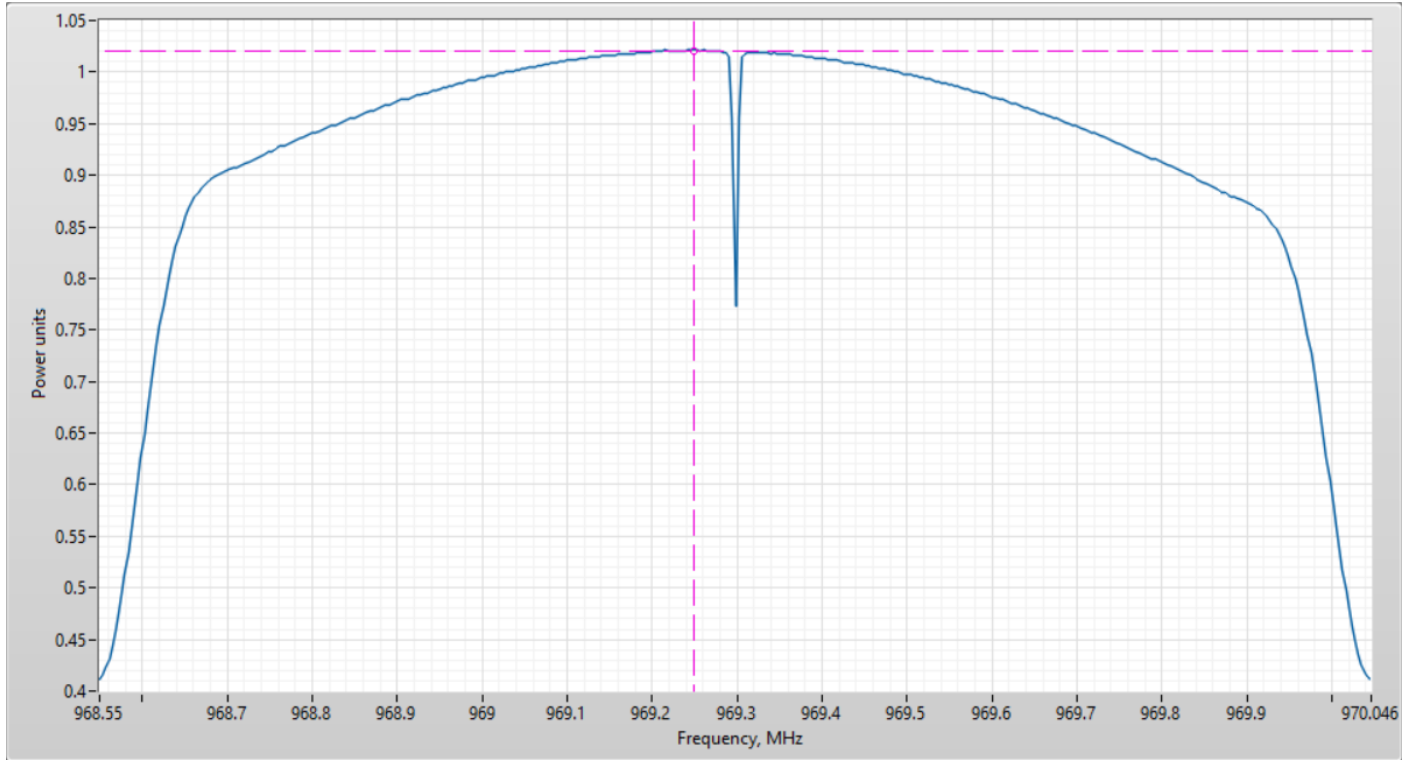


Figure 4. Frequency response of Ettus USRP B200mini in linear power units. Here $F_s=1.5$ MHz, $F_{LO}=969.3$ MHz.

As an example, see the frequency response of my receiver (Ettus USRP B200mini) in linear power units, Figure 4; it is bell shaped definitely, and a final correction of the frequency response will be desperately needed for a maser

receiver. The anomaly at the center frequency is connected to DC (zero frequency) suppression features in USRP devices.

In any case, one should remember a real receiver bandwidth Δf may be somewhat less the sample rate F_s due to anti-aliasing and digital filtering in FPGA (Field Programmable Gate Array); therefore, the sample rate F_s should be chosen somewhat higher. FPGA is now a customary element of SDR receivers, it allows to improve the receiver control and performance.

IQ samples in two channels are often presented by complex numbers S , i.e. $S = I + i Q$, where i – imaginary unit, $i^2 = -1$, I or Q presents here real samples in I or Q channels. Such presentation is convenient for programmers of following software blocks in Figure 3.

The sequence of complex samples is going to the first of software blocks in Figure 3 where it is converted to spectrum data. This conversion is made using the Fast Fourier Transform (FFT), which is a quick version of the Discrete Fourier Transform (DFT). One should choose the number of FFT points N for conversion; the FFT takes N samples from the input sequence and gives an array with N complex points of the frequency spectrum. This number is a nearest integer to F_s / RBW ,

$$N = \text{round} (F_s / RBW), \tag{5}$$

but a nearest $N = 2^k$, k is natural >0 , $N \geq F_s / RBW$, can be preferable to speed up the conversion. Output spectrum is divided to N equal frequency bins; the RBW value becomes the width of bins. A larger number N leads to a longer time of conversion; the time of conversion rises with N as $N \ln(N)$. One should also check the FFT spectrum is properly arranged; the zero frequency has to be at the center of the spectrum array.

For my 6.7 GHz maser telescope Figure 2 the sample rate F_s was chosen $=1.5 \text{ MHz} = 1\,500\,000 \text{ Hz}$. For $RBW = 4.5 \text{ kHz} = 4500 \text{ Hz}$ the number of FFT points is $N = \text{round} (1\,500\,000 / 4500) = 333$. We can also find a nearest higher power of 2 and choose $N = 2^9 = 512$. In this case RBW becomes smaller, $RBW = 1\,500\,000 / 512 \approx 2930 \text{ Hz} = 2.93 \text{ kHz}$, and the integration time Δt longer.

Windowing before FFT mitigates drawbacks, which stem from their discrete nature; windowing suppresses unavoidable spectrum sidelobes, lowers the spectral leakage from bin to bin, smooths the bin shape, and makes the dynamic range of the transform higher. Some popular window functions are collected in Table 1. Windows (except rectangular) also bring some losses to the passed signal.

Table 1. Characteristics of window functions by [9].

Name	Peak sidelobe level (to peak of the main lobe)	Integrated sidelobe level (power in sidelobes)	Equivalent Bandwidth (ENB) to nominal	Noise to nominal
Rectangular (no windowing)	-13.3 dB	-10.1 dB	1.00	
Hamming	-42.7 dB	-34.4 dB	1.36	
Blackman-Harris (Nuttall) 3 term	-71.5 dB	-60.3 dB	1.70	
Flat Top 3 term	-44.4 dB	-38.6 dB	2.97	

As one can see, window filters are characterized also by the Equivalent Noise Bandwidth (ENB), which is wider than the nominal bin width (predefined RBW). It means more noise is coming to every bin when windowing is applied. Equations (4), (4a) tell that the integration time Δt can be shorter with windowing, and it helps to uphold the "5 times rule" for RBW. I usually applied the Hamming window with RBW by "5 times rule" or narrower, but for other RBWs wider windows may help better.

The output of transform has to be a spectrum in power units,

$$\mathbf{P}_{N \text{ bins}} = \text{FFT}(\mathbf{S}_N) \text{FFT}^*(\mathbf{S}_N) / \mathbf{N}^2 \quad (6)$$

where * means the complex conjugate, $\mathbf{P}_{N \text{ bins}}$ – means the array of power spectrum with \mathbf{N} points, and the function $\text{FFT}(\mathbf{S}_N)$ presents the FFT procedure over time domain array with \mathbf{N} complex samples \mathbf{S}_N . Operations of multiplication, division and complex conjugation in (6) are element-wise. Next block at schematic Figure 3 has to perform the integration (averaging) of power spectrums. The power spectrum points are just usual real numbers.

Following averaging procedures can be performed on-fly without saving current FFT spectrums. Let \mathbf{M} is a number of power spectrums needed to be averaged. The spectrum power at \mathbf{k} -th step of averaging ($\mathbf{k} = 1, 2, \dots$) will be

$$\begin{aligned} \bar{\mathbf{P}}_{N \text{ bins}}(\mathbf{k}) &= ((\mathbf{k}-1) \bar{\mathbf{P}}_{N \text{ bins}}(\mathbf{k}-1) + \mathbf{P}_{N \text{ bins}}) / \mathbf{k}, \quad \mathbf{k} \leq \mathbf{M}; \\ \bar{\mathbf{P}}_{N \text{ bins}}(\mathbf{k}) &= ((\mathbf{M}-1) \bar{\mathbf{P}}_{N \text{ bins}}(\mathbf{k}-1) + \mathbf{P}_{N \text{ bins}}) / \mathbf{M}, \quad \mathbf{k} > \mathbf{M}. \end{aligned} \quad (7)$$

Here $\mathbf{P}_{N \text{ bins}}$ without overbar means a current power spectrum with \mathbf{N} points obtained from FFT, eq. (6). Formula (7) describes the feedback loop with arrows from Figure 3; a next step of averaging uses results from the previous step. All summations, multiplications and divisions in (7) are element-wise. The current value $\bar{\mathbf{P}}_{N \text{ bins}}(\mathbf{k})$ is called sometimes "running mean"; the feedback procedure (7) – is called correspondingly "running integration". The bar over $\bar{\mathbf{P}}_{N \text{ bins}}(\mathbf{k})$ means that we operate with averaged spectrum. As the result of averaging $\bar{\mathbf{P}}_{N \text{ bins}}$ one should take the value $\bar{\mathbf{P}}_{N \text{ bins}}(\mathbf{k})$ when $\mathbf{k} \geq \mathbf{M}$. The integration time Δt will be then

$$\Delta t = \mathbf{M} \mathbf{N} / \mathbf{F}_s. \quad (8)$$

Needed number of averages \mathbf{M} is a nearest integer to $\Delta t \mathbf{F}_s / \mathbf{N}$,

$$\mathbf{M} = \text{round}(\Delta t \mathbf{F}_s / \mathbf{N}). \quad (8a)$$

Above example with 6.7 GHz telescope from Figure 2, $\Delta t = 2 \text{ hours} = 7200 \text{ s}$, $\mathbf{F}_s = 1.5 \text{ MHz} = 1\,500\,000 \text{ Hz}$, $\mathbf{N} = 333$, gives for needed numbers of averages by (8a) $\mathbf{M} = \text{round}(7200 \cdot 1\,500\,000 / 333) = 32\,432\,432$.

The averaging procedure by formulas (7) works well and even is capable to save computer resources when the sampling and the samples processing would be made simultaneously. When the sampling and processing are sequential, one after other, there are reasons for some modifications. Samples could be fetched from the SDR module by large packets. For each packet, the size is $\mathbf{N} \cdot \mathbf{L}$, where \mathbf{L} is a rather large integer, and the sampling time t_{sampling} has to be much longer the processing time,

$$t_{\text{sampling}} = \mathbf{N} \mathbf{L} / \mathbf{F}_s \gg \text{processing time}. \quad (9)$$

Then a total observation time will be just a little longer the integration time. The FFT takes data from this packet by portions with \mathbf{N} samples at a time giving \mathbf{L} raw spectrum arrays. Afterwards these \mathbf{L} spectrums have to be element-wise averaged taking usual arithmetic mean, and then the running procedure with feedback by (7) can be applied to these mean over a packet spectrums. In this case the number \mathbf{M} will be smaller by \mathbf{L} times approximately,

$$\mathbf{M} = \text{round}(\Delta t \mathbf{F}_s / (\mathbf{N} \mathbf{L})), \quad (9a)$$

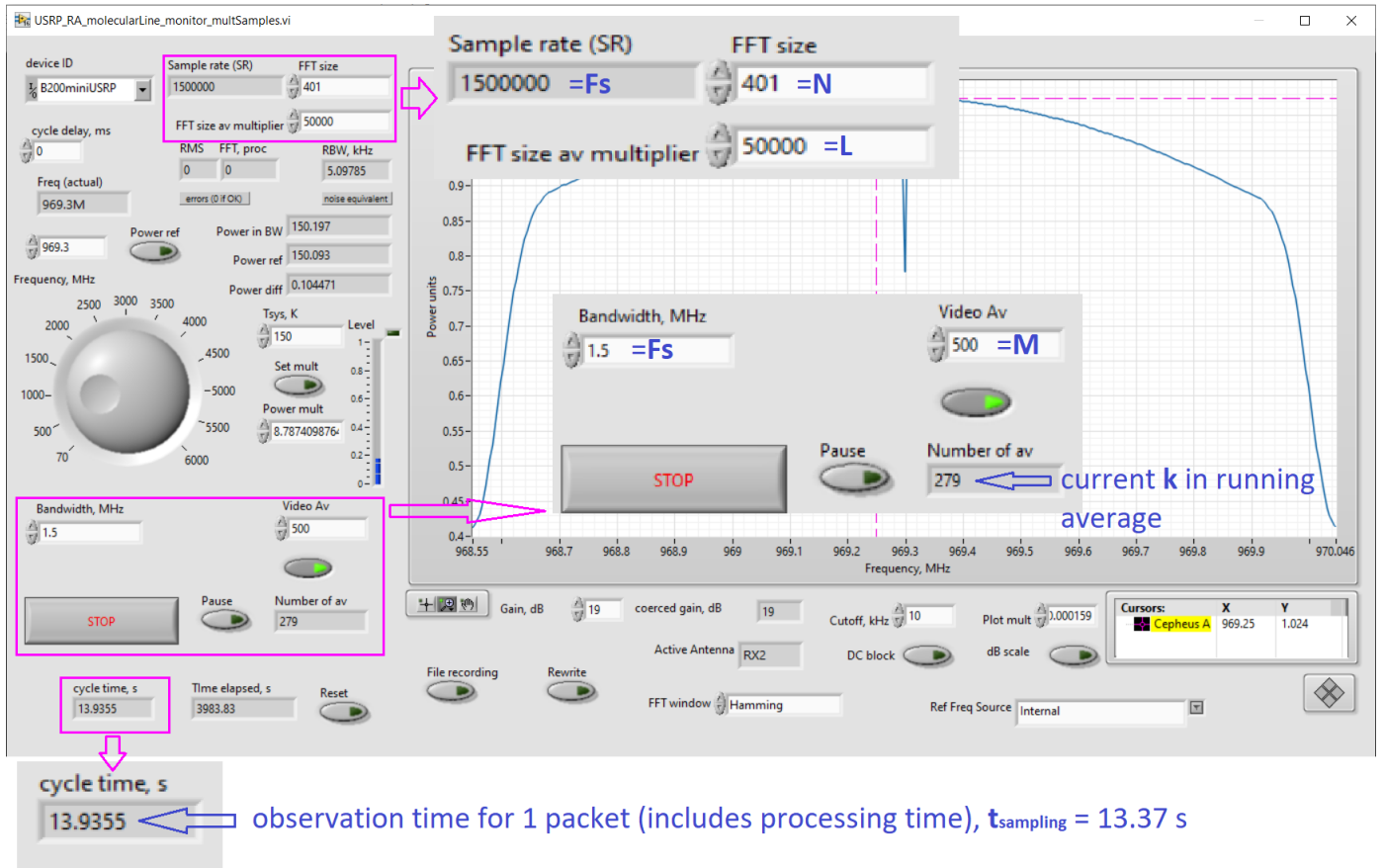


Figure 5. Receiver screen with sequential sampling and processing. Taken during 6.7 GHz maser observation process.

Now the integration time formula is modified,

$$\Delta t = M L N / F_s. \quad (9b)$$

The 6.7 GHz telescope example with $L=50\,000$ gives now $M = \text{round}(7200 \cdot 1\,500\,000 / (333 \cdot 50\,000)) = 649$ and for the sampling time $t_{\text{sampling}} = 333 \cdot 50\,000 / 1\,500\,000 = 11.1$ s, which is expectedly much longer the processing time for $L=50\,000$ raw spectrums.

The sequential algorithm was realized in my LabVIEW soft for Ettus USRP receivers, see the screen from practical observations at Figure 5; the relation (9) is satisfied definitely.

Postprocessing procedures

The last block at Figure 3 makes the frequency response (FR) correction and other procedures to get a well readable spectrum picture. For such correction, one need the background spectrum obtained when antenna is directed to the empty sky. Then the corrected, normalized to 1, and shifted to 0 spectrum $\bar{A}_{N \text{ bins}}$ with N points will be

$$\bar{A}_{N \text{ bins}} = \bar{P}_{N \text{ bins}} / \bar{P}_{N \text{ bins, background}} - 1. \quad (10)$$

Here $\bar{P}_{N \text{ bins}}$ designates the result of averaging procedures described above, $\bar{P}_{N \text{ bins, background}}$ – the same, but when antenna is directed to the empty sky and all other condition and tunings are preserved; operations of division and subtraction in (10) are element-wise. It is recommended to collect $\bar{P}_{N \text{ bins, background}}$ shifting the antenna beam just a bit aside in azimuth; then the atmosphere noise will be the same, what is mostly significant for H_2O 22 GHz observations. For OH lines 1.6 GHz possible remnants of the galaxy noise at centimeters can contribute to the

empty sky noise; then the shifting antenna aside from the source would be by small deviations in RA and DEC with further tracking. As expected, the atmosphere noise is small at 1.6 GHz. The bar over $\bar{A}_{N \text{ bins}}$ reminds that we operate with an averaged spectrum still.

For example of FR correction procedure (10) see Figure 6 with results for $\bar{A}_{N \text{ bins}}$ in practical Cepheus A observations 2023-09-21.

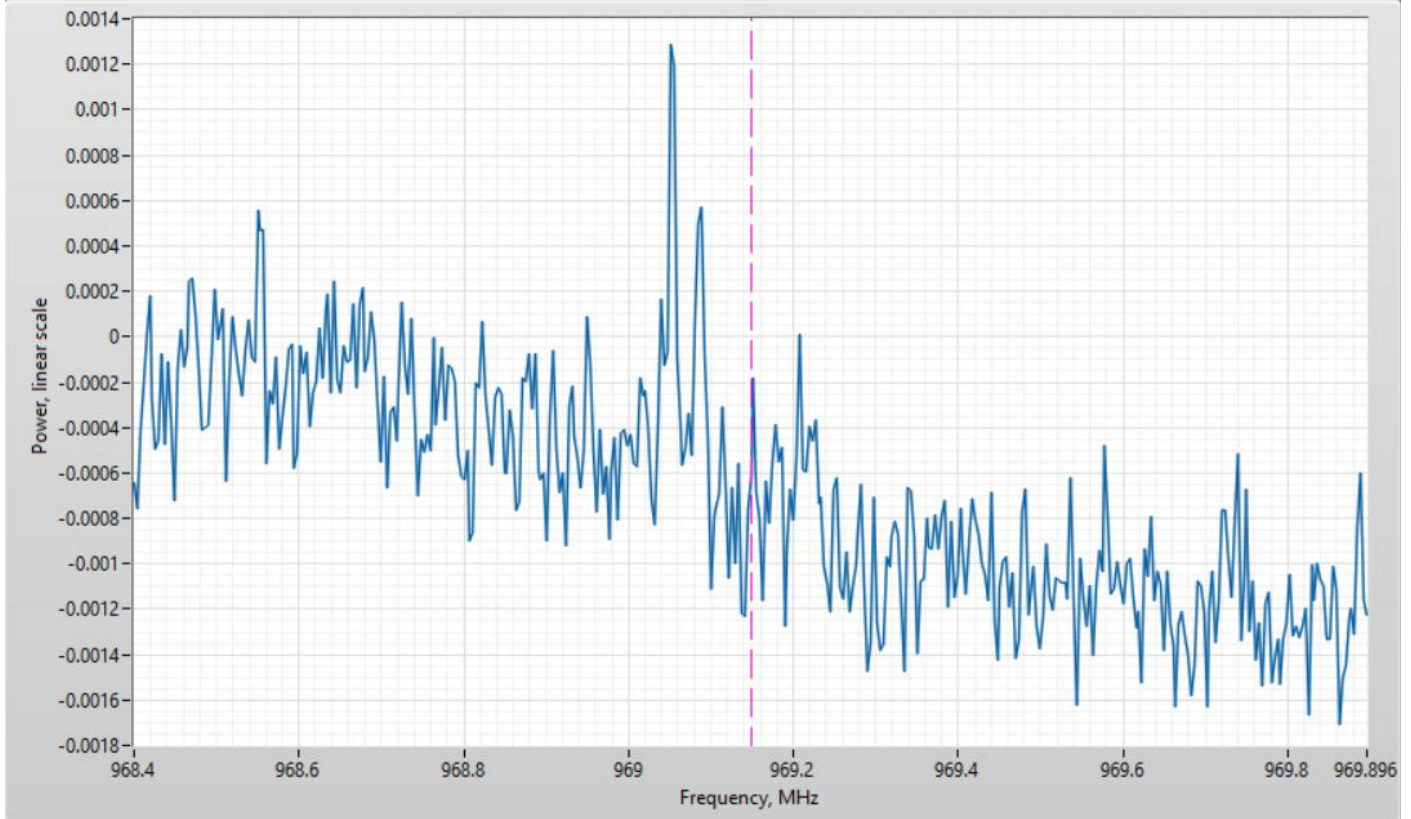


Figure 6. FR correction result $\bar{A}_{N \text{ bins}}$ by (10) for Cepheus A 6.7 GHz observations 2023-09-21. Integration time $\Delta t \approx 1.5$ hours, for background ≈ 3 hours.

Nevertheless, in practice the background in $\bar{P}_{N \text{ bins}}$ and $\bar{P}_{N \text{ bins, background}}$ come out slightly different due to inevitable gain drift of the receiver, changes in weather conditions etc. Then $\bar{P}_{N \text{ bins, background}}$ can be adjusted to be maximally close to the background in $\bar{P}_{N \text{ bins}}$,

$$\bar{A}_{N \text{ bins}} = \alpha \cdot \bar{P}_{N \text{ bins}} / \bar{P}_{N \text{ bins, background}} - 1, \alpha \approx 1. \quad (10a)$$

Parameter α would be slightly adjusted around 1 to get a better result for $\bar{A}_{N \text{ bins}}$ around 0. Nevertheless, even after this has done some slant adjustments of the plot and a little zero correction finally can be desirable for a better view.

The important note is the FR correction procedure (10) or (10a) adds a noise to the spectrum leading to inevitable loss in the sensitivity of maser receiving system as a whole; some residual noise in $\bar{P}_{N \text{ bins, background}}$ still presents and comes to $\bar{A}_{N \text{ bins}}$ with the residual noise in $\bar{P}_{N \text{ bins}}$. If the integration time Δt is the same for $\bar{P}_{N \text{ bins}}$ and $\bar{P}_{N \text{ bins, background}}$ the noise in $\bar{A}_{N \text{ bins}}$ will be $\sqrt{2}$ times higher in comparison to a noiseless background. Therefore, the integration time for collecting $\bar{P}_{N \text{ bins, background}}$ has to be as long as possible to reduce the background noise in $\bar{A}_{N \text{ bins}}$ and the loss in sensitivity.

For spectrum in flux units $F_{N \text{ bins}}$ one can write out a simple formula,

$$F_{N \text{ bins}} = \text{SEFD} \cdot \bar{A}_{N \text{ bins}} \quad (11)$$

Since SEFD is measured in Jy the results by (11) will be also in Jy; the multiplication here is also element-wise as previously.

The equation (11) uses the spectrum array $\bar{A}_{N \text{ bins}}$, which is already normalized to 1 (and shifted additionally to 0 to show the maser spectrum up from a zero level). Nevertheless, I would demonstrate an example of F_{peak} estimation before the FR correction procedure (10) or (10a) is applied. Figure 7 shows the raw spectrum from USRP receiver. Its spectrum monitor is just zoomed to see appearing maser peaks; the formula for estimation F_{peak} is also drawn there. The background of peak of interest a is different from 1, therefore, the peak size from the picture Δa has to be normalized to the background a .

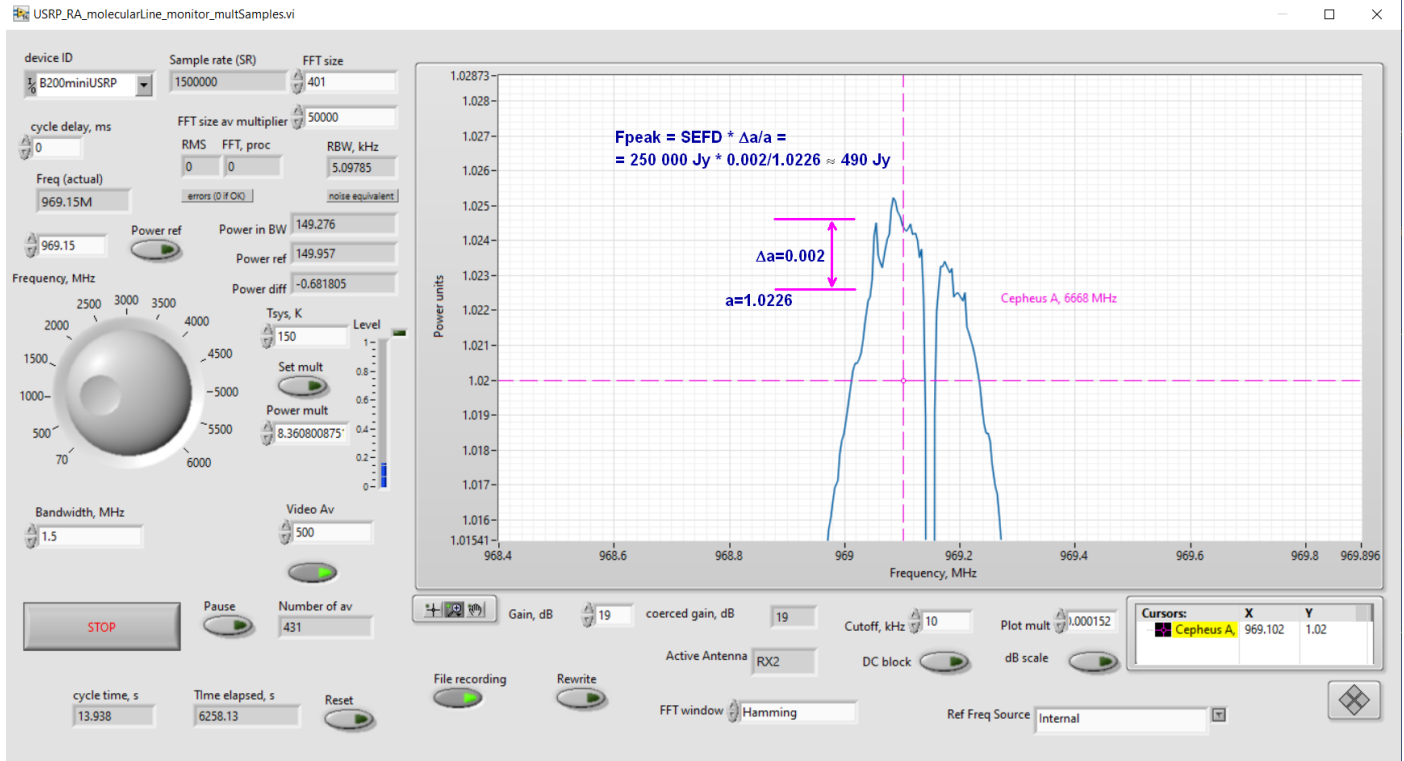


Figure 7. USRP receiver screen zoomed to see how maser peaks are appeared during the integration time, taken from observations of Cepheus A 2023-09-21.

After that, the multiplication by SEFD gives the peak size in Jy. The local background a like on the picture *de facto* corresponds to SEFD (or to T_{sys} in the temperature scale), and if a peak is not too wide such estimation would give nice results. The same spectrum but by formula (11) with FR correction by (10) (and with small slant and zero adjustments) is shown on Figure 8. Highest peak on Figure 8 corresponds to estimated peak at Figure 7. All pictures Figure 6, Figure 7, Figure 8 are taken from one observation of Cepheus A maser 6.7 GHz.

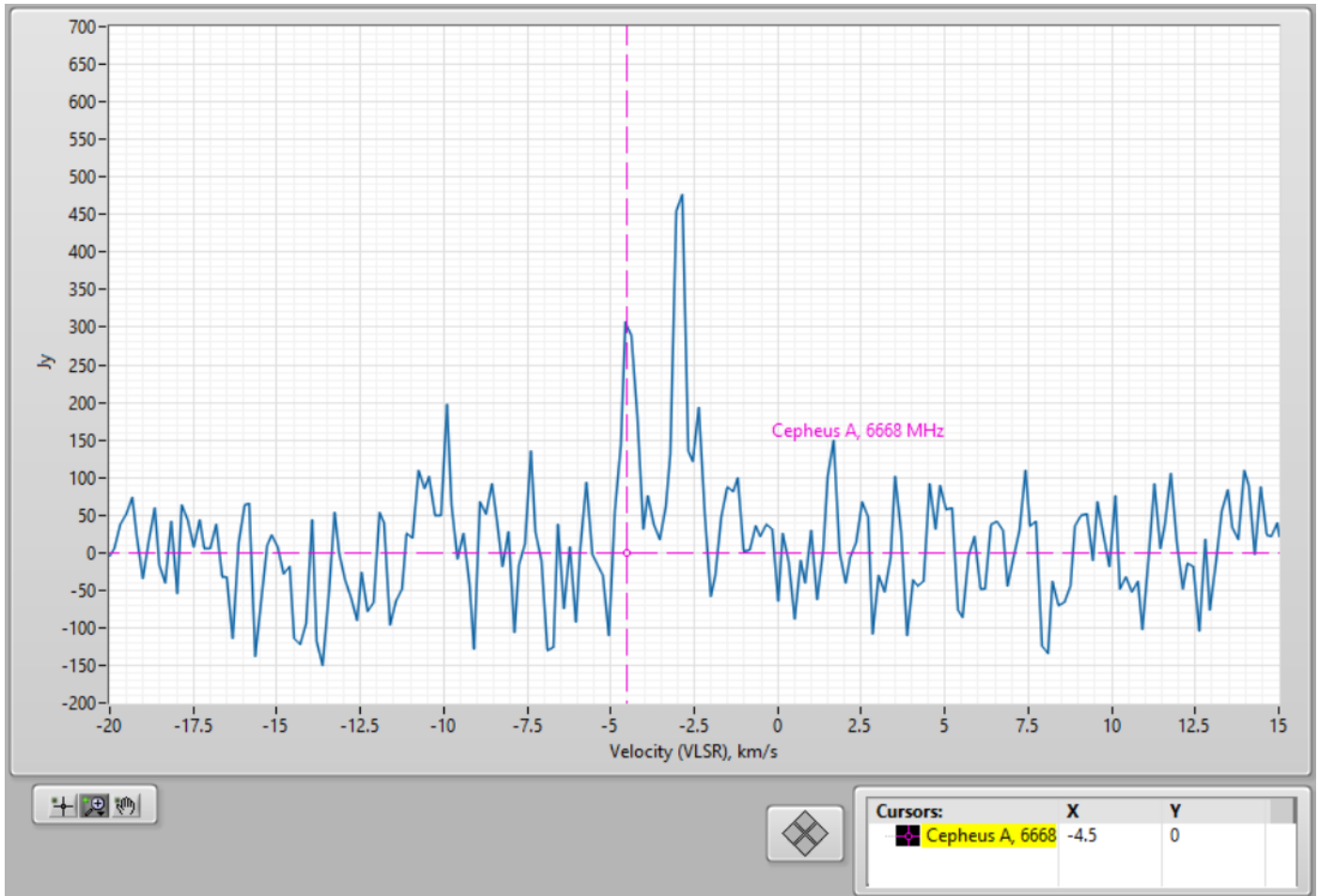


Figure 8. Final spectrum of Cepheus A maser 6.7 GHz in observations 2023-09-21. Integration time $\Delta t \approx 1.5$ hours, for background ≈ 3 hours.

The VLSR scale on Figure 8 is obtained using Java scripts from page [10]. A spectrum versus frequency from the receiver is converted to the same, but versus VLSR. Higher frequencies corresponds to lower velocities and vice versa; the example Figure 7 gives an estimation for the line with highest velocity in the Cepheus A spectrum Figure 8. Velocities in the range of interests \ll than speed of light c , and the Doppler shift depends on velocities linearly. Therefore, it is enough to calculate velocities by [10] only for bounds of the receiver bandwidth. A view of spectrum versus velocities would be horizontally flipped in comparison with the frequency spectrum.

Concluding notes and comments

In conclusion, I would note the radiometer equation (4a) describes conditions of picking out a spectral line from the background noise in observations. It uses System Equivalent Flux Density (SEFD) as a sensitivity parameter of the telescope. The coefficient $K=3$ corresponds to the level of appearance of the line over noise peaks. The resolution bandwidth (RBW) plays a role of frequency band from the classic radiometer equation, see ch. 4.2.1 in [5].

I told nothing about multiday observations. As expected, the receiver provides saving the averaged spectrum results with N bin points. Next day the observation can be done again with same tunings of SDR; the result together with the previous day result could be averaged arithmetically obtaining new observation result with lower background noise. The same can be done for long collection of the background receiver response, $\bar{P}_{N \text{ bins, background}}$; then, the FR correction procedure (10) or (10a) will bring less noise to the output and displayed spectrum at all.

In above consideration the system temperature T_{sys} corresponds to measured background when the telescope antenna is directed to the sky. Therefore, T_{sys} has to include the atmosphere noise, and the SEFD parameter takes into account the atmosphere too. For H₂O 22 GHz observations, the atmosphere influence, i.e. attenuation and thermal noise, cannot be ignored already. Atmospheric effects can be estimated by ITU methods for current weather [11,12]. Attenuation by [11] works well for clear weather; dense clouds and precipitations bring difficulties in estimation. I haven't a better idea how to exclude the atmosphere attenuation from observation results than enhancing a maser spectrum artificially by expected attenuation value within the spectrum width.

The most of issues in building a maser receiver using SDRs were considered above; I hope many of communicated things can be applied to receivers based on other SDR modules besides USRP. LabVIEW Virtual Instrument (VI) files for my USRP receiver are placed in GitHub repository https://github.com/ua3avr/USRP_maser_line_receiver.git; if you interested in installation files for the compiled Windows application, please, ask the author. I performed the postprocessing procedures in a separate utility; its VI is also shared.

References

- [1] Ibaraki methanol maser line 6.7 GHz database iMet, <http://vlbi.sci.ibaraki.ac.jp/iMet/> (data are retrieved by galactic coordinate identifiers).
- [2] Eduard Mol, *Recent observations of 22.2 GHz H₂O masers with the 1-metre Mini Maser Telescope*, Radio Astronomy, Journal of the Society of Amateur Radio Astronomers, September – October 2023, p. 138.
- [3] D. Fedorov UA3AVR, *Methanol maser lines 12 GHz observations*, Radio Astronomy, Journal of the Society of Amateur Radio Astronomers, September – October 2022, p. 71.
- [4] D. Fedorov UA3AVR, *Methanol maser line 6.7 GHz observations*, Radio Astronomy, Journal of the Society of Amateur Radio Astronomers, May – June 2023, p. 120.
- [5] T.L. Wilson, K. Rohlfs, S. Hüttemeister, *Tools of Radio Astronomy*, 6th ed, Springer, 2013.
- [6] Wolfgang Herrmann, *Refurbishing an SRT, Part 4: Characterization and Observation Examples*, Radio Astronomy, Journal of the Society of Amateur Radio Astronomers, September – October 2022, p. 42.
- [7] D. Fedorov UA3AVR, *Methanol maser 6.7 GHz in Cepheus A in August-September 2023*, Radio Astronomy, Journal of the Society of Amateur Radio Astronomers, September – October 2023, p. 146.
- [8] Sophocles J. Orfanidis, *Introducing to Signal Processing*, <https://eceweb1.rutgers.edu/~orfanidi/intro2sp/>, Rutgers University (2010).
- [9] Armin W. Doerry, *Catalog of Window Taper Functions for Sidelobe Control*, SAND2017-4042, Sandia National Laboratories, 2017, <https://doi.org/10.2172/1365510>.
- [10] HawkRAO VLSR Calculator, modifications by F4KLO/N5CNB, <http://f4klo.ampr.org/vlsrKLO.php>, RadioTélescope de la Vilette.
- [11] *Attenuation by atmospheric gases* by ITU recommendations P.676, <https://www.itu.int/rec/R-REC-P.676>.
- [12] *Radio noise* by ITU recommendations P.372, <https://www.itu.int/rec/R-REC-P.372/en>.

About the author



Dimitry Fedorov was first licensed as radio amateur since 1982, as UA3AVR since 1983. In 1990 graduated as MS in electronics in Moscow Power Engineering University. Now works as research and development engineer in wireless industry, LTE/5G NR, RF and microwave modules development. Previous scientific experience in nuclear and particle physics, worked in Moscow State University, Institute of Nuclear Physics and Universität Tübingen, Institut für Theoretische Physik, see profile blog at <https://www.researchgate.net/profile/Dimitry-Fedorov-2>. Radio Astronomy hobby since 2012, mainly in applications for weak signals reception. You can contact the author at ua3avr@yandex.ru.

Errata to: System temperature Tsys by measurements the Moon radiation

by Dimitry Fedorov UA3AVR

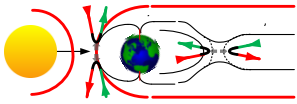
in Radio Astronomy, Journal of the Society of Amateur Radio Astronomers, January – February 2024, p. 62.

In comments after formula (6) about L_{atm} (page 65):

"Clouds and weather with precipitations make calculations hardly predictable." have to be read as "Clouds and weather with precipitations make atmosphere losses and noise hardly predictable."

Solar & Geomagnetic Storms 23-24 March 2024

Whitham D. Reeve



Solar activity reached high levels during the early UTC morning on 23 March with an X1.1 x-ray flare first observed at 0058 and peaking at 0133 (figure 1). Associated with the flare were radio bursts over a very wide frequency range including a Type II slow radio sweep, which was detected between 30 and 75 MHz at the Coho Radio

Observatory in Alaska in e-CALLISTO data at 0109 (figure 2). Type II sweeps and coronal mass ejections (CME) often go together. In this case, a halo CME was observed by the SOHO spacecraft during the same time period (figure 3). According to the Space Weather Prediction Center (SWPC) Forecast Discussion for 24 March at 0030, the CME signature *contained plasma from multiple sites on the Sun*.

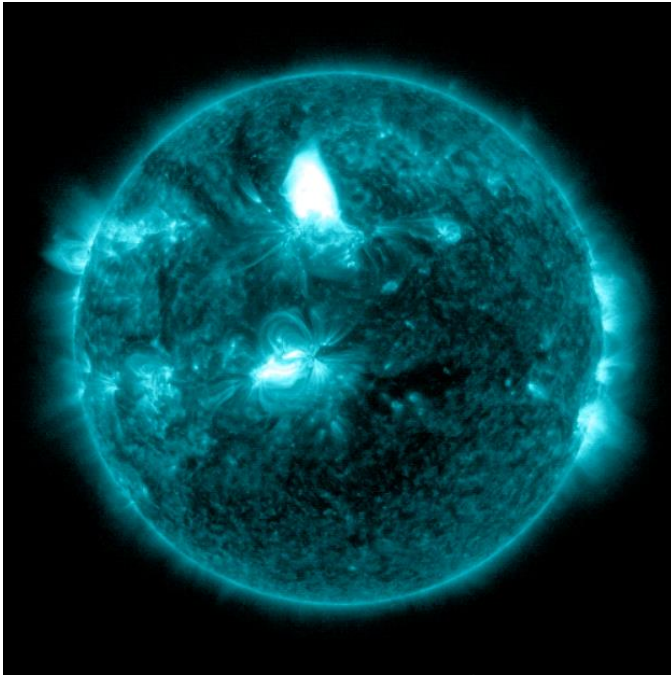


Figure 1 ~ Simultaneous x-ray flares early on 23 March from two different sites and pointed practically head-on toward Earth. This false-color image was produced by the SDO spacecraft using an extreme ultraviolet (EUV) sensor designed to highlight the extremely hot material in flares.

The flares produced a variety of radio bursts including Type VI (series of Type III fast sweep bursts over a period lasting more than 10 minutes and no period longer than 30 minutes without activity), long-lived broadband continuum over 3 octaves in the VHF band and Type II. Image credit: NASA/SDO

About 2.5 hours after the flare, at 0400, the 10 MeV proton flux measured by the GOES-18 spacecraft started to rise and reached the warning threshold of $10 \text{ particles cm}^{-2} \text{ s}^{-1} \text{ sr}^{-1}$ at about 0800 (figure 4). The average speed for these particles was about $16\,700 \text{ km s}^{-1}$ or 5.6% of the speed of light. The 50 MeV proton flux also increased but did not exceed the warning threshold. The high proton flux was able to penetrate the geomagnetosphere, causing a solar energetic particle (SEP) event. The SEP, in turn, increased the electron density in the high-latitude D-region ionosphere, which induced high levels of absorption in the HF band that lasted a few days (figure 5).

Transient CME effects were observed by the ACE spacecraft (1.5 million km from Earth along the Sun-Earth line) at 1411 on 24 March. The travel time from Sun to ACE was only 37 hours, giving an average speed of 1100 km s^{-1} for the plasma mass. The subsequent impact of the CME with Earth's magnetosphere 26 minutes later at 1437 rapidly compressed the magnetosphere and produced a sudden storm commencement (SSC) in the form of a sudden impulse. At the time of the shock, the solar wind speed measured at the ACE spacecraft was 800 km s^{-1} .

The CME impact and associated relatively high solar wind speed directly affected the *auroral oval* and the *auroral electrojet*. The auroral oval, which maps the footprint on Earth of open magnetic field lines and along which aurora is produced, was significantly expanded and pushed equatorward by fast high solar wind (figure 6). The auroral electrojet is a huge current system that flows in the neighborhood of 90 to 150 km altitude (ionosphere's E-region) in the auroral oval. It is the only magnetospheric current system whose effects can be measured by ground magnetometers.

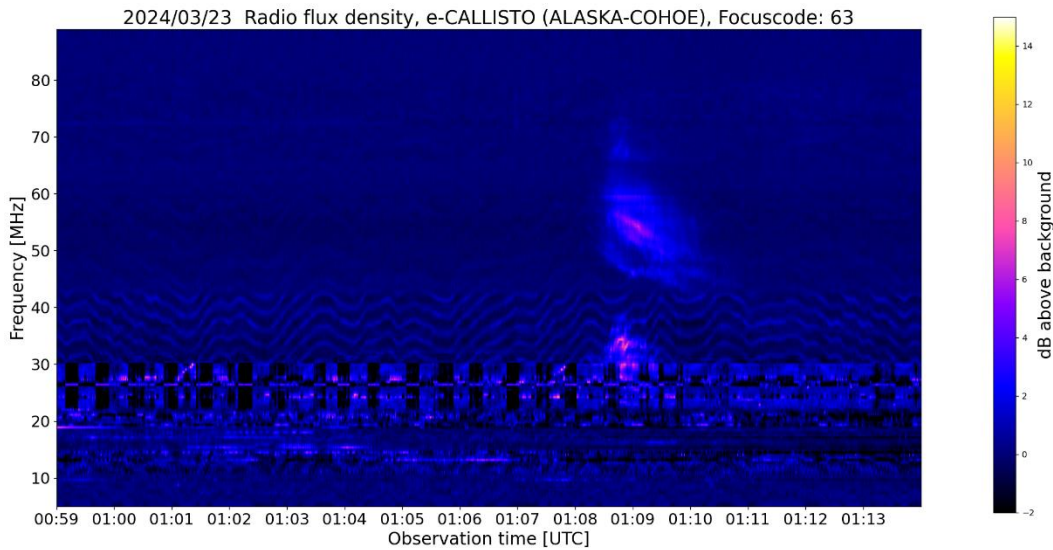


Figure 2 ~ Type II slow radio sweep between 25 and 75 MHz seen as two puffy features one of which is seen to sweep downward in frequency. The horizontal features below 30 MHz are shortwave stations. Image credit: FHNW Brugg/Windisch and IRSOL Locarno, Switzerland and W. Reeve

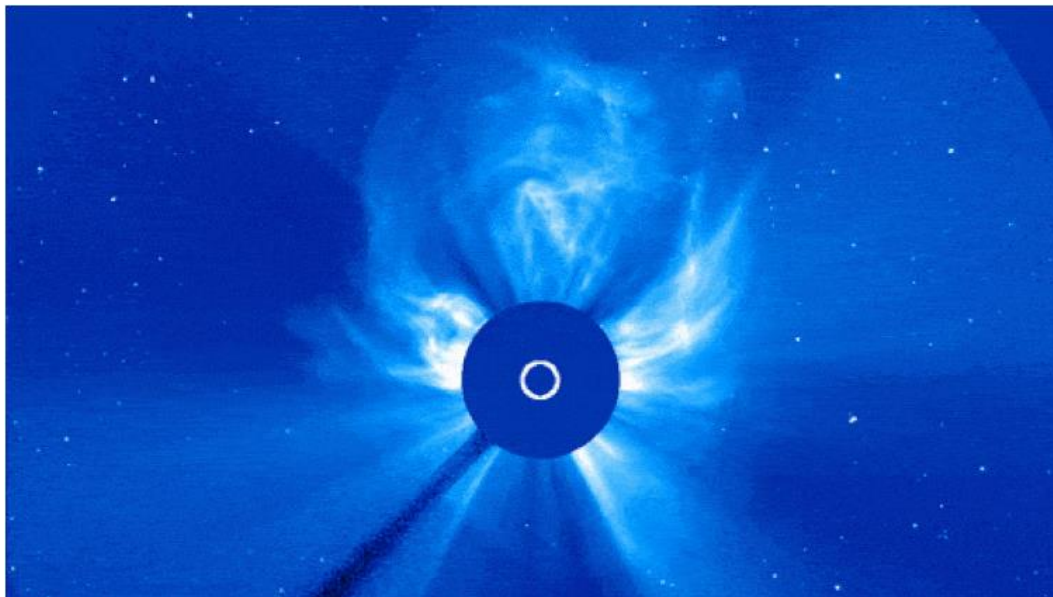


Figure 3 ~ Halo CME resulting from the flares on 23 March. The dark-blue occulting disk is designed to block the bright Sun from the SOHO spacecraft coronagraph so it can image the relatively dim CME structures. The Sun is represented to scale by the white circle. Image credit: NASA/SOHO

The open magnetic field lines, with footprints on Earth below the auroral oval, opened a gap in the magnetosphere and allowed precipitation of solar energetic particles into the upper atmosphere where they collided with atoms and molecules. The collisions increased the ionization and, thus, the electron density and conductivity in the region. Charge imbalances in the region produced strong horizontal electric fields, which along with the high conductivity caused large variations in the electrojet current.

GOES Proton Flux (5-minute data)

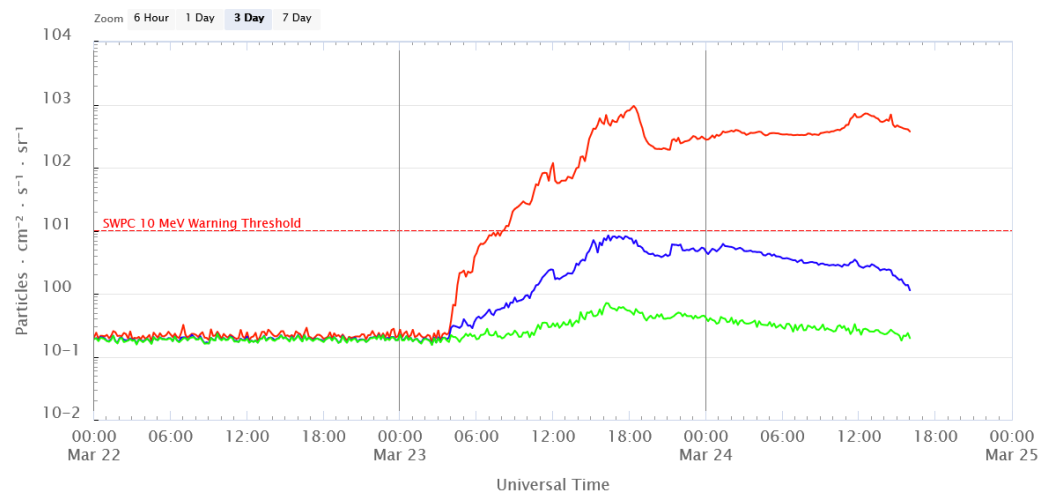
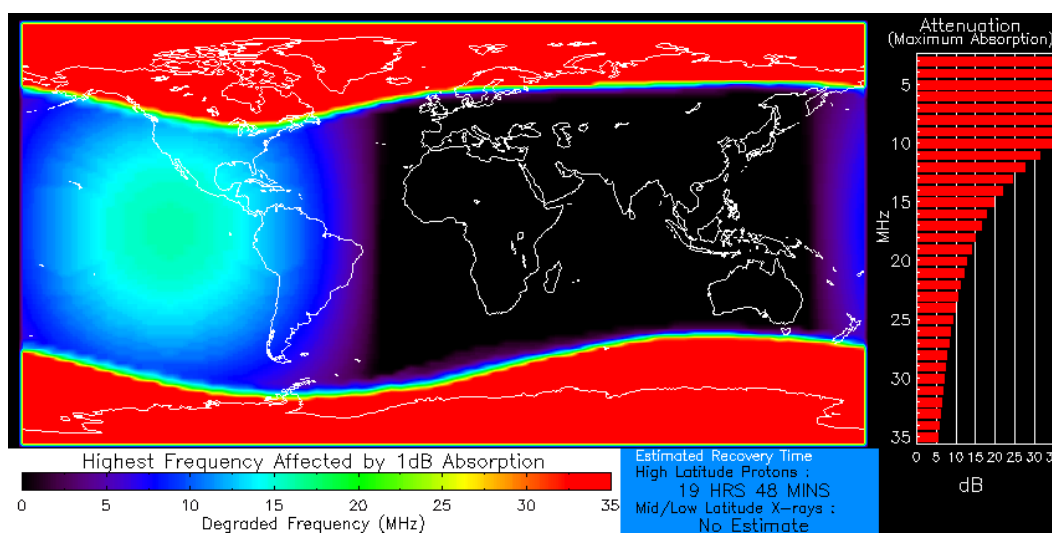


Figure 4 ~ 3-day GOES-18 Proton Flux plot showing 10, 50 and 100 MeV measurements. The flux began to rise at 0400 on 23 March giving 2.5 hour time of flight from Sun to spacecraft and an average speed of 5.6% speed of light. Image credit: NOAA/SWPC

Updated 2024-03-24 16:00 UTC

— GOES-18 ≥ 10 MeV — GOES-18 ≥ 50 MeV — GOES-18 ≥ 100 MeV

Space Weather Prediction Center



Elevated X-ray flux
Product Valid At : 2024-03-24 19:45 UTC

Minor Proton Flux
NOAA/SWPC Boulder, CO USA

Figure 5 ~ D-region absorption prediction at 1945 on 24 March showing heavy absorption, which are indicated by the red bands at high latitudes. This plot shows that absorption was still at elevated levels almost 2 days after the x-ray flares on 23 March and was expected to continue for another 20 hours. Note the very high levels of absorption at lower frequencies indicated on the right-side bar graph. The elevated absorption likely led to radio blackouts on HF radio propagation paths within the red areas. The green-blue round feature over the Pacific Ocean west of Panama is the predicted effect of a relatively low level flare about 1 hour earlier. Image credit: NOAA/SWPC

The auroral electrojet effects are characterized by the AE index, which is composed of the AU, AL, AE and AO indices (figure 7). The AU and AL define the upper and lower envelopes of magnetic measurements from selected northern hemisphere high-latitude stations and express the strongest current intensity of the eastward and westward auroral electrojets, respectively, at any given time.

AE is the difference between AU and AL and AO is the average of AU and AL at any given time. Thus, AE represents the overall or peak-to-peak activity of the electrojets and is always positive. AO provides a measure of the equivalent current flows and may be positive or negative at any given time. AO was primarily negative during the disturbance on 24 March, indicating a westward current flow in the auroral oval. Both AE and AO ran off-scale at about 1600.

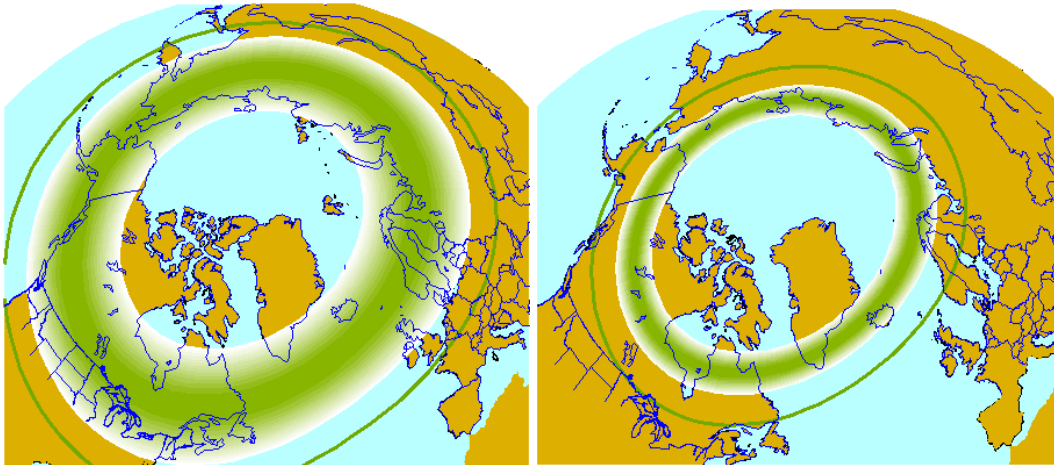


Figure 6 ~ Left: Prediction of the northern hemisphere Auroral Oval, shown by the green belt, for the time period following the solar flares of 23 March. The thinner green line circling the oval shows the boundary of the auroral zone, above which aurora may be observed. Right: Magnetically quiet day for comparison. Image credit: University of Alaska Fairbanks Geophysical Institute.

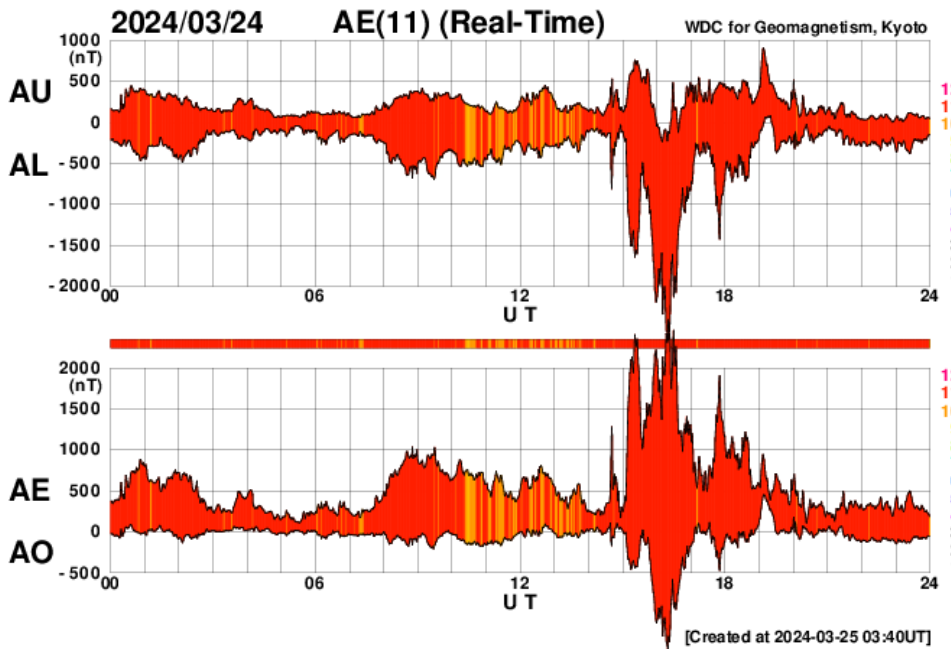


Figure 7 ~ Auroral Electrojet Indices AU, AL, AE and AO (see text). Image credit: World Data Center for Geomagnetism, Kyoto

The westward current flow produced a magnetic field that opposed Earth’s internal magnetic field measured on the ground at Anchorage and HAARP (figure 8). The opposition manifested as a decrease (bay) in the horizontal component of the geomagnetic field that may be directly compared to the AE index plots. During the 1500 to 1800

UTC synoptic period, the SAM-III magnetograms at Anchorage Radio Observatory and HAARP Radio Observatory in Alaska both displayed the highest possible K-index of K9. The K-index provides a 3-hour summary of peak-to-peak magnetic activity. It generally is designed to represent the horizontal (H-) component of the magnetic field, but the SAM-III reports a pseudo-index for each of the three magnetic components, X, Y and Z.

As seen in the Anchorage and HAARP magnetograms, the X- (east-west) and Y- (north-south) components of the magnetic field were reduced from the baseline by 1750 and 750 nT, respectively, at Anchorage and 2000 and 1850 nT, respectively, at HAARP. The reductions in the east-west component represent roughly 50% of the steady-state east-west magnetic flux densities measured on the ground. For the north-south component, the reductions represent roughly 5% at Anchorage and 14% at HAARP of the steady-state magnetic flux densities. These changes highlight the immensity of the enhanced current flow during the geomagnetic storm.

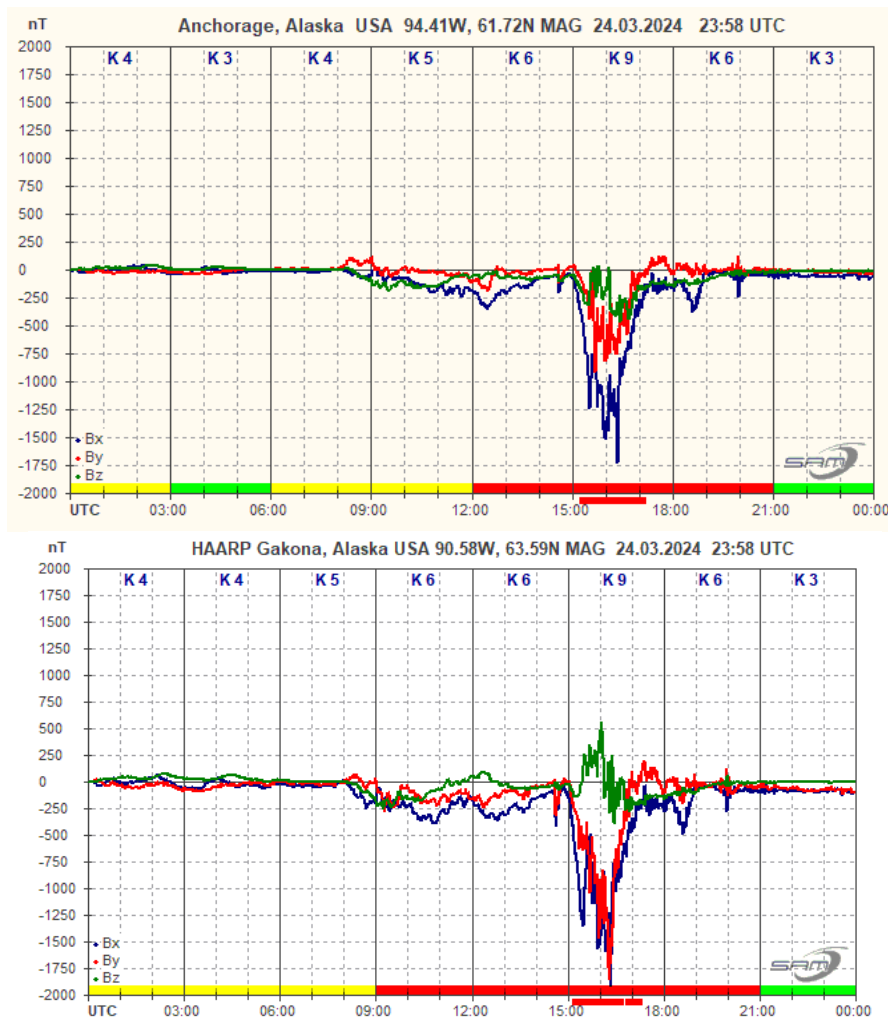


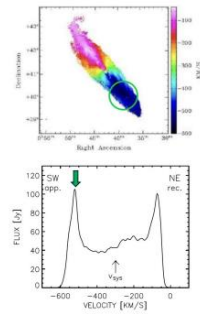
Figure 8 ~ Magnetic field measurements at Anchorage Radio Observatory (upper) and HAARP Radio Observatory (lower) for 24 March. The sudden impulse is clearly identifiable as the downward pulse between 1400 and 1500 UTC at both locations. The sudden impulse amplitude at Anchorage, approximately 200 nT, is one-half the amplitude as at HAARP but still considered quite strong. The reductions in the X- and Y-components around 1620 UTC are a significant percentage of Earth’s internal magnetic field (see text). Image credit: © 2024 W. Reeve

Hydrogen Line Drift Scan Detection of M31 and M33 with a Portable 2.64 Meter Dish

By Jason Burnfield
11 April 2024

Origins of This Project

Ever since I first saw the double-peaked "Batman Signal" spectral profile of M31 in published research papers, I was "hooked"! One way or another, I was determined to capture this "Batman Signal" myself!



Phase 1: Dish Design, Build, and Test

Dish Profile Design in Excel

Radius [m]	Height [m]	...
0.00	0.00	...
0.05	0.01	...
0.10	0.02	...
0.15	0.03	...
0.20	0.04	...
0.25	0.05	...
0.30	0.06	...
0.35	0.07	...
0.40	0.08	...
0.45	0.09	...
0.50	0.10	...
0.55	0.11	...
0.60	0.12	...
0.65	0.13	...
0.70	0.14	...
0.75	0.15	...
0.80	0.16	...
0.85	0.17	...
0.90	0.18	...
0.95	0.19	...
1.00	0.20	...

Original Dish
was
Cumbersome
and Impractical
but a good proof
of concept



Frame Built
from
Plywood



Original Cover was
Duct Tape and Foil
Tape



2nd Design was
Collapsible
Like an
Umbrella with
 f/D 0.5 (too
long)



3rd Version of
Dish
Redesigned
and Rebuilt
with f/D 0.35



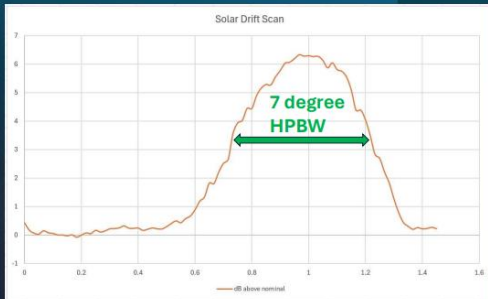
Switched cover
material to
Aluminum
Window Screening
and moved to front
of frame to reduce
loss



Nooelec Sawbird H1+ LNA/BPF



Nooelec Smartee SDR mounted on Large Heat Sink for Temperature Stability



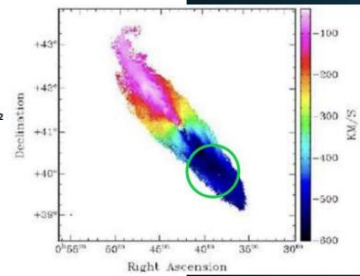
My Setup

- Antenna: homemade, portable, collapsible, parabolic dish, diameter 2.64 meters, f/D 0.35
- Feed: homemade "Super" VE4MA with choke ring
- LNA/BPF: Nooelec Sawbird H1+
- Receiver: Nooelec Smartee SDR
- Software: Airsty SDR# with IF Averaging Plug-In
- Data Analysis: Microsoft Excel

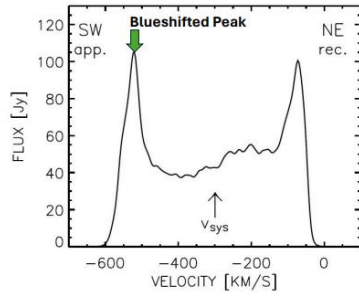


Phase 2:
M31 Drift Scan
Observations

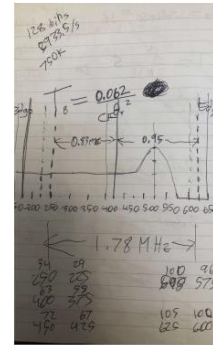
- Target Area:
RA 39m Dec 40 degrees₂



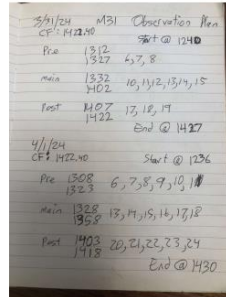
M31 Reference Profile₂



- Center Frequency Chosen to place blueshifted peak halfway between center of band and edge of band.
- Center Frequency was adjusted each day to account for the VLSR correction factor.⁴



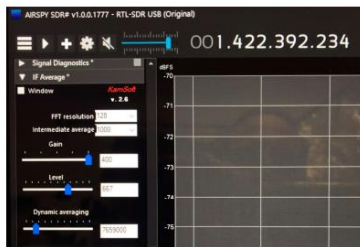
- Observation Plan to maximize time "on target" and ensure pre and post scans are captured.



Dish tilted 1 degree due North of Zenith



SDR# IF Averaging Plug-In Settings



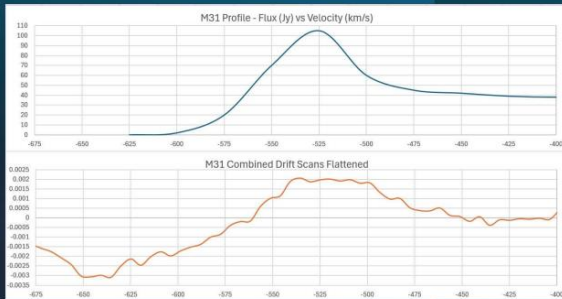
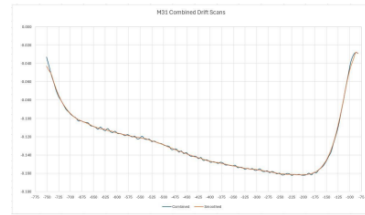
M31 Pre-Scan



Analysis of Data in a Nutshell:

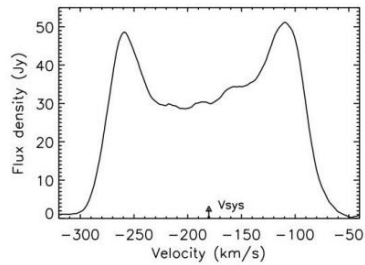
- Raw Linear Amplitude Values for Pre and Post Scans Averaged together to Create a Reference Scan.
- Main Scan divided by Reference Scan and the result converted to dB using $20 \log(\text{Amplitude Ratio})$.
- Resulting Data Flattened using leveling points on the expected profile to create a linear flattening function.

Blueshifted Peak clearly visible even in unflattened plot!

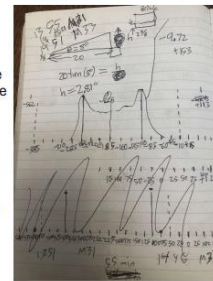


Phase 3: M33 Drift Scan Observations

M33 Reference Profile₃



- Center Frequency chosen to center the entire spectral profile of M33 in the bandwidth of the receiver.
- Center Frequency was adjusted each day to account for the VLSR correction factor.⁴



- Observation Plan to maximize time "on target" and ensure pre and post scans are captured.

4/6/24 M33 Observation Plan
 CF: N21,24 side 1300
 pre 329 side 1300
 359 4,5,6,7,8,9
 main 1404 11,12,13,14,15
 1439 17,18,19,20,21,22
 1909 End @ 1515

Dish tilted 8 degrees due South of Zenith



M33 Pre-Scan

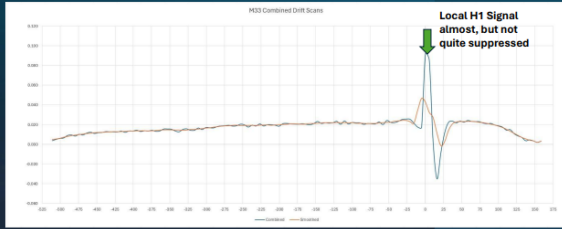


M33 Main Scan



M33 Post-Scan





Success!

Thank-you to Jean-Jacques Maintoux whose paper was my inspiration and guide in this endeavor!₅



References

1. Tadeja Saje, Matjaz Vidmar – A Compact Radio Telescope for the 21cm Neutral Hydrogen Line <https://antena.fe.uni-lj.si/literatura/Razno/Diplome/Radioteleskop/cianek/radioteleskop.pdf>
2. Laurent Chemin, Claude Carignan and Tyler Foster – H I Kinematics and Dynamics of Messier 31 <https://arxiv.org/pdf/0909.3846v1.pdf>
3. S. Z. Kam, C. Carignan, L. Chemin, T. Foster, E. Elson, T. H. Jarrett – H I Kinematics and Mass Distribution of Messier 33 <https://arxiv.org/pdf/1706.04248.pdf>
4. HawkRAO VLSR Calculator (modifications by F4KLO/NSCNB) <https://f4klo.ampr.org/vlsr/klo.php>
5. J. J. Maintoux – Amateur radio astronomy : 21 cm hydrogen survey of M31 and M33 galaxies <https://articles.adsabs.harvard.edu/pdf/2018O%26T...86...2M>

Observation Reports

Small Aperture Antenna Drive with 3D Printed Components Nathaniel Butts - SOKYRAD

Abstract

I've had the desire to add motor controls to my 1m telescope since the day I built it. While letting the antenna perform meridian drift scans at manually adjusted declinations, I started my research into possible solutions. Many proved to be overly powered and overly expensive for my needs of a sub 5kg dish. I found a potential solution using 3D printed slew drives powered by NEMA 17 stepper motors, so I set out to test the effectiveness of this solution.

Equipment

I found a design for a parametric slew drive on Printables.com [1] which showed great promise. The slew drive is designed using 3D printed components for the housing, gear/bearing, and worm. It is designed to utilize 6mm (0.12g) airsoft bb's for the bearing balls (figure 1).

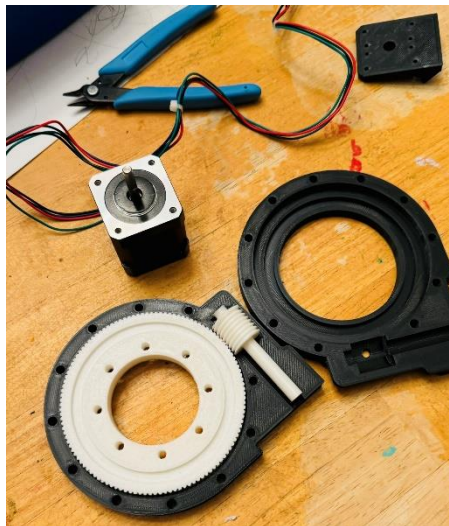


Figure 9 - Drive Internals

I printed everything in PLA with a 65% gyroid infill to increase the ability to handle rotational loads and spent some time cleaning up the bearing side of the worm to ensure it rotated smoothly. The first print had too much play in the worm to gear mating, so I printed another set with 0.0mm horizontal expansion which made the connection more rigid. A thick coating of white lithium grease was used on all friction points, threads, and bearings.

For a motor I used a NEMA 17, 2A bipolar stepper motor rated at 59Ncm of torque. These motors are designed for desktop CNC or 3D printers, making them small but with a good amount of torque for the package size. For

electronics I attached a Waveshare Stepper motor hat [3] to a Raspberry PI 3b+ and powered everything using a 24v dc, 3a power supply.

The motor turns at 200 steps for 1.8° of rotation of the stepper motor shaft. The drive gear printed is 100mm in diameter and 120 tooth count, and an 8mm diameter worm. This calculates to a 50:1 drive ratio since the worm has 2 starting threads, or a theoretical max torque output of 35.4Nm.

Testing Method

Bench testing

On the bench, I first laid the slew drive on its side and stacked weights directly onto the white bearing and drove the motor using the hat and Python script. I increased weights up to 25kg and the motor never strained, skipped, or bound up, and recorded maximum amperage was 1.2A. Testing was concluded prematurely due to these findings, as I never expected to put more than 25kg of axial load to these drives.

I then printed a 100mm arm to test torque holding capability. I started at 1.2kg and continued adding weight hanging from the arm until failure. Lifting was tested between 20-65 degrees to horizontal. The maximum torque reached was 6.67Nm with failure, in the form of skipping threads, occurring at 7.8Nm, but the motor was able to complete the full arc sweep. This maximum efficiency calculates to 22%, which seems to be comparable to other 3D printed gear testing performed in the past with this filament.



Figure 11 - Test Setup



Figure 10 - Coupler

A second arm was printed, and testing was performed with a balanced load (equal weight on each arm). Testing was performed up to 10kg/arm, 20kg total, with no signs of distress from the slew drive or motor.

Performance testing

A test bed was created (figure 2) using a sawhorse, PVC pipe, my 1m grid antenna with waveguide, a 3d printed coupler (figure 3) to attach the slew drive to the PVC pipe, and a 4lb hammer used as ballast. The weight of the antenna, waveguide, and support structure totaled 3035g.

The antenna was moved in elevation through several rounds of testing: 1) from 0° to 85° back to 0° for several iterations, 2) from 0° to 80° to 0° in 10° increments with 5s pauses in between, 3) from 0° to 80° to 45° in 1° increments with 2 second pauses in between moves. All tests were performed without any indication of stress or failure from the system.

The system was then set to 55° elevation and unplugged, where it remained overnight (approximately 12 hours) without any additional support. The pressure of the worm to the drive gear was sufficient to keep the antenna from rotating any measurable amount during this dwell period, suggesting this configuration has a large safety factor built into the design. However, adequate braking is still recommended.

Conclusions

The slew drive system as designed appears to be more than capable of moving up to a 1m antenna of reasonable mass. A second set of slew drives is currently under production to create a system with Alt-Az capabilities for this antenna so that real-world, longer-term testing can be conducted. Consideration must be given to mounting and protection from the elements. PLA is known to weaken during high heat/UV exposure so that will be monitored as well. I envision attaching weather sensors and temperature monitoring sensors to the drive itself to keep more accurate data in the event of future damage.

Next steps are already underway which involve controlling the drives programmatically, or better yet through a planetarium and scheduling system for automated measurement and tracking projects. Afterward, the author hopes to test multiple configurations (thicker drive gear, different number of teeth, different motors, various filaments) to find the upper limits of this technology.

References

- [1] bostwickinator, <https://www.printables.com/model/144450-parametric-slew-drive-v2> (accessed on 3/1/24)
- [2] Stepper Motor, https://www.amazon.com/gp/product/B00PNEQKC0/ref=ppx_yo_dt_b_search_asin_title?ie=UTF8&psc=1 (accessed on 2/26/24)
- [3] Waveshare Stepper Motor Hat, [https://www.waveshare.com/wiki/Stepper_Motor_HAT_\(B\)?Amazon](https://www.waveshare.com/wiki/Stepper_Motor_HAT_(B)?Amazon) (accessed 3/20/24)



About the author: The author is a graduate of Western Kentucky University for Mechanical Engineering. He studied Physics and Astronomy where he found a love, but not a career, for Astronomy. The spark has stayed alive, and he is an avid Wannabe Astronomer, dedicated to advancing the cause of Amateur Astronomers the world over.

Observation report: OH masers observed with the Dwingeloo telescope

Eduard Mol, Tammo Jan Dijkema and Thomas Telkamp

Abstract

On January 21, 2024, observations of eight OH maser sources were performed with the 25- metre Dwingeloo telescope. This was mostly aimed as a test to see whether it was possible to detect maser sources in the 1.6- 1.7 GHz band with the current front-end installed on the dish, which is not optimized for this band. This test was a success: six maser sources were detected at the 1612 MHz line, and two sources were detected at the 1665 and 1667 MHz lines.

Introduction

What are OH Masers?

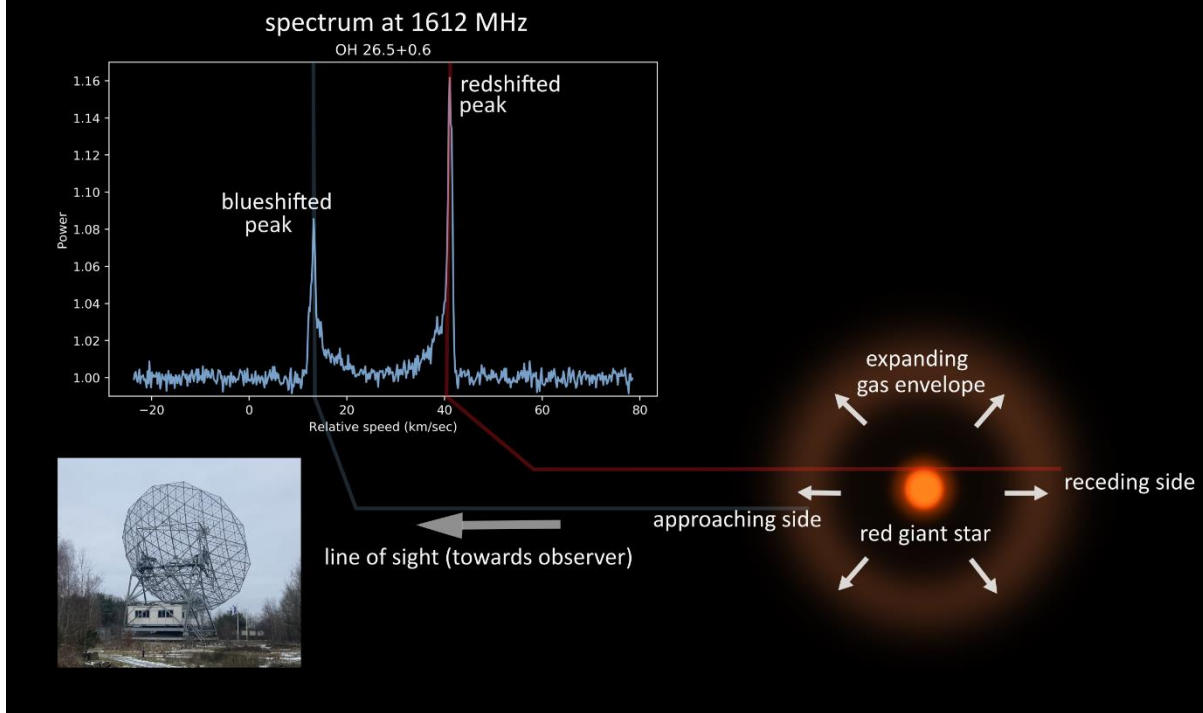
Astrophysical masers- the naturally occurring microwave equivalents of lasers- can be detected at several different frequencies in the radio spectrum, depending on the type of molecule producing maser emission [1, 2]. Hydroxyl (OH)- masers are a particular class, emitting at four spectral lines of the OH molecule at frequencies of around 1.6- 1.7 GHz [3]

Spectral line	Transition [4]	Rest frequency (MHz) [4]
OH satellite line 1	$^2\Pi_{3/2} J=3/2 F=1-2$	1612.2310
OH main line 1	$^2\Pi_{3/2} J=3/2 F=1-1$	1665.4018
OH main line 2	$^2\Pi_{3/2} J=3/2 F=2-2$	1667.3590
OH satellite line 2	$^2\Pi_{3/2} J=3/2 F=2-1$	1720.5300

These frequencies are relatively close to the 1420 MHz hydrogen line, unlike most other maser types of other molecules which mainly occur at cm- to mm- wavelengths. This makes it possible to detect OH masers with a system designed for receiving the hydrogen line with few adaptations [5]. The brightest OH masers are in the order of several hundred Jansky, and have been successfully detected by amateurs using dishes in the 3- metre size range [6, 7].

Based on their respective environments OH-masers can be roughly subdivided into two main categories: circumstellar and interstellar OH masers. The circumstellar type is found in the dusty envelopes of some red giant stars and emits most strongly at the 1612 MHz line. These masers typically have a characteristic double- peaked spectrum. This could be explained by the expansion of the gas envelope: the part of the shell in front of the star (as seen from the perspective of the observer) is moving towards the observer, thus we see a blueshifted peak from this area. Conversely, the maser emission from the far side of the shell behind the star is redshifted. Maser amplification is strongest along the paths across the near and far sides of the shell and weaker along the rim. Thus, we observe two peaks from the most blue- and redshifted parts of the gaseous shell [3, 8].

Circumstellar OH maser



Because the circumstellar masers are pumped by the IR radiation of the central red giant star, the masers also respond to changes in the star's IR luminosity. Many of these stars pulsate with periods of several hundreds of days to years. It is therefore not surprising that this periodic variability is also reflected in the maser brightness [8, 9].

Interstellar masers occur mostly in the dense gas clouds deep inside star forming regions, and emit most strongly at the main OH lines at 1665 and 1667 MHz. Their spectra are often more complex with several different peaks, and there is no simple model to visualize them like for the circumstellar masers. This probably reflects the much more complex and chaotic velocity fields within star forming regions, with many different maser clouds moving at different velocities with respect to the observer [8]. Interstellar OH masers may also exhibit a large degree of circular polarization (tens of percent to nearly 100% in some cases), which reflects the magnetic fields inside star forming regions [8].

The Dwingeloo telescope

The 25-metre Dwingeloo telescope is a historical radio telescope located in the province of Drenthe in the northeastern part of the Netherlands. It saw "first light" in 1956 and played an important role in the early days of radio astronomy. The telescope was primarily used for observations at the 1420 MHz hydrogen line, which was used to map the Milky Way galaxy in detail. Other work performed with the Dwingeloo telescope included continuum observations at 800- 1400 MHz as well as observations of the OH lines at 1.6- 1.7 GHz [9].

In 1998 the observatory was closed, and the telescope was no longer maintained by the Dutch radio astronomy institute ASTRON. Plans were made to dismantle the telescope, but eventually this did not happen. In 2007 the CAMRAS foundation was founded, with the aim of renovating the telescope and use it for amateur radio as well as give public tours of the site. Currently the telescope is operational again; steering and tracking are functional,

and the dish is equipped with a new front-end for 400 MHz and 1200- 1420 MHz. The dish is primarily used for Earth- Moon- Earth (EME) communications at the 70cm and 23cm amateur bands, as well as pulsar and hydrogen line observations at 400 MHz and 1420 MHz respectively [9].



Figure 12: the Dwingeloo telescope. (Photo by E. Mol)

The feed currently installed on the dish is a circularly polarized septum horn built for the 1200- 1420 MHz band. Surrounding the opening of the horn are also four dipole antennas for the 70cm band. The G4DDK LNA installed in the front-end is also optimized for 1200-1420 MHz; its performance at 1600-1700 MHz was not measured but is likely not as good as on 1420 MHz.

We wanted to see whether it was possible to observe OH masers, despite the limitations of the feed and the LNA which are not optimized for 1.6- 1.7 GHz. Normally this would not be possible due to the bandpass filters installed on the front-end, but these had temporarily been removed for maintenance.

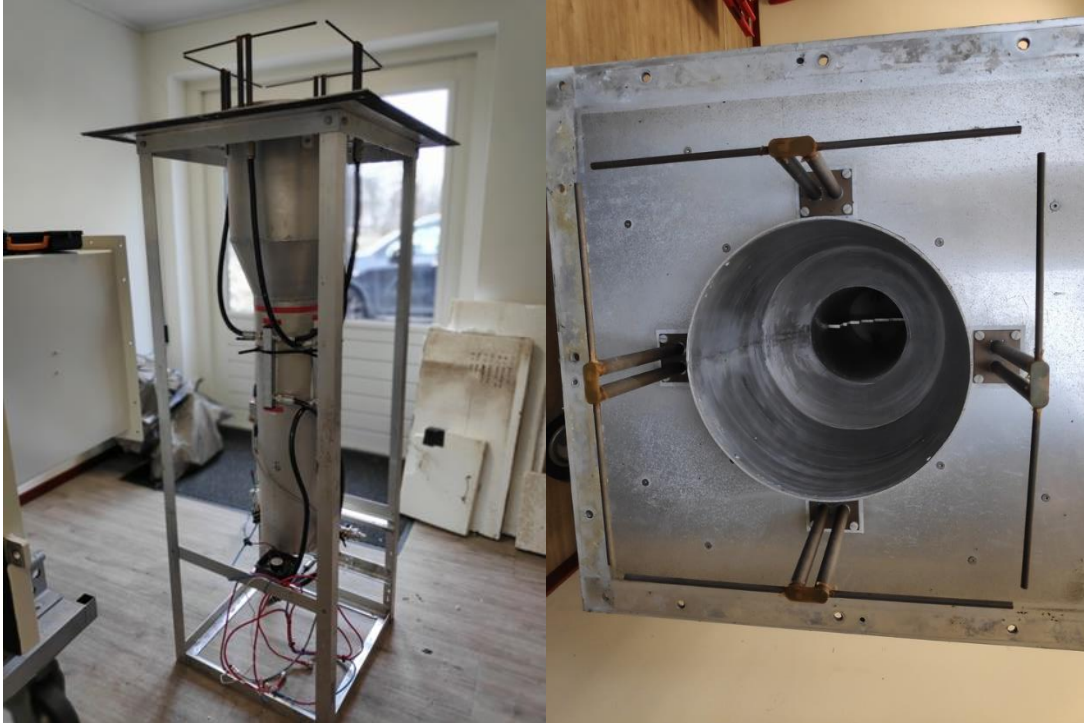


Figure 13: left: front-end of the Dwingeloo telescope when it was brought down to the workshop for maintenance. Right: close-up of the feed, the waveguide in the centre is a septum feed built for the 23 cm amateur band and the 21 cm astronomical band; the four copper rods around the feed are dipole antennas for the 70cm band. (Photos by T. J. Dijkema)

Target selection and observation

The target list was based on a selection of bright maser sources compiled from the Database of Circumstellar Masers [10] and the MaserDB database [11]; the complete list can be found in the March 2023 SARA journal [12]. From this list the objects which were well above the horizon during the observing session were observed roughly in the order from the brightest to the weakest source. Observations were done in left-hand circular polarization (LHCP), integration times ranged from two to five minutes. In about two hours we managed to observe eight sources; all of which were successfully detected at least at one frequency.

Data collection was done using an Ettus USRP B210 SDR; integrated spectra were saved every second to a CSV file using a python script developed in-house at CAMRAS. The individual 1 second spectra were later averaged after excluding the spectra affected by strong RFI. Bandpass correction was done by switching the SDR a few MHz away from the OH line frequency and fitting a polynomial through the bandpass, which could be later subtracted from the averaged spectra. The frequency axis was converted to velocity with respect to the Local Standard of Rest (LSR) using the Astropy- based script by T. J. Dijkema [13]. The velocities of the peaks in the spectra were compared with velocity data published in the Database of Circumstellar Masers and MaserDB for verification [10, 11]. Furthermore, for some of the masers sample spectra are available on the Nancay maser monitoring webpage [14].

Results

Circumstellar masers at 1612 MHz

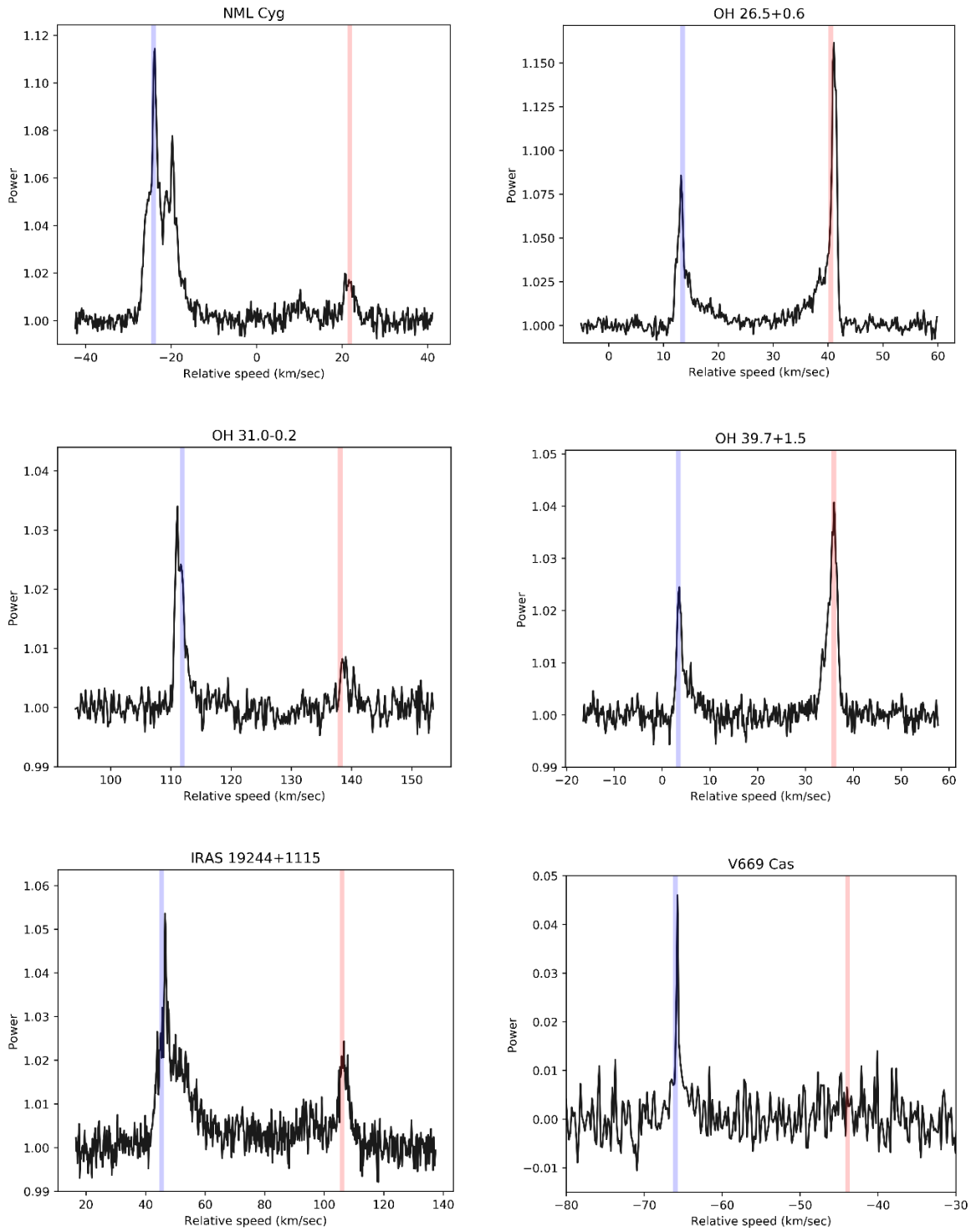


Figure 14: 1612 MHz maser spectra of selected OH/IR stars. Spectral resolution is 1KHz, integration times were 4.7 minutes for OH 31.0-0.2, 5 minutes for OH 39.7+1.5 and 2 minutes for all other sources. The blue and red shaded vertical lines represent the most recent reported LSR velocities of the blue- and redshifted peaks in the Database of Circumstellar Masers [10].

Six circumstellar masers were observed; all six sources were detected at the 1612MHz line. Attempts to detect the two strongest sources (NML Cygni and OH 26.5+0.6) at the other three OH lines were unsuccessful. This was somewhat expected, since circumstellar OH masers are known to emit most strongly at the 1612 MHz transitions, with the other three transitions typically being weaker by about an order of magnitude [5, 8]. Five out of six circumstellar masers exhibit the classical “double peak” spectral profile, with peak velocities matching the velocities of the blue- and redshifted peak as reported in the literature to within 1 km/s. Only for V669 Cas we did not detect the redshifted peak. Most of the masers had a relatively simple peak profile, except for NML Cygni and IRAS 19244+1115. NML Cyg has multiple overlapping features in the blueshifted part of its spectrum, which suggests that the maser cloud around this star has a more complex structure than a simple expanding shell. The blueshifted peak in the spectrum of IRAS 19244+1115 has a narrow spike on top of a very broad (~20 km/s) hump. The velocity difference between the red- and blueshifted peaks of this maser (62 km/s) is also notably more than the other observed sources, implying that the circumstellar envelope of this star is expanding much faster.

Interstellar masers at 1665 and 1667 MHz

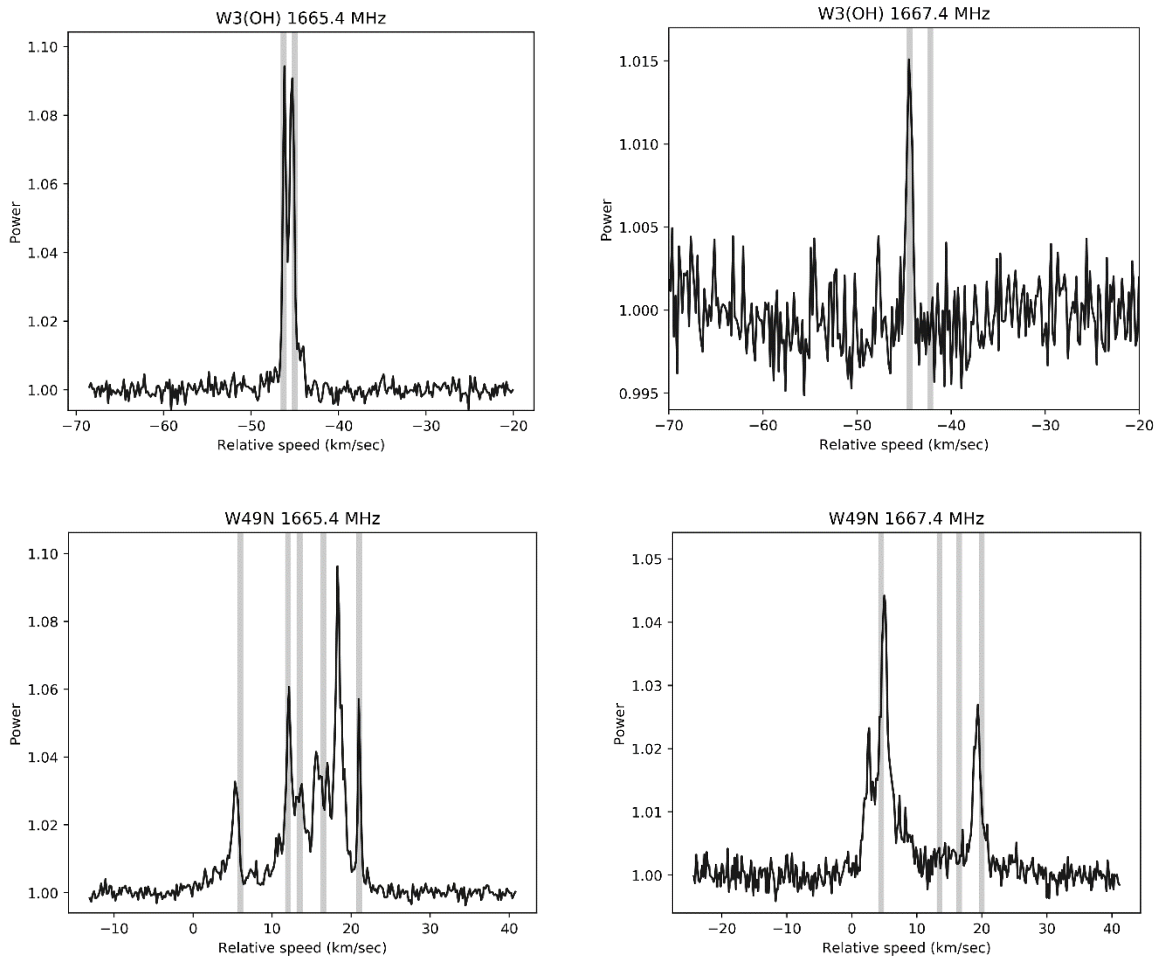


Figure 15: interstellar maser sources observed at 1665 MHz (left) and 1667 MHz (right). Spectral resolution 1 KHz, integration times were 5.1 minutes on W3(OH) and 7 minutes on W49N.

In addition to the circumstellar masers, the two star forming regions Westerhout 3-OH (W3OH) and Westerhout 49 (W49) were observed. Both regions were initially discovered in the late 1950s by the Dutch radio-astronomer

Gart Westerhout as part of a continuum survey with the Dwingeloo telescope [15]. There is a certain symbolic to using the same telescope more than 60 years later to observe the same sources.

OH masers were detected at the 1665 and 1667 MHz line in both the W3(OH) and W49 regions; attempts to detect these sources at 1612 MHz were unsuccessful. We also tried to detect W49 at 1720 MHz but intense RFI made detection of weak astronomical signals unfeasible. The 1665 MHz spectrum of W3(OH) at 1665 MHz consisted of two partially overlapping narrow peaks, while at 1667 MHz only one weak feature was detected. W49 has a much more complex spectrum with many overlapping features at 1665 MHz. The 1667 MHz line from this source is only about half as strong and has fewer peaks. Apparently, the conditions needed for the 1667 MHz maser emission to occur are not as common in these star forming regions.

RFI issues

As noted, before, observations of all four OH lines were regularly affected by RFI. At 1612 MHz and 1665-1667 MHz the RFI occurred in short bursts every few minutes, so it was still possible to exclude the “bad” spectra and gather sufficient data while there was no RFI. At 1720 MHz the RFI was more or less continuous making observations very difficult.

Conclusion and outlook

The OH maser observations with the Dwingeloo telescope were a success: we detected more sources than expected. This demonstrates that with a sufficiently large dish these relatively weak sources can be easily detected despite the reduced sensitivity of the 1.2- 1.4 GHz front- end at 1.6- 1.7 GHz. The OH maser spectra from this experiment could also provide comparison data for amateurs trying to detect these sources with much smaller dishes.

However, these initial experiments still do not address the question of the actual sensitivity of the Dwingeloo telescope at 1.6 GHz. In order to constrain the system temperature and aperture efficiency we would have to perform hot-cold measurements and observe a “standard” source with a known flux density. The masers themselves are not that useful for this purpose because of their intrinsic variability, although comparison of our spectra with recent observations by Astropfeiler could be interesting.

Sources:

- 1) <https://astronomy.swin.edu.au/cosmos/m/Masers>
- 2) https://en.wikipedia.org/wiki/Astrophysical_maser
- 3) S. Deguchi “Masers; interstellar and circumstellar.”
<https://ned.ipac.caltech.edu/level5/ESSAYS/Deguchi/deguchi.html>
- 4) Lovas, F. J. (2004). NIST recommended rest frequencies for observed interstellar molecular microwave transitions—2002 revision. *Journal of Physical and Chemical Reference Data*, 33(1), 177-355.
- 5) “The Astropfeiler Stockert story part 5: Spectral observations Hydroxyl (OH) masers and absorption”, Wolfgang Herrmann. https://www.astropfeiler.de/wp-content/uploads/2023/05/Astropfeiler_Story_5.pdf
- 6) “The 3- metre dish at the “Astropfeiler Stockert” part 2: characterisation and observations” Wolfgang Herrmann. https://astropfeiler.de/wp-content/uploads/2017/12/Part2_The_3-Meter_Dish_Astropfeiler_Stockert_Characterisation_and_Observations.pdf
- 7) “Observations OH raies 18cm”, J. J. Maintoux F1EHN. https://f1ehn.org/wp-content/uploads/2023/07/pages_radioastro/Images_Docs/Radioastro_18cm_OH_2019.pdf

- 8) Gray, M. (1999). Astrophysical masers. *Philosophical Transactions of the Royal Society of London. Series A: Mathematical, Physical and Engineering Sciences*, 357(1763), 3277-3298.
- 9) Official website of CAMRAS: <https://www.camras.nl/>
- 10) Engels, D., & Bunzel, F. (2015). A database of circumstellar OH masers. *Astronomy & Astrophysics*, 582, A68. (www.hs.uni-hamburg.de/maserdb)
- 11) Ladeyschikov D.A., Bayandina O.S., Sobolev A.M., *Astronomical Journal*, 2019, Vol. 158, P. 233. (<https://maserdb.net/>)
- 12) Mol, E. (2023). Catalogue of the brightest astrophysical maser sources. *SARA journal* March-April 2023, 90-94.
- 13) <https://gitlab.camras.nl/dijkema/HPIB/blob/185d241ad9bd7507ed90c9fa91fe0a63009d3eee/vlsr.py>
- 14) Nancay 1612 MHz maser monitoring programme: https://hsweb.hs.uni-hamburg.de/projects/nrt_monitoring/index.html
- 15) Westerhout, G. (1958). A survey of the continuous radiation from the galactic system at a frequency of 1390 Mc/s. *Bulletin of the Astronomical Institutes of the Netherlands*, Vol. 14, p. 215, 14, 215.

Journal Archives and Other Promotions

The rich and diverse legacy of member contributed content is available in the SARA Journal Archives. Table of contents for journals is available online at: [SARA-Journal-Master-Index.xlsx \(live.com\)](#)

The entire set of The Journal of The Society of Amateur Radio Astronomers is available by online download. It goes from the beginning of 1981 to the present (over 6000 pages of SARA history!)

All SARA journals and conference proceedings are available through the previous calendar year.

SARA Store (radio-astronomy.org/store.)

SARA offers the above USB drives, DVDs, printed Proceedings and Proceedings on USB drive and other items at the SARA Store: <http://www.radio-astronomy.org/e-store>. Proceeds from sales go to support the student grant program. Members receive an additional 10% discount on orders over \$50 US. Payments can be made by sending payment by PayPal to treas@radio-astronomy.org.

SARA Online Discussion Group

SARA members participate in the online forum at <http://groups.google.com/group/sara-list>. This is an invaluable resource for any amateur radio astronomer.

SARA Conferences

SARA organizes multiple conferences each year. Participants give talks, share ideas, attend seminars, and get hands-on experience. For more information, visit <http://www.radio-astronomy.org/meetings>.

What is Radio Astronomy?

Radio Astronomy is just what the name implies.... Astronomy observed at radio wavelengths instead of optical. But why do radio astronomy? Radio astronomy has expanded the knowledge of the universe about as much since its discovery in 1932 as optical has since humans first looked up at the sky. (The sky in the different frequencies or colors of radio are as different and varied as all of the flowers on Earth. Each frequency has its own information about what is happening in the universe.) This knowledge has been gained by both professional astronomers as well as amateurs, with amateurs contributing to this day.

Do I need a big dish and expensive equipment?

No. Complete beginner projects are available at the [SARA store](#) at very reasonable prices. You can monitor the Sun's effects upon our planet with [SuperSID](#). This information is gathered for Stanford for research into our ionosphere and radio signal propagation. Another project is the detection the hydrogen line just like Dr. Ewen had done in 1951 for a fraction of the cost using the [Scope in a Box](#) kit.

That said, radio astronomy is like optical astronomy in that you can spend as much as you want to. Many amateurs push the lower boundaries of cost by using very low-cost receivers and low-noise low-cost amplifiers that were not available even a few years ago. (See the [Scope in a Box](#) kit in the store for examples of both.)

Is everything 'plug and play' and boring?

The kits mentioned above are a starting point which are mostly plug-and-play... that gets you started. After you have mastered the basics, where you go from there depends upon your interests. Monitoring pulsars is done by amateurs. (One even noticed a [pulsar glitch](#) before the professionals!) These amateurs are pushing the boundaries of what can be done. Papers are being published and discussions had about pulsar detection as well detection of a MASER with a 50-inch dish. Techniques on new detection methods are posted in the [SARA forum](#) and elsewhere. You are free to build your own equipment to receive the signals as well as software to collect and analyze the data.

What is SETI?

SETI is the Search for Extra-Terrestrial Intelligence. Some amateurs scan the sky and search for signals that might be from aliens. To date no one has received a definitive alien signal (professional or amateur), but the search continues. The search has resulted not just in better receiving equipment but also wide and lively discussions about how aliens might communicate and how they might be trying to contact us. Some of these techniques have interesting ideas for our own communication techniques here on Earth!

What should I do to get started?

You should start with reading our [Introduction to Radio Astronomy](#) and joining our online [SARA Forum](#). Look at the [SARA store](#) to get a project to get your feet wet without much expense and minimal risk. We will work with you so you can succeed.

Administrative

Officers, directors, and additional SARA contacts

The Society of Amateur Radio Astronomers is an all-volunteer organization. The best way to reach people on this page is by email with SARA in the subject line SARA Officers.

President: Dr. Rich Russel, AC0UB, <https://www.radio-astronomy.org/contact/President>

Vice President: Jay Wilson, <https://www.radio-astronomy.org/contact/Vicepresident>

Secretary: Bruce Randall, NT4RT, <https://www.radio-astronomy.org/contact/Secretary>

Treasurer: Tom Jacobs, <https://www.radio-astronomy.org/contact/Treasurer>

Asst. Treasurer: Donna Hallin, <https://www.radio-astronomy.org/contact/Treasurer>

Past President: Dennis Farr

Founder Emeritus and Director: Jeffrey M. Lichtman, KI4GIY, jeff@radioastronomysupplies.com

Board of Directors

Name	Term expires	Email
Ed Harfmann	2024	edharfmann@comcast.net
Dr. Wolfgang Herrmann	2025	messbetrieb@astropeiler.de
Paul Butler	2025	paul.butler.melbourne@gmail.com
Charles Osborne	2025	k4cso@twc.com
Bob Stricklin	2024	bstrick@n5brg.com
Steve Tzikas	2024	Tzikas@alum.rpi.edu
Ted Cline	2025	TedClineGit@gmail.com
David Westman	2024	david.westman@engineeringretirees.org

Other SARA Contacts

All Officers	http://www.radio-astronomy.org/contact-sara	
All Directors and Officers	http://www.radio-astronomy.org/contact/All-Directors-and-Officers	
Eastern Conference Coordinator	http://www.radio-astronomy.org/contact/Annual-Meeting	
All Radio Astronomy Editors	http://www.radio-astronomy.org/contact/Newsletter-Editor	
Radio Astronomy Editor	Dr. Richard A. Russel	drrichrussel@radio-astronomy.org
Contributing Editor	Bogdan Vacaliuc	bvaculiuc@iee.org
Educational Co-Chairs	Ken Redcap, Tom Hagen: http://www.radio-astronomy.org/contact/Educational-Outreach	
Grant Committee	Tom Crowley	grants@radio-astronomy.org
Membership Chair	http://www.radio-astronomy.org/contact/Membership-Chair	
Technical Queries (David Westman)	http://www.radio-astronomy.org/contact/Technical-Queries	
Webmaster	Ciprian (Chip) Sufitchi, N2YO	webmaster@radio-astronomy.org

Resources

Great Projects to Get Started in Radio Astronomy

Radio Observing Program

The Astronomical League (AL) is starting a radio astronomy observing program. If you observe one category, you get a Bronze certificate. Silver pin is two categories with one being personally built. Gold pin level is at least four categories. (Silver and Gold level require AL membership which many clubs have membership. For the bronze level, you need not be a member of AL.)

Categories include.

- 1) SID
- 2) Sun (aka IBT)
- 3) Jupiter (aka Radio Jove)
- 4) Meteor back-scatter
- 5) Galactic radio sources

This program is a collaboration between NRAO and AL. Steve Boerner is the Lead Coordinator and a SARA member.

For more information:

Steve Boerner

2017 Lake Clay Drive

Chesterfield, MO 63017

Email: sboerner@charter.net

Phone: 636-537-2495

<http://www.astroleague.org/programs/radio-astronomy-observing-program>

Radio Jove



The Radio Jove Project monitors the storms of Jupiter, solar activity and the galactic background. The radio telescope can be purchased as a kit, or you can order it assembled. They have a terrific user group you can join. <http://radiojove.gsfc.nasa.gov/>

INSPIRE Program



The INSPIRE program uses build-it-yourself radio telescope kits to measure and record VLF emissions such as tweeks, whistlers, sferics, and chorus along with man-made emissions. This is a very portable unit that can be easily transported to remote sites for observations.

<http://theinspireproject.org/default.asp?contentID=27>

SARA/Stanford SuperSID



Stanford Solar Center and the Society of Amateur Radio Astronomers have teamed up to produce and distribute the SuperSID (Sudden Ionospheric Disturbance) monitor. The monitor utilizes a simple pre-amp to magnify the VLF radio signals which are then fed into a high-definition sound card. This design allows the user to monitor and record multiple frequencies simultaneously. The unit uses a compact 1-meter loop antenna that can be used indoors or outside. This is an ideal project for the radio astronomer that has limited space. To request a unit, send an e-mail to supersid@radio-astronomy.org

Radio Astronomy Online Resources

SARA YouTube Videos: https://www.youtube.com/@radio-astronomy	Pisgah Astronomical Research Institute: www.pari.edu
AJ4CO Observatory – Radio Astronomy Website: http://www.aj4co.org/	A New Radio Telescope for Mexico - ORION 2021 01 20. Dr. Stan Kurtz https://www.youtube.com/watch?v=Q9aBWr1aBVc
Radio Astronomy calculators https://www.aj4co.org/Calculators/Calculators.html	National Radio Astronomy Observatory http://www.nrao.edu
Introduction to Amateur Radio Astronomy (presentation) http://www.aj4co.org/Publications/Intro%20to%20Amateur%20Radio%20Astronomy,%20Typinski%20(AAC,%202016)%20v2.pdf	NRAO Essential Radio Astronomy Course http://www.cv.nrao.edu/course/astr534/ERA.shtml
RF Associates Richard Flagg, rf@hawaii.rr.com 1721-1 Young Street, Honolulu, HI 96826	Exotic Ions and Molecules in Interstellar Space -- ORION 2020 10 21. Dr. Bob Compton https://www.youtube.com/watch?v=r6cKhp23SUo&t=5s
RFSpace, Inc. http://www.rfspace.com	The Radio JOVE Project & NASA Citizen Science – ORION 2020.6.17. Dr. Chuck Higgins https://www.youtube.com/watch?v=s6eWAXjywp8&t=5s
CALLISTO Receiver & e-CALLISTO http://www.reeve.com/Solar/e-CALLISTO/e-callisto.htm	UK Radio Astronomy Association http://www.ukraa.com/
Deep Space Exploration Society http://DSES.science	CALLISTO software and data archive: www.e-callisto.org
Deep Space Object Astrophotography Part 1 -- ORION 2021 02 17. George Sradnov https://www.youtube.com/watch?v=Pm_Rs17KlyQ	Radio Jove Spectrograph Users Group http://www.radiojove.net/SUG/
European Radio Astronomy Club http://www.eraonet.org	Radio Sky Publishing http://radiosky.com
British Astronomical Association – Radio Astronomy Group http://www.britastro.org/baa/	The Arecibo Radio Telescope; It's History, Collapse, and Future - ORION 2020.12.16. Dr. Stan Kurtz, Dr. David Fields https://www.youtube.com/watch?v=rBZIPOLNX9E
Forum and Discussion Group http://groups.google.com/group/sara-list	Shirleys Bay Radio Astronomy Consortium marcus@propulsionpolymers.com
GNU Radio https://www.gnuradio.org/	SARA Twitter feed https://twitter.com/RadioAstronomy1
SETI League http://www.setileague.org	SARA Web Site http://radio-astronomy.org
NRAO Essential Radio Astronomy Course http://www.cv.nrao.edu/course/astr534/ERA.shtml	Simple Aurora Monitor: Magnetometer http://www.reeve.com/SAMDescription.htm
NASA Radio JOVE Project http://radiojove.gsfc.nasa.gov Archive: http://radiojove.net/archive.html https://groups.io/g/radio-jove	Stanford Solar Center http://solar-center.stanford.edu/SID/
National Radio Astronomy Observatory http://www.nrao.edu	

For Sale, Trade and Wanted

At the SARA online store: radio-astronomy.org/store.

Scope in a Box

radio-astronomy.org/store.

Kit of parts and software to build a working Radio Telescope to detect Hydrogen Line emissions. Available to USA addresses only at this time.

SuperSID Complete Kit

radio-astronomy.org/store.



SARA Publication, Journals and Conference Proceedings (various prices)

radio-astronomy.org/store.

SARA Journal Online Download

radio-astronomy.org/store.

The USB drive covers the society journal "Radio Astronomy" from the founding of the organization in 1981 thru the present. Articles cover a wide range of topics including: cosmic radiation, pulsars, quasars, meteor detection, solar observing, Jupiter, Radio Jove, gamma ray bursts, the Itty Bitty Telescope (IBT), dark matter, black holes, the Jansky antenna, methanol masers, mapping at 408 MHz and more. This CD contains all of the above and more with over 4800 pages of articles on radio astronomy. Also included is a copy of Grote Reber's handwritten, 34-page document "Carriage and Mirror Detail" of his historic antenna now on display at the National Radio Astronomy Observatory (NRAO) in Greenbank, WV. You also get an electronic copy of the 109 page "Basics of Radio Astronomy" from JPL Goldstone-Apple Valley Radio Telescope. Also included is the NRAO 40-foot radio telescope "Operators Manual", which by the way, you get to operate if you attend the Eastern SARA conference in July.

SARA Advertisements

There is no charge to place an ad in Radio Astronomy; but you must be a current SARA member. Ads must be pertinent to radio astronomy and are subject to the editor's approval and alteration for brevity. Please send your "For Sale," "Trade," or "Wanted" ads to edit@radio-astronomy.org. Please include email and/or telephone contact information. Please keep your ad text to a reasonable length. Ads run for one bimonthly issue unless you request otherwise.

Radio-Astro-Machine, zzblac@gmail.com

Elevation rotation adapter plate for Scope in a Box and custom machining. For further information visit <https://radio-astro-machine.wixsite.com/my-site> or send an email.

Typinski Radio Astronomy, Inc., info@typinski.com

Antenna systems and feed line components for HF radio astronomy

Jeff Kruth, WA3ZKR, kmec@aol.com

RF components from HF to MMW, various types including mixers, RF switches, amplifiers, oscillators, coaxial components, waveguide components, etc. I have a very large collection of stuff and the facilities to test and provide data. Please email with your needs and I will see if I have something for you. Have fun!

Stuart and Lorraine Rumley, sales@valontechnology.com

The Valon Technology 2100 Downconverter, when combined with our 5009 frequency synthesizer module, provides a high-performance, compact receiver downconverter system. Applications include hydrogen line studies at 1420MHz and radio astronomy in the protected 30MHz segment of the 21 cm band. For more information visit <http://www.valontechnology.com/2100downconverter.html> or send an email.

Radio2Space, filippo.bradaschia@primalucelab.com

SPIDER radio telescopes and turn-key-systems designed specifically for education.

<https://www.radio2space.com>

We developed our SPIDER radio telescopes as turn-key-system just to avoid the problem you perfectly highlighted in your website: "Purchasing a radio telescope isn't like buying an optical telescope. They are harder to find, and usually require assembly and software troubleshooting. In some cases, a radio telescope must be built from components." Our SPIDER radio telescopes are not designed for amateurs that prefer to build a radio telescope but to schools, universities, museums, and other science institutes that needs for a complete and ready-to-use system, just like the optical telescopes they can normally buy!

SARA Brochure



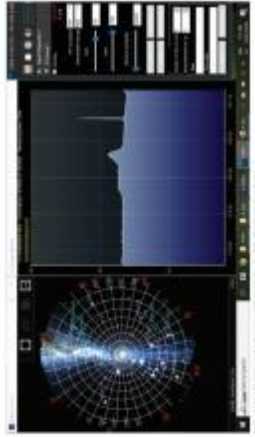
Society of Amateur Radio Astronomers, Inc.
Founded 1981

Membership supported, nonprofit [501(c) (3)]
Educational and Radio Astronomy Organization
**Knowledge through Common Research,
Education and Mentoring**



How to get started?

SARA has made a kit of software and parts to detect the Hydrogen line signal from space. This is an excellent method to get started in radio astronomy. It teaches the principles of antenna design, signal detection, and signal processing. Read more about this and other projects on our web site.



Membership Information

Annual SARA dues individual \$20, Classroom \$20, Student \$5 (US funds) anywhere in the world. Membership includes a subscription to Radio Astronomy, the bimonthly Journal of The Society of Amateur Radio Astronomers, delivered electronically (via a secure web link, emailed to you as each new issue is posted). We regret that printing and postage costs prevent SARA from providing hardcopy subscriptions to our Journal.

We would appreciate the following information included with your check or money order, made payable to SARA:

Name: _____
 Email Address: _____
(required for electronic Journal delivery)
 Ham call sign: _____ (if applicable)
 Address: _____
 City: _____
 State: _____
 Zip: _____
 Country: _____
 Phone: _____

Please include a note of your interests. Send your application for membership, along with your remittance, to our Treasurer.

For further information, see our website at:
<http://radio-astronomy.org/membership>



SARA members have been privileged to use this forty foot diameter drift-scan hydrogen line radio telescope every year at their annual meeting in Green Bank.

Why Radio Astronomy?

Because about sixty five percent of our current knowledge of the universe has stemmed from radio astronomy alone. The discovery of quasars, pulsars, black holes, the 3K background from the "Big Bang" and the discovery of biochemical hydrogen/carbon molecules are all the result of professional radio astronomy.



<http://radio-astronomy.org>

The Society of Amateur Radio Astronomers

SARA was founded in 1981, with the purpose of educating those interested in pursuing amateur radio astronomy.

The society is open to all, wishing to participate with others, worldwide.

SARA members have many interests, some are as follows:

SARA Areas of Study and Research:

- Solar Radio Astronomy
- Galactic Radio Astronomy
- Meteor Detection
- Jupiter
- SETI
- Gamma Ray/High Energy Pulse
- Detection
- Antennas
- Design of Hardware / Software

The members of the society offer a friendly mentor atmosphere. All questions and inquiries are answered in a constructive manner. No question is silly!

SARA offers its members an electronic bi-monthly journal entitled Radio Astronomy. Within the journal, members report on their research and observations. In addition, members receive updates on the professional radio astronomy community and, society news.

Once a year SARA meets for a three-day conference at the Green Bank Observatory in Green Bank West Va.

There is also a spring conference held at various cities in the Western USA. Previous meetings have been at the VLA in Socorro, NM and at Stanford University.



How do I get started?

Just as a long journey begins with the first step, the project you elect must start with a clear idea of your objectives. Do you wish to study the sun? Jupiter? Make meteor counts? Do you wish to engage in imaging radio astronomy? What you decide will not only determine the type of equipment you will need, but also the local radio spectrum.

How do amateurs do radio astronomy?

Radio astronomy by amateurs is conducted using antennas of various shapes and sizes, from smaller parabolic dishes to simple wire antennas. These antennas are connected to receivers and most of these receivers are software defined radios these days. Data from the receivers are collected by computers, and the received signals will be displayed as charts, graphs or maybe even sky maps. As diverse as the observed objects, so is the instruments and tools used. SARA members will always be supportive to find good solutions for what one wishes to observe.

Is amateur radio astronomy instrumentation expensive?

Technical information freely circulated in our monthly journal helps amateurs to obtain good low noise equipment from off the shelf assemblies, or to build their own units. The actual cash investment in radio astronomy equipment need not exceed that of any other hobby.

What are amateurs actually looking for in the received data?

The aim of the radio amateur is to find something new and unusual. Just as an amateur optical observer hopes to notice a supernova or a new comet, so does an amateur radio observer hope to notice a new radio source, or one whose radiation has changed appreciably.



The Reber Telescope at NRAO. Constructed by Grote Reber in 1937 in his back yard in Wheaton, Illinois



SARA Members discussing the IBT (Itty Bitty Telescope)

